Protocoles de routage opportunistes et avec qualité de service pour les réseaux véhiculaires VANETs

Guang Yu Li

Université Paris-Sud

Ecole Doctorale Informatique Paris Sud
Laboratoire Recherche en informatique

Discipline: Informatique

Thèse de doctorat

Soutenue le 21/07/2015 par

Guangyu Li

Adaptive and Opportunistic QoS-based Routing Protocol in VANETs

Directeur de thèse :	Dr. Lila Boukhatem	Université Paris-Sud

Composition du jury :

Rapporteurs :	Prof. Mohamed Yacine Ghamri-Doudane	Université de La Rochelle
	Prof. Paul Mühlethaler	INRIA Rocquencourt
Examinateurs :	Prof. Guy Pujolle	Université Pierre et Marie Curie
	Prof. Véronique Vèque	Université Paris-Sud
	Prof. Steven Martin	Université Paris-Sud
	Dr. Jinsong Wu	Université Chile

Abstract

Adaptive and Opportunistic QoS-based Routing Protocol in VANETs

by

Guangyu Li

Vehicular ad hoc networks (VANETs) are able to supply scalable and cost-effective solutions for various applications such as road safety, traffic efficiency and entertainments through multi-hop vehicle-to-vehicle wireless communications. However, developing multi-hop communications in VANET environments is a very challenging problem due to the rapid topology changes and frequent network disconnections, which lead to routing failure or inefficiency in traditional mobile ad hoc routing protocols. This dissertation proposes a novel class of routing protocols (AQRV, AQRV-1 and AQRV-2), which can account for specific characteristics of VANETs. Based on real-time QoS of road segment (namely connectivity probability, packet delivery ratio and delay), these three routing protocols rely on dynamic intersection-based best QoS route selection to cope with the scalability challenge in large-scale urban scenarios and meet varying requirements of a large number of applications. In order to explore the best QoS routing path, we regard the corresponding routing issue as an optimization problem, and propose an ACO-based (Ant Colony Optimization) algorithm to solve it. Besides, to reduce routing exploration time and decrease network overhead, an opportunistic method is proposed to explore the network and search available routing paths in terms of local/global QoS. In addition, by taking benefit from traffic information, such as vehicle density, vehicle speed and road length, we design mathematical models to estimate real-time QoS for 1-lane and 2-lane road scenarios. The main advantages of these models are twofold: provide accurate estimations of road segments' QoS metrics and decrease the overhead compared with the estimation method by forwarding periodic packets. Furthermore, a TI-based (Terminal Intersection) concept is proposed to make a group of communication pairs share the same back-bone best route, which is beneficial to update latest routing information, decrease overhead and reduce transmission delay. Upon best route identification, data packets forwarding process is initiated including a dynamic road segment selection at intersections based on the updated global QoS, and a simple greedy carry-and-forward scheme to relay data packets between two neighboring intersections. Finally, to further reduce signaling overhead and alleviate network congestion, the one-hop geographical forwarding is improved using a distributed receiver-based election concept and utilized in AQRV-2 routing protocol to avoid periodic Hello packets exchanges. Extensive simulations are implemented to prove the effectiveness of the proposed protocols and the

accuracy of the derived mathematical QoS models. A thorough analysis showed the better performance of our routing protocols in terms of overhead, delay and packet delivery ratio compared with reference routing protocols, and investigated the effects of related influencing factors.

Acknowledgements

First and foremost, I would like to express my utmost admiration and deepest gratitude to my supervisor Dr. Lila Boukhatem for her continuous guidance and kind support. *"Ancient scholars certainly had teachers. A teacher is one who could propagate the doctrine, impart professional knowledge and resolve doubts" (from the article called "On Teachers" written by Han Yu, who is a very famous poet and essayist in Tang dynasty in China).* In my opinion, the behaviors of Dr. Lila Boukhatem fulfill the description of Han Yu in terms of an excellent teacher, and I draw a lot of inspirations from her words and actions, such as how to become a qualified researcher, how to choose the career direction and what is the meaning of life, etc. In the past four years, there are many memorable instants: I can not forget the moment she helped me revise my papers in the deep of night, I can not forget the moments she arrived at the lab and supervised my research progress when she gave birth to a child at once, I can not forget the moment she had a call to me to discuss my thesis when she suffered from the illness and so on. There is an ancient saying in China: *One day is teacher, life long is family.* I wish to take this opportunity to thank her for the constant encouragement and patience and that was a tremendous pleasure to work with her.

I would like to thank my jury committee members: Prof. Ghamri-Doudane Mohamed Yacine, Prof. Mühlethaler Paul, Prof. Guy Pujolle, Prof. Véronique Vèque, Prof. Martin Steven and Dr. Wu Jinsong for their invaluable comments and support to make me improve this work.

Special thanks to Prof. Martin Steven for his strong support in the past four years, and for his painstaking and thoughtful preparations during my defense period.

I am also thankful to my fellow colleagues and friends in the LRI lab at the University of Paris Sud who inspired me along the way with their constructive comments, continuous support and great friendships.

I am deeply indebted to my family for their full backing, and especially to my parents and my brothers for their love, guidance and vision. I believe I have been blessed by the God for granting me such wonderful and supportive family.

Finally, great thanks to my beloved wife Dr. Shanshan Zhang. It is her love and support that give me power and confidence to cope with the challenges and difficulties.

Contents

List of Figures

List of Tables

Abbreviations

VANET	**V**ehicular **A**d hoc **NET**works
ACO	**A**nt **C**olony **O**ptimization
TI	**T**erminal **I**ntersection
AQRV	**A**daptive **Q**oS-based **R**outing for **V**ANETs
AQRV-1	**A**daptive **Q**oS-based **R**outing for **V**ANETs in **1**-lane scenarios
AQRV-2	**A**daptive **Q**oS-based **R**outing for **V**ANETs in **2**-lane scenarios
WLAN	**W**ireless **L**ocal **A**rea **N**etwork
ITS	**I**ntelligent **T**ransportation **S**ystems
MANET	**M**obile **A**d hoc **NET**work
V2V	**V**ehicle-**t**o-**V**ehicle
V2I	**V**ehicle-**t**o-**I**nfrastructure
OBU	**O**n-**B**oard **U**nit
RSU	**R**oad **S**ide **U**nit
DSRC	**D**edicated **S**hort **R**ange **C**ommunications
GPS	**G**eographic **P**osition **S**ystem
QoS	**Q**uality **o**f **S**ervice
BER	**B**it **E**rror **R**ate
EDD	**E**xpected **D**isconnection **D**egree
VRP	**V**ehicular **R**outing **P**roblem
NP	**N**on-deterministic **P**olynomial
SA	**S**imulated **A**nnealing
GA	**G**enetic **A**lgorithm
TS	**T**abu **S**earch
RREQ	**R**oute **REQ**uest
RREP	**R**oute **REP**ly

LQM	**L**ocal **Q**oS **M**odels
TID	**T**erminal **I**ntersection of the **D**estination vehicle
TIS	**T**erminal **I**ntersection of the **S**ource vehicle
RTS/CTS	**R**equest **T**o **S**end/**C**lear **T**o **S**end
PDR	**P**acket **D**elivery **R**atio
FC	**F**ully **C**onnected road segment
PC	**P**artly **C**onnected road segment
FB	**F**ully **B**roken road segment
CDF	**C**umulative **D**istribution **F**unction
VanetMobiSim	**V**ehicular **a**d hoc **net**works **Mobi**lity **Sim**ulator
CI	**C**onfidence **I**ntervals
CTR	**C**hannel **T**ransmission data **R**ate
NP	**N**etwork **P**artitions
NC	**N**etwork **C**onnections
DP	**D**isconnection **P**hase
CP	**C**onnection **P**hase
PDF	**P**robability **D**ensity **F**unction
CBR	**C**onstant **B**it **R**ate
VSC	**V**ehicle **S**afety **C**ommunications
VII	**V**ehicle **I**nfrastructure **I**ntegration
PATH	**P**artners for **A**dvanced **T**ransit and **H**ighways
CooPerCom	**Coo**perative **Per**ception and **Com**munication in Vehicular Technologies
CVIS	**C**ooperative **V**ehicles and **I**nfrastructure **S**ystems
PRECIOSA	**PR**ivacy **E**nabled **C**apability **I**n c**O**operative Systems and **S**afety **A**pplications
EVITA	**E**-safety **V**ehicle **I**n**T**rusion protected **A**pplications
ASV	**A**dvanced **S**afety **V**ehicle Program
AOMDV	**A**d hoc **O**n-demand **M**ulti-path **D**istance **V**ector
TORA	**T**emporally **O**rdered **R**outing **A**lgorithm
ZRP	**Z**one **R**outing **P**rotocol
GPSR	**G**reedy **P**erimeter **S**tateless **R**outing
GSR	**G**eographic **S**ource **R**outing
GPCR	**G**reedy **P**erimeter **C**oordinator **R**outing
GPSRJ+	**G**reedy **P**erimeter **S**tateless **R**outing **J**unction+

A-STAR	**A**nchor-based **S**treet and **T**raffic **A**ware **R**outing
LOUVRE	**L**andmark **O**verlays for **U**rban **V**ehicular **R**outing **E**nvironments
RBVT	**R**oad-**B**ased using **V**ehicular **T**raffic
RMRV	**R**oad-based **M**ultipath **R**outing protocol for urban **V**ANETs
CAR	**C**onnectivity **A**ware **R**outing
VADD	**V**ehicle-**A**ssisted **D**ata **D**elivery routing
IGRP	**I**ntersection-based **G**eographical **R**outing **P**rotocol
ARP-QD	**A**daptive **R**outing **P**rotocol based on **Q**oS and vehicular **D**ensity
MURU	**MU**lti-hop **R**outing protocol for **U**rban VANETs
IACO	**I**mproved **A**nt **C**olony **O**ptimization

Symbols

y	Routing path
e_k	Road segment
$F(y)$	Route objective function
$PC(y)$	Route connectivity probability
$PDR(y)$	Route packet delivery ratio
$DV(y)$	Route delay variance
$PC(e_k)$	Road segment connectivity probability
$PDR(e_k)$	Road segment packet delivery ratio
$DV(e_k)$	Road segment delay variance
χ	Weight value of distance on TI selection
p_{ij}	Probability of choosing the next intersection j at intersection i
$Nb(i)$	Neighboring intersections set of intersection i
GP_{ij}	Global pheromone of the route from intersection i to destination/destination's terminal intersection going through next intersection j
LP_{ij}	Local pheromone of the road segment between intersection i and intersection j
PGP_{ij}	Previously updated global pheromone of the route from intersection i to destination/destination's terminal intersection going through next intersection j
τ_{min}	Floor level of pheromone
N_{fant}	Reactive forward ants number
a	Weight value of cell size
N_{inf}	Number of interfering nodes
P_{FC}	Probability of FC case

P_{FB}	Probability of FB case	
P_{PC}	Probability of PC case	
PDR_{FC}	Packet deliver ratio in the FC case	
PDR_{FB}	Packet deliver ratio in the FB case	
PDR_{PC}	Packet deliver ratio in the PC case	
$Score\,(I_i)$	Score value of TI candidate of intersection i	
α	Weight value of local pheromone	
β	Weight value of global pheromone	
φ_1	Weight value of connectivity probability	
φ_2	Weight value of packet delivery ratio	
φ_3	Weight value of delay	
PC_{th}	Threshold of connectivity probability	
PDR_{th}	Threshold of packet delivery ratio	
PDR_{NP}	Packet delivery ratio in the NP case	
PDR_{NC}	Packet delivery ratio in the NC case	
r_{dp}	Probability of dp phase	
r_{cp}	Probability of cp phase	
t_k	Waiting time to reply CTS to packet transmitter	s
λ_1	Vehicle spacing density on the Eastbound lane	vehicles/m
λ_2	Vehicle spacing density on the Westbound lane	vehicles/m
v_1	Vehicle speed on the Eastbound lane	m/s
v_2	Vehicle speed on the Westbound lane	m/s
$D\,(y)$	Route delay	s
$D\,(e_k)$	Road segment Delay	s
R	Communication range	m
λ	Vehicle spacing density in 1-lane road	vehicles/m
$P_r(x)$	Received signal power	W
$psize$	packet size	byte
L_f	Forwarding link length	m
L_c	Carry links length	m
L	Road segment length	m
R_{inf}	Interference range	m
T_{GP}	updated time interval of global pheromone	m

D_{th}	Threshold of delay	s
D_{NP}	Delay in the NP case	s
D_{NC}	Delay in the NC case	s
D_{FC}	Delay in the FC case	s
D_{FB}	Delay in the FB case	s
D_{PC}	Delay in the PC case	s
v	Vehicle speed on 1-lane road	m/s
t_p	1 hop delay	s
DPR	Data packet sending rate	packets/s

Chapter 1

Introduction

1.1 Background

Wireless communications become significantly available and inexpensive with the development of various network technologies, such as Wireless Local Area Networks (WLANs) and 4G cellular system [1–3], all of which promise rapid advancements of Intelligent Transportation Systems (ITS) witnessing the global development of smart cities [4, 5] and provide new attractive and cost effective services to users. As a key component of ITS and smart cities, Vehicular Ad hoc NETworks (VANETs) [6] are attracting enormous attentions of more and more institutes and companies.

VANETs are a special type of Mobile Ad hoc NETworks (MANETs)[7, 8], and they are composed of a group of vehicles which can communicate without relying on fixed infrastructure support. In VANETs, the vehicles are able to act as routing nodes to exchange information (which may be various depending on different applications, for example, video, security notifications, location messages and so on) by means of either Vehicle-to-Vehicle (V2V) or Vehicle-to-Infrastructure (V2I) communications. V2V communication takes place among On-Board Units (OBUs) equipped in each vehicle, and V2I communication occurs between OBUs and Road Side Units (RSUs), which can transmit available information to servers through Internet based on different network access technologies (RFID, 3G/4G, Wi-Fi, ect.). VANETs have tremendous potential to improve vehicle and road security, increase traffic efficiency, and enhance convenience and comfort to both drivers and passengers.

1.2 Research motivations and problem statements

Because of their wide variety of applications, high effectiveness and low-cost constructions, VANETs become a major research motivation of governments, car manufacturers and academic institutions, and attract more and more interests of them. However, the successful deployment of VANETs consists of a number of important components, a key one of which is how to establish adaptive and efficient routing paths from sources to destinations in the complex and dense urban scenarios. The benefits of VANETs will be limited without the available solution of this routing problem. Based on profound investigations and detailed considerations, the main challenges of VANET routing issue in urban scenarios are as follows.

Firstly, real-time and accurate QoS routing obtainment. Routing QoS metrics, such as delay, packet delivery ratio and connectivity probability, play an important role in establishing available routing paths, as they offer characterization of the routes quality which is highly relevant to instantaneous and precise operational traffic information (e.g., vehicle density, vehicle distribution and road segment length). Besides, routing QoS can directly affect the availability and efficiency of various applications, for example, emergent collision warning is required to be transmitted with low delay and the connectivity of this routing path should be favorable, while providing available VoIP and E-payment service to customers, reliable and robust routing paths with high packet delivery ratio are necessary. Moreover, the spatial-temporal features of traffic conditions in VANETs are dynamic, for example, the spatial vehicle density can vary from very sparse to far dense, and the temporal vehicle density in one area can be variant depending on the time of the day. As a result, real-time and accurate routing QoS is very difficult to be estimated in VANET urban scenarios.

Secondly, network congestion. Large-scale urban environments are characterized by a high concentration of vehicles in VANETs especially during hush hours, and their communication exchange can easily burden the wireless channel with high traffic loads and may result in significant impairment of end-to-end packet delivery ratio and transmission delay. Actually, these traffic loads include not only data packets but also a number of Hello packets, which are used to broadcast geographic information among neighbor nodes. Besides, DSRC (Dedicated Short Range Communications) standard provides VANET communications with a bandwidth of only 75 MHz [9], and this spectrum is divided into 7 channels, one of which only owns 10 MHz capacity. Obviously, higher traffic loads and limited bandwidth can easily induce network congestion and then exacerbate routing performance. Therefore, how to alleviate network congestion and reduce overhead in VANETs are very challenging issues that we want to address in this thesis.

Thirdly, low QoS performance. It is very important but difficult to keep the best QoS for packets forwarding in urban scenarios. The possible reasons are given as follows: (1) urban environments are usually large-scale scenarios and the communication distance from a source to its destination may be very great, (2) global QoS of candidate routing paths are difficult to be known by a source vehicle, so routing exploration processes in large-scale networks are always based on local traffic information with random characteristics, which may result in the end-to-end routes including network-partitioned/congested road segments, (3) most traditional VANET routing protocols lack of self-adaptation features and can not cope with topology changes availably, which can disturb the process of packets forwarding, and (4) different communication pairs are usually absent of cooperation and do not make use of explored routing paths, so more routing exploration processes are implemented, which may result in redundant overhead and higher transmission delay.

Fourthly, scalability and stability. Guaranteeing a stable and scalable routing mechanism over VANETs is an important and necessary step toward the realization of effective vehicular communications. However, due to varying vehicle mobility and network topologies, routing paths are disrupted frequently, and it is very difficult to ensure their stability. In addition, end-to-end node-based or intersection-based source-driven routing paths are not available in large-size urban environments as they can not handle the scalability issue.

Finally, heterogeneity conveyed data packets. VANETs are supposed to provide a wide variety of applications ranging from safety to infotainment applications. Road safety applications usually require low transmission delay and high reliability whereas resource utilization, packet loss and fairness are the common performance measures for infotainment applications. Besides, different QoS metrics maybe counterproductive to each other in some communication scenarios, for example, dense vehicles are advantageous to the improvement of connectivity but may increase packet loss ratio because of channel congestion and interference. By means of different traffic information, the best QoS routing selection with multiple QoS thresholds to satisfy with heterogeneous applications should be considered.

There have been many proposals in the literature to deal with above challenges of routing protocols in VANETs. Geographic-based routing protocols [10–12] are considered to be more stable and suitable for large-scale VANETs compared with topology-based routing protocols [13]. In GPSR [14], each node just forwards the packets to its neighboring node which is nearest to the destination, so it can efficiently solve the scalability issue but frequently suffers from link failure problems. GPCR [15] and GSR [16] are intersection-based routing protocols and search the shortest path towards the destination. However, they neglect the traffic information along the route and may easily undergo the network-partition/ network congestion problems. A-STAR [17] uses the statistical traffic information of city buses to identify high connectivity anchor-based paths, but this information may be out of data and not sufficient to reflect comprehensive routing performance. CAR [18] and ACAR [19] take advantage of real-time routing information to choose the best QoS path, whereas this information is gathered through the on-the-fly collection process and shows instantaneous characteristics and can not reflect accurate transmission quality. In addition, blind routing explorations in these routing protocols result in high delay and redundant overhead. TADS [20] makes use of local link quality to select the next best intersection, but it neglects global route quality and may make packets forwarding face extreme forwarding conditions in future routing selection processes. According to above descriptions, even if the literature on routing issues are abundant and rich, there are still several problems to be solved, such as how to make use of global rather than only local routing information, real-time rather than historical/instantaneous traffic data and so on, to dynamically and adaptively choose the best QoS routing path in large-scale urban scenarios.

1.3 Research objectives and contributions

To support a wide range of applications, routing protocols of VANETs must be able to efficiently transmit packets to related destinations. In order to cope with the challenges described in section 1.2, we propose in this thesis intersection-based QoS routing protocols suitable for large-scale urban scenarios. One objective of these routing protocols is to search the best QoS routing path which satisfies with different applications requirements based on real-time QoS of road segments expressed in terms of namely connectivity probability, delay and packet delivery ratio. Besides, these routing protocols are adaptive and scalable, and can effectively decrease redundant overhead to cope with network congestion and limited bandwidth in VANETs. In order to realize our objectives, the main research contributions are conducted as follows.

(1) Formulate corresponding QoS-based system models. Our routing protocols aim at finding the best route that maximizes QoS evaluated in terms of three metrics including connectivity probability, packet delivery ratio and delay, while satisfying different QoS constraints. In order to achieve this purpose, we set up useful system models, which regard various routing issues as respective optimization problems.

(2) Propose an ACO-based optimization algorithm on which the exploration function of routing protocols rely. Because of special characteristics of ACO algorithm [21], e.g., scalability, adaptation, fault tolerance, etc., we propound an ACO-based algorithm to solve related routing issues. This method makes different network exploration processes

and communication pairs closely cooperate with each other to search as many as available candidate routing paths and update the latest routing information along the routes. Such behaviors are beneficial to adaptively choose the best routing path based on the current network conditions.

(3) An opportunistic method is proposed to explore the network and search for the best routing paths based on both local and global QoS. In order to make use of real-time routing information efficiently and increase the exploring randomness of our routing protocols, we adopt local road segment QoS which is advantageous to explore new routing paths. In addition, global route QoS is used to attract network exploration to be inclined to the selection of the established best route, and to prevent our routing protocol from making inappropriate routing decisions on the upcoming road segments (for example, choose some road segments with network holes/congestion). Obviously, this method can keep the balance between the new routing paths exploration and the prior route exploitation, and compared to the blind flooding mechanism (CAR [18] and AODV [22]), our method can accelerate the convergence of the best route, reduce routing exploration time and decrease network overhead.

(4) Propose analytical models to estimate real-time local road segment QoS for 1-lane and 2-lane roads scenarios. Local QoS performance of a road segment play a key role in our routing protocols. By considering related traffic information, such as vehicle density, vehicle distribution, communication range, channel transmission rate, road length and so on, mathematical QoS models are set up to obtain road segment's connectivity probability, delay and packet delivery ratio, respectively. We validate these models through a series of simulations, and compared to other costly methods, for example, the periodic packets to get the real-time routing information (SADV [12]), on-the-fly collection process to achieve the instant routing information (CAR [18]) and direct utilization of historical routing data (VADD [23]), our models can easily evaluate more accurate local road segment QoS, decrease operation time, decline energy consumption and alleviate network congestion.

(5) A Terminal Intersection (TI) concept is presented. Based on two factors: a source/destination vehicle's moving direction and the corresponding distance separating it from its neighboring intersections, we propose a TI concept, so that available backbone intersection-based routes are explored between two TIs instead of from the source to its destination. As a result, TI concept makes a group of communication pairs with the same TID (Terminal Intersection of the Destination vehicle) and QoS requirements directly implement data packets forwarding sessions by sharing the already explored paths, which can decrease routing exploration time and signal overhead. In addition, intersection-based

routes are more stable and scalable compared with complete node-based routing protocol in large-scale urban environments.

(6) Data packet forwarding schemes are improved. Firstly, data packets are forwarded by dynamically choosing the next best intersection using the updated global QoS, which helps cope with varying network topology. Then, in order to decrease the number of Hello packets exchanging geographical information among neighboring nodes and alleviate network congestion especially in high traffic load scenarios, we propose a useful method to relay data packet between two intersections based on the both RTS/CTS mechanism and receiver-side relay election approach.

1.4 Thesis outline

The outline of this thesis is organized as follows:

Chapter 1 firstly introduces the background of VANETs, and then illustrates the motivations, problem statements, research objectives and main contributions of this thesis.

Chapter 2 presents the related works for this research. In this chapter, we introduce the applications, characteristics and technical challenges of VANETs, followed by the presentations of some vehicular networking projects undertaken by various groups and organizations in USA, Japan and European Union. Then we survey the related routing protocols and packet forwarding algorithms.

Chapter 3 describes the original version of our designed routing protocol called AQRV (Adaptive QoS-based Routing for VANETs using ACO). This routing protocol is to set up the best QoS route with a delay constraint from a source vehicle to its destination in terms of three QoS metrics, namely, connectivity probability, packet delivery ratio and delay. In order to achieve above objectives, we firstly design the system model and derive a function expression to regard the routing issue as an optimization problem. Then a new mechanism is proposed, which makes use of periodic packets forwarding, to estimate real-time QoS of a road segment. In addition, based on the proposed ACO-based algorithm, the reactive and proactive components in AQRV are used to establish and maintain the best route by means of global QoS, respectively. When the best route is obtained, the source vehicle implements data packets forwarding sessions, which are carried out by dynamic intersection by intersection selections. In order to reduce the effects of individual vehicle movement on the routing paths, a simple greedy carry-and-forward mechanism is adopted to relay packets between two adjacent intersections. Simulation results show that the performances of AQRV are better than reference routing protocols.

Chapter 4 illustrates the improved routing protocol AQRV-1 suitable for 1-lane road-layout scenarios. In order to decrease network overhead and reduce power consumption, we firstly propose three mathematical models to estimate real-time road segment QoS making use of traffic information such as vehicle distribution, vehicle density, road segment length, etc. Besides, a Terminal Intersection (TI) concept is proposed to update latest routing information and make different communication pairs to share the explored best route so as to decrease overhead and transmission delay. Moreover, we take advantage of reactive ants to explore and establish the best route based on both global and local QoS, which are able to maintain the balance between the new routing paths exploration and the best route exploitation better than only global QoS used in AQRV. Furthermore, a new routing maintenance scheme is proposed instead of the proactive mechanism used in AQRV to decrease overhead and alleviate network congestion especially in high traffic load scenarios. Simulation results validate our derived road segment QoS models in different scenarios, indicate the effectiveness of AQRV-1 in terms of delay, packet delivery ratio and overhead, and analyze the influences of related designed factors.

Chapter 5 proposes the further enhanced routing protocol AQRV-2 which is to establish the best route with different QoS thresholds (delay, packet delivery raito and connectivity probability) to meet various applications requirements, and this routing protocol is appropriate in 2-lane road scenarios. We firstly set up a new system model to constitute the best route and meet above QoS requirements while relaying on the same ACO-based concept introduced in AQRV-1. Then, we propose mathematical QoS models used in 2-lane road scenarios to obtain real-time road segment QoS consisting of connectivity probability, packet delivery ratio and delay. In addition, a new packet forwarding algorithm is proposed to select next relaying hop based on a receiver-side relay election concept, which is beneficial to decrease network overhead. Finally, we implement a series of simulations to prove the derived QoS models, evaluate and analyze the performances of AQRV-2 and related reference routing protocols.

Chapter 6 summarizes the thesis and provides potential directions for the future research.

Chapter 2

Background and related works

In this chapter, we introduce the basic characteristics and applications of VANETs, followed by an overview of their technical issues and associated projects. In addition, a number of appropriate routing protocols and packet forwarding algorithms for VANETs are described.

2.1 Characteristics and applications of VANETs

The advances in mobile communications and the current trends in ad hoc networks allow different deployment architectures for vehicular networks in highways, urban and rural environments to support many applications with different QoS requirements. The goal of a VANET architecture (as shown in Fig. 2.1) is to allow the communication among vehicles and between vehicles and fixed roadside equipments. The communication in VANETs consists of three possibilities: (1) Vehicle-to-Vehicle (V2V) communication: making use of the OBUs (On Board Units) installed on the vehicles, the direct vehicular communication can be established without relaying on a fixed infrastructure; (2) Vehicle-to-Infrastructure (V2I) communication: allows a vehicle to communicate with the roadside infrastructure through equipped RSUs (Road Side Units), and this communication is mainly used for information and data gathering applications; (3) Hybrid communication: combines both Vehicle-to-Vehicle (V2V) and Vehicle-to-Infrastructure (V2I), and in this scenario, a vehicle can communicate with the roadside infrastructure either in a single hop or multi-hop fashion, so it enables long distance connection to the Internet or to vehicles that are far away with each other.

As a specific class of MANETs, VANETs inherit several characteristics of them, e.g., both of them are self-organizing networks and composed of mobile nodes. However, VANETs still are in possession of many particular features as follows.

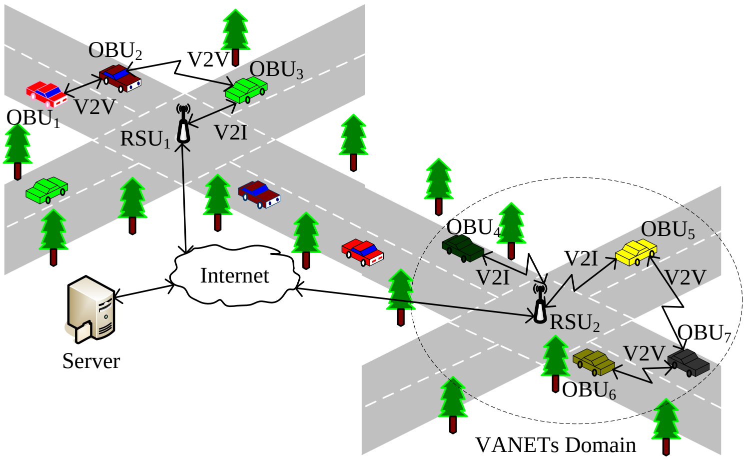

FIGURE 2.1: Basic architecture of VANETs.

(1) Sufficient power. Power scarcity is less serious in VANETs compared with MANETs, as communication devices installed in vehicles are supported by stronger batteries, which are in possession of extensive storage and rechargeable property.

(2) Fruitful capabilities. There is relative big space in vehicles, so various devices owning significant computing, communication and sensing capacities can be installed, which make vehicles capable of powerful functions and high computational abilities.

(3) Predictable mobility. Unlike MANETs in which mobile nodes move randomly, the movements of vehicles in VANETs are controlled by street topologies, traffic light and regulations, and the future position of a vehicle can be predicted based on roadway information (such as street digital map and destination location).

(4) Large scale application scenarios. VANETs are always laid out in highway/urban environments which constitute large networks and include a high number of mobile nodes, while MANETs are usually studied in limited-size environments.

(5) Rapid network topologies changes. Vehicles in VANETs are moving with high and different speed, and they are also changing their directions constantly, so network topologies are very dynamic and communication links are not stable, which may lead to network partitions.

The above typical characteristics of VANETs promote the development of attractive and various applications, which can be categorized into three main different groups as follows: road safety applications, traffic efficiency and management applications, and infotainment applications.

First of all, road safety applications [24–27] primarily provide drivers with assistance to avoid vehicle collisions and decrease crash death ratios. Therefore, these applications are sensitive to the delay and related traffic information should be transfered as soon as

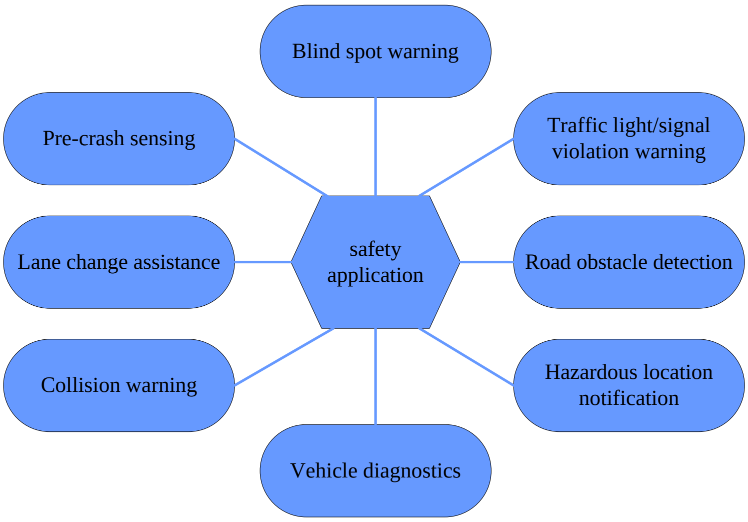

FIGURE 2.2: Typical road safety applications in VANETs.

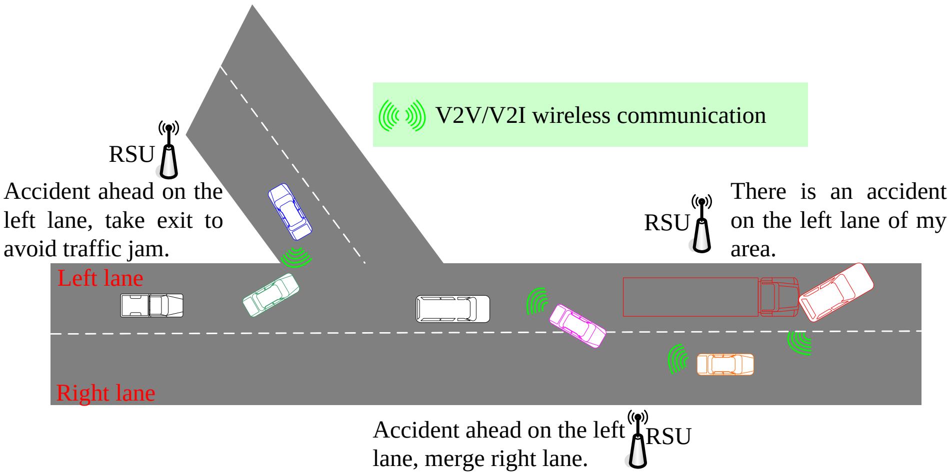

FIGURE 2.3: A concrete example of road safety applications in VANETs.

possible. Another requirement is the reliability, all vehicles close to the hazard should be alerted. These applications include lane change assistance, collision waring and so on, as shown in Fig. 2.2. A concrete example of road safety applications is presented in Fig. 2.3. When there is a traffic accident on the left lane, safety messages including this accident information are broadcasted to the posterior vehicles by V2V/V2I wireless communications to make them change to the right lane or directly leave the left lane at the exit, so this scheme can avoid serious traffic congestion and further traffic accident.

In addition, the applications of traffic efficiency and management focus on improving the vehicle traffic flow, supplying faster routes, giving adaptive traffic lights and providing real-time local traffic information. In this category, most of the applications require a high availability, because the drivers have to use the provided information to make decisions during the trip. These applications mainly consist of speed management and cooperative navigation systems. Speed management system [28, 29] aims to assist the

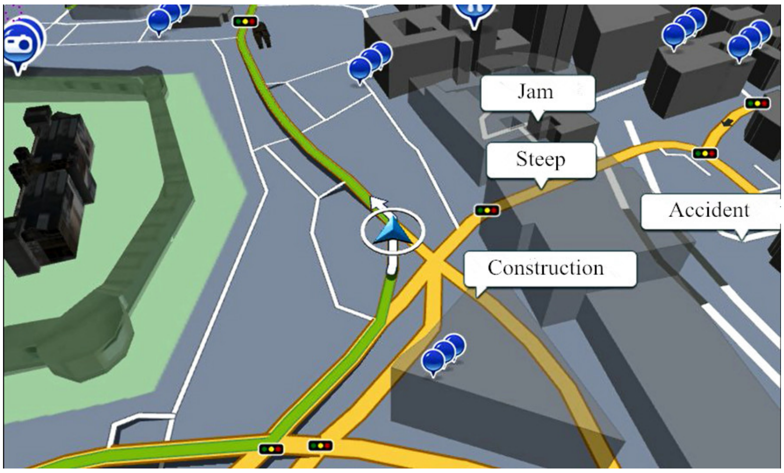

FIGURE 2.4: Navigation application in VANETs.

driver to manage the speed of a vehicle for smooth driving and to avoid unnecessary stopping. Besides, this system provides regulatory/contextual speed limit notification and green light best speed advisory to related drivers. Cooperative navigation system [30–32] is used to increase the traffic efficiency by managing the navigation of vehicles through V2V and V2I communications. Fig. 2.4 gives an example of cooperative navigation application in VANETs. Real-time traffic information and road situations can be collected by moving vehicles, such as traffic jam, road accidents, road segments being under construction and steep roads (implying that these roads require more energy consumption), etc. Then above information need to be transmitted in real-time to related vehicles through VANETs to be processed by the navigation system to choose the optimal moving path.

Finally, infotainment applications [33–36] are referred to as non-safety fields which are beneficial to improve drivers and passengers comfort levels and make trips more pleasant. Normally, the typical requirements of these applications are reliability, availability and connectivity, so as to provide the information in the right moment that the drivers need. Main infotainment applications are presented in Fig. 2.5 and these applications can supply drivers or passengers with weather forecast, location of the nearest restaurant, on-line games and so on. Fig. 2.6 illustrates the applications of Carplay system [37] used in VANETs. It's a system that integrates the iPhone apps with the vehicle's digital systems, allows the driver to use all the iPhone's functionality (such as playing the music, finding the favorable shops, taking phone calls, reading text messages) without actually touching it, which make the driver control the devices more easily and conveniently.

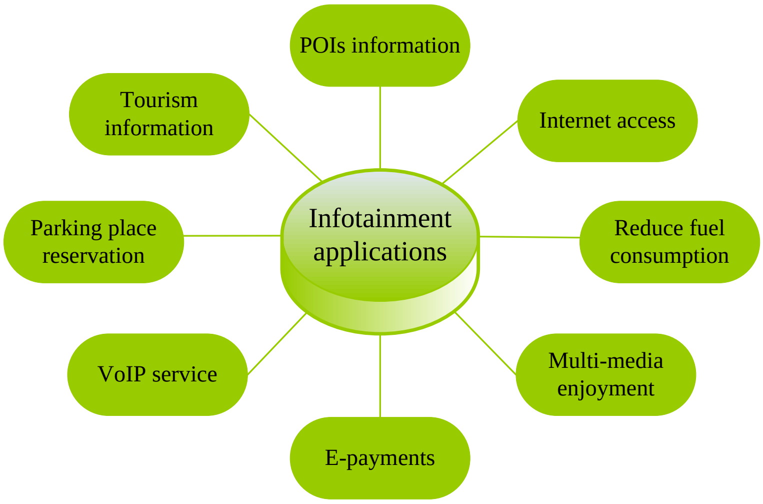

Figure 2.5: Main infotainment applications in VANETs.

2.2 Technical issues in VANETs

According to above descriptions in section 2.1, VANETs are expected to be more and more used in our daily lives and helpful to the promotion of ITS and smart cities. However, many factors which have a critical impact on VANET objectives have to be taken into consideration, so it is vital to specify the key issues that still need to be solved. The key problems from the technical perspectives are given as follows.

(1) Signal fading. Obstacles located between two communication vehicles are one of the challenges that can prevent the signal from reaching its destination, increasing the fading in the wireless channel and reducing the transmission efficiency. These obstacles may be other vehicles or buildings distributed along roads especially in urban scenarios [38].

(2) Bandwidth limitations. VANETs are lack of a central coordinator to regulate V2V/V2I communications, bandwidth management and contention operation restriction. In addition, the range of bandwidth frequency for VANET applications is limited and only 75 MHz are allocated in the DSRC (Dedicated Short Range Communications), so channel congestion can occur easily especially in high density environments. Obviously, it is necessary to efficiently optimize bandwidth utilization [39], which has an important impact on QoS based routing. For example, if the wireless channel is busy, a vehicle requiring packet forwarding has to wait for some time for the idle statement of this channel, so that the transmission delay of packet increases particularly in high traffic-load scenarios.

(3) Connectivity. Due to the high vehicle mobility and rapid changes of topology, network fragmentations take place frequently in VANETs [40], so it is better to elongate the time duration of link communication as long as possible. This task can be accomplished by increasing transmission power, but at the expense of serious interferences and throughput

FIGURE 2.6: Entertainment applications of Carplay.

degradation. Therefore, connectivity is considered to be an important issue in VANETs. Although many studies in MANETs [41, 42] have focused on solving this problem, it still occupies a wide portion of the efforts gathered towards the development of VANETs.

(4) Small effective diameter. Because of the small effective network diameter of VANETs, the QoS of the link between two nodes is degraded and the maintenance of complete global network topology is impracticable for a node. The restricted effective diameter results in problems that existing routing algorithms available in MANETs can not be directly used in VANETs [39].

(5) Security and privacy. It is very important to guarantee the security and privacy in VANETs. In the case of security challenges, for example, selfish vehicles may attempt to clear up the way ahead or mess up the way behind with false traffic information, which can result in serious accidents and even loss of lives. The other issue is to protect the vehicles' privacy. It is very easy to collect vehicle information about the speed, status, trajectories and so on because of sharing and open properties in VANETs, and by mining this vehicle information, malicious observers can make inferences about a driver's personality, living habits and social relationships, which can be traded in underground markets and may bring threats to this driver.

(6) Routing protocol. Because of complex vehicle movements and highly varying topology changes, designing an efficient routing protocol that can deliver a packet successfully within lowest delay is considered to be a critical challenge in VANETs. In this thesis, we mainly focus on the problems related to routing protocols.

2.3 Vehicular networking projects

Motivated by the development of new valued-added applications, several consortia (e.g., automotive industries, highway control authorities, toll service providers and safety organizations) have engaged in a large number of VANET projects. These collaborations have come to actual implementations, which are an essential and necessary part of the verification of VANET systems. We present in the following some typical projects for VANETs carried out in USA, European Union and Japan.

2.3.1 USA

(1) Vehicle Safety Communications (VSC and VSC-A)
The VSC consortium [43] is to support the development of traffic safety applications, especially in the fields of cooperative forwarding collision warning, curve speed warning, stop movement assistant and so on. In order to deepen the research of VSC, a new project called VSC-A [44] was initiated, and its objectives are as follows: 1) assess how previously identified critical safety scenarios can be improved by means of DSRC technology along with positioning systems, 2) determine the minimum system requirements and related performance parameters for vehicle safety applications operating in conjunction with the DSRC system, and 3) implement communication models deployment for vehicle safety systems.

(2) Vehicle Infrastructure Integration (VII)
The VII Consortium [45] supplies coordination to key automobile manufacturers (such as Ford, General Motors, Daimler-Chrysler, etc.), state transportation departments and professional associations. The test environment of VII covers 50 square kilometers near Detroit, USA, and it is used to test a variety of prototype VII applications, which are composed of: 1) warning drivers of unsafe conditions and imminent collisions, 2) supplying real-time information to system operators concerning congestion, weather conditions, and other potentially hazardous incidents, and 3) providing operators with real-time information on corridor capacity.

(3) California Partners for Advanced Transit and Highways (PATH)
The project of PATH [46] is implemented by University of California, in cooperation with several state and federal administrations. The PATH project mainly focuses on policy and behavior research, transportation safety, traffic operation research (e.g., traffic managements and traveler information systems), and technologies to improve transmission solutions for dependent drivers.

2.3.2 European Union

(1) Cooperative Perception and Communication in Vehicular Technologies (CooPerCom)
One objective of the CooPerCom project [47] is to determine how we can improve the reliability and robustness of the vehicular embedded systems and sensors which are becoming more ubiquitous, numerous and complex over time. As the number of sensors and systems increases, the challenges of insuring sufficient reliability and safety are becoming overwhelming. In addition, vehicular environment is highly dynamic and thus requires a high level of connectivity, which in turn requires reliability and robustness as well. The other objective of this project is to explore and develop intelligent signal and information processing tools so as to make use of multiple vehicles presences and inter-vehicles communication capabilities to collect sources information, validate individual data pieces, assess the level of uncertainty and exploit potential redundancies, which are beneficial to mitigate risk of unexpected failures and optimize reliability as well as robustness.

(2) Cooperative Vehicles and Infrastructure Systems (CVIS)
CVIS [48] is in charge of traffic control systems and implements a variety of driver routing systems based on hazardous conditions. The main objectives of this trial are to develop standards for V2V and V2I communications, provide greater precision in vehicle location and supply the generation of more dynamic and accurate mapping using recent location referencing methods. In addition, the trials address systems for cooperative traffic and network monitoring in both vehicle and roadside infrastructure along with the ability to detect potentially dangerous incidents. Moreover, it deploys a "floating car data" application by updating the service center with individual vehicle's operational parameters.

(3) Privacy Enabled Capability in Cooperative Systems and Safety Applications (PRECIOSA)
PRECIOSA [49] is implemented to demonstrate cooperative systems which comply with future privacy regulations and protect related location data. The objectives of this project are as follows: 1) define an approach to evaluate cooperative systems in terms of communication and data storage privacy, 2) design privacy aware architectures for cooperative systems which involve suitable trust models as well as ontologies, 3) propose and validate guidelines for privacy aware cooperative systems and 4) investigate specific privacy challenges.

(4) E-safety Vehicle Intrusion Protected Applications (EVITA)
EVITA [50] is proposed to address safe threats by preventing un-authorised manipulation of on-board systems, so as to successfully prevent the intrusion into the in-vehicular

systems and the transmission of corrupted data to the outside. Actually, EVITA complements SEVECOM [51] and NoW [52] which focus on communication protection. The main contributions of EVITA are given as follows: 1) the overall security requirements are defined through identifying the necessary industrial use cases and compiling substantial scenarios of possible threats, 2) a secure trust model is proposed, and 3) a secure on-board architecture and protocol are specified.

2.3.3 Japan

(1) Advanced Safety Vehicle Program (ASV)
ASV [53, 54] is composed of a series of ongoing development projects (ASV-1, ASV-2, ASV-3 and ASV-4) covering various trial phases and supported by Japanese Ministry of Transport, automobile manufacturers (Honda, Mitsubishi, Suzuki and Toyota in particular) as well as academic and research organizations. The trials focus on two aspects including active and passive safety. In the case of active safety, some related systems (such as systems for drowsiness warning, vision enhancement, navigation, automatic collision avoidance and lane departure) are designed and tested to assist in the prevention of a crash. In the case of passive safety, several systems for impact absorption, occupant protection, pedestrian protection and door lock sensing are designed to protect occupants during a crash.

(2) Public Private Cooperations program (ITS-Safety 2010)
ITS-Safety 2010 [55] is a project that performs on-road verification tests to present current ITS technologies and verify the effectiveness of ITS services installed along public roads. As the result of ITS-Safety 2010, two V2I cooperative systems have been actualized in Japan from 2011: 1) ITS spot on highway service to provide wide area traffic information, hazard warning, road condition ahead, etc., and 2) DSSS (Driving Safety Support Systems) on ordinary roads to satisfy with stop sign recognition enhancement, crossing collision and rear end collision prevention support.

(3) Electronic Toll Collection (ETC)
ETC [56, 57] is a V2I collaboration system that offers driving support services enabled by high-throughput bidirectional communication through ITS spots installed alongside the highways. This system is able to produce the reduction of traffic volume in specific locations, the decrease of time periods prevention of accidents and the mitigation of the deterioration of roadway structures. As a result, limited resource of road networks can be used more efficient and intelligent in longer period of time. In addition, ETC provides a wide variety of services. 1) Safe driving support: the system presents visual and audible alerts when there is a falling object found or a hazardous point of lane

merging ahead as well as invisible traffic congestion being occurred around the corner, etc. 2) Congestion avoidance support: vehicle drivers can select the optimum route when entering into the metropolitan area based on traffic information and they can also find out necessary time of each route by using a car navigation device equipped with ETC. 3) Support under disaster: the system provides assistance information when disasters occur, and this information consists of ongoing situation of disasters and their impacts.

According to the above descriptions, vehicular networking standardizations and research activities in USA, Europe and Japan have been investigated and promoted for the development of relevant technologies in VANETs, so as to improve traffic safety, reduce road congestion and advance traffic efficiency. Besides, these projects reveal that different designing objectives for specific applications require diverse QoS guarantees (such as delay, robustness, scalability, etc.), which are still challenging in the field of VANETs.

2.4 Routing protocols in VANETs

A large number of routing protocols have been proposed for VANETs [9, 13, 38, 58, 59] and the main goal of these routing protocols is to provide the best path through multi-hop wireless communications. In this section, we provide most representative literature in vehicular routing area and present briefly the different protocols classified according to their core concepts, namely topology-based, geographic-based, QoS-based and ACO-based (Ant Colony Optimization) protocols.

2.4.1 Topology-based routing protocols

Topology-based routing protocols [13] usually make use of link's information which is stored in the routing table to forward packets from source to destination.

AOMDV (Ad hoc On-demand Multi-path Distance Vector) routing protocol [60] is a multi-path on-demand protocol which is an enhancement of AODV routing protocol [22]. AOMDV takes advantage of same control messages used in AODV but just adds extra fields to reduce the overhead occurring during discovering multiple paths process, in which AOMDV keeps all available paths in the routing table, then the source selects the first established route as the preferred one. Compared with single-path based routing protocols, the performance of AOMDV is better in reducing route discovery retransmission, improving robustness and decreasing transmission delay.

R-AOMDV [61] is an extension of AOMDV routing protocol. In R-AOMDV routing protocol, a source node sends a route discovery packet when it does not own an available path to its destination. The route discovery process of R-AOMDV is similar to AOMDV and it depends on route request and route reply control packets. It is a cross-layer routing protocol and adds two fields to route replay message fields (maximum retransmission count at MAC layer and total hop count at network layer) to compute quality of the whole path. R-AOMDV protocol inherits all good properties of multi path routing protocols, such as reducing rebroadcast route discovery and enhancing robustness. Besides, this protocol presents better performance compared with AOMDV in both rural and city vehicular networks [61, 62], as well as improves the routing operations based on the quality of routes. However, the routing based on IP addresses is not convenient for VANETs because it has to send the packets to nodes' IPs even though they change their locations, and in this situation the source node must search for a new intermediate forwarding node, which may lead to increase the packet delay and packet loss.

ZRP (Zone Routing Protocol) [63] is a hybrid routing protocol, and it can be divided into several zones in terms of many factors, namely transmission power, signal strength, speed, etc. ZRP makes use of reactive and proactive routing schemes for outside and inside zone, respectively. On one hand, it limits the scope of the proactive procedure only to the node's local neighborhood. As we shall see, the local routing information is frequently referred to in the operation of ZRP, minimizing the waste associated with the purely proactive schemes. On the other hand, the search throughout the global network can be performed efficiently by reactively querying selected nodes in the network, as opposed to querying all the network nodes.

TORA (Temporally Ordered Routing Algorithm) [64] is a distributed routing protocol using multi hop routes and it is designed to reduce the communication overhead related to adapting frequent network changes. TORA constructs a directed graph which regards the source node as the tree root. Packets should be forwarded from higher nodes to lower nodes in the tree. Once a node broadcasts a packet to a particular destination, its neighbor needs to broadcast a route reply to check if it has a downward link to the destination, if not, it just drops the packet. TORA ensures multi path loop free routing since the packet always flows downward to the destination and don't flow upward back to the sending node. The advantages of TORA are that it offers a route to every node in the network and reduces the control messages broadcast. However, it causes routing overhead in maintaining routes to all network nodes, especially in highly dynamic networks, such as VANETs.

2.4.2 Geographic-based routing protocols

Geographic-based routing protocols rely on the geographical information in the routing process so the source sends a packet to the destination using its position rather than using its network address [65]. These protocols require each node to be able to retrieve its location and the location of its neighbors through a location service such as the G-PS (Geographic Position System). When the source needs to send a packet, it usually stores the position of the destination in the packet header which will help in forwarding the packet to the destination without route discovery and route maintenance process. Therefore, geographic-based routing protocols are considered to be more stable and suitable for for large scale networks such as VANETs, compared to topology-based routing protocols.

GPSR (Greedy Perimeter Stateless Routing) [14] is a reference geographic-based routing protocol, and it uses two routing strategies to relay data packets towards destination including greedy forwarding and perimeter forwarding. Greedy forwarding algorithm is utilized if the forwarding vehicle finds a neighbor of which the location is the closest to the destination. While the current forwarding vehicle is the closest one to reach its destination, GPSR shifts to perimeter forwarding in which the right hand rule is applied to select the next hop. The major advantage of GPSR lies in determining the geographical information of its neighbors through Hello packets. A forwarding vehicle selects next hop on the basis of local optimal which is geographically closest to the destination. However, the recovery strategy of GPSR is inefficient and time consuming especially in highly dynamic VANET environments. In addition, GPSR is best suited to open environments with even distribution of nodes but it suffers in a presence of obstacles. When applied in city environment, it shows poor performance [15, 16], because direct communication between two nodes is difficult to establish under the presence of obstacles such as buildings and trees.

GSR (Geographic Source Routing) [16] is a source routing protocol specifically designed for city environments to overcome the disadvantages of GPSR. In GSR, the source takes advantage of city digital map to find shortest path towards destination via Dijkstra shortest path algorithm. This shortest path is composed of a sequence of intersections and each packet must follow the computed sequence of intersections to reach its destination. Greedy forwarding is used to forward data packets between two involved intersections. When suffering from local maximum problem, packets are forwarded through carry and forward strategy. The drawback of GSR is that the distance-based shortest path is not the best path since it does not consider vehicular traffic information along the path. In addition, GSR is a source-driven routing protocol and uses fixed intersection selection mechanism, which results in worse performance in highly dynamic networks.

GPCR (Greedy Perimeter Coordinator Routing) [15] is proposed to tackle the planarization problem in GPSR by considering urban streets as a planar graph. Here each road segment is regarded as an edge of the network topology graph, and each junction is defined as a vertex. Based on the distance towards destination, GPCR makes actual routing decisions at intersections to determine which next road segment is the best option for packet forwarding. Therefore, packets should be forwarded to a node on the junction, and this node is known as the coordinator node, and it is elected based on two methods. The first one is to make use of beaconing services so that each node is aware of position information of its neighbors, and a node can be considered a coordinator node when it has two neighbors that are within communication range of each other, but do not list each other as a neighbor. This indicates that the two neighbors are hidden to each other and the coordinator node is able to forward messages between them. The second method is derived by calculating the correlation coefficient that relates a node to its neighbors. A correlation coefficient close to zero indicates that there is no linear coherence between the positions of the neighbors which indicates that the node is located at a junction.

GpsrJ+ (Greedy Perimeter Stateless Routing Junction+) [66] is proposed to further improves the packet delivery ratio based on minimal modification of GPCR. GpsrJ+ utilizes two-hop beaconing to predict the next road segment in which the packet should be forwarded toward a destination. If the current forwarding node has the same direction as a coordinator node, the prediction mechanism bypasses the intersection and forwards the packet to the node ahead of the junction node. However, if the coordinator node has a different direction from the current forwarding node, it selects the coordinator node as a next relay hop. In comparison with GPCR and GPSR, GpsrJ+ increases packet delivery ratio and reduces the number of hops in the perimeter mode of packet forwarding.

A-STAR (Anchor-based street and traffic Aware Routing) [17] is an operable routing protocol in city environments. It removes one of the drawbacks of GSR by taking into account the vehicular traffic on the street. A-STAR makes use of vehicular traffic on the street and then assigns weight to each street according to the number of bus lines that the road possesses. The more bus lines a road owns, the less weight it is assigned and vice versa. A digital map facilitates computation of anchors or junctions by using Dijkstra shortest path algorithm. Packet relaying from source to destination is based on greedy forwarding algorithm. When packets get stuck in a local maximum, a new recovery strategy is introduced. The road segment where the local maximum problem occurs is marked as "out of service" for a short duration and this information is propagated throughout the network so that other data packets can avoid this "out of service" street. A-STAR routing protocol is traffic aware by considering the number of bus lines but it does not take into account vehicular traffic density. Besides, most of network traffic is shifted towards major streets owning many bus lines (which may induce bandwidth congestion) rather than secondary streets, even if these streets provide better connectivity and may supply best path.

LOUVRE (Landmark Overlays for Urban Vehicular Routing Environments) [67] builds an overlay on top of an urban topology. That is, the overlay is composed of the connected roads in the network, and thus a routing path from source to destination can be established based on the overlay. In addition, LOUVRE uses a P2P (Peer-to-Peer) protocol to discover and distribute traffic density information of each road, and each node exchanges density information with its neighbors by beacon service. However, the scalability of the overlay is limited due to the P2P exchange delay in the whole network.

RBVT (Road-Based using Vehicular Traffic) [68] creates road-based paths consisting of successions of road intersections. The authors proposed two routing protocols including a reactive protocol (RBVT-R) and a proactive protocol (RBVT-P). The route discovery scheme in RBVT-R is similar to source driven routing protocols [22]. But the routing information piggybacked in the packet' header is a succession of road intersections instead of nodes. RBVT-P is similar to LOUVRE. Nodes periodically discover and disseminate the road-based network topology to maintain a global view of the network connectivity. The performance of RBVT-R depends on the stability of road segments' connectivity, and the performance of RBVT-P depends on the efficiency of network connectivity information exchange. However, RBVT requires the exchange and maintenance of non-local information, which causes high network overhead. In addition, data packet headers carry a list of junctions that the packets should pass through and it might lead to scalability issues. Furthermore, the direction of vehicles is not taken into consideration in the optimized geographical forwarding.

On the basis of above descriptions, geographic-based routing protocols are very suitable for VANET environments, but there are still some drawbacks we need to overcome: how to make use of real-time rather than historical/statistical, complete rather than local/global traffic information to dynamically choose useful routing paths in large-scale VANET scenarios.

2.4.3 QoS-based routing protocols

VANETs support a number of applications for safety and comfortability, so efficient QoS-based (Quality of service) routing protocols [12, 69–72] are necessary to forward packets within the required QoS constraints in the targeted regions so as to satisfy various applications.

RMRV (Road-based Multipath Routing protocol for urban VANETs) [73] is a road-based QoS-aware multipath routing protocol in urban scenarios. The proposed routing protocol is used to find multiple paths according to the road layout and estimate paths' lifetime so as to select the most stable path. A space-time planar graph approach has been proposed to predict the connectivity of each road segment, and thus a path's future lifetime and life periods can be derived. Nevertheless, the routing paths are explored by flooding mechanism, which causes a large number of overhead and decreases exploration efficiency. Besides, different communication pairs are lack of cooperation to cope with dynamic vehicular environments.

CAR (Connectivity Aware Routing) [18] is a connectivity-aware routing protocol designed specially for inter-vehicle communications in the urban scenarios. When requiring an available routing path to the destination, the source initiates a path discovery process by broadcasting exploring messages, and these messages record the velocity vector of the mobile nodes through which it goes. If the velocity vector direction of the current node is different from that of the previous forwarding node, these two nodes are regarded as an anchor pair and are added to the header of the message. When a broadcast message reaches the destination using the shortest delay, the route this message passing through is regarded as the selected routing path, which is established as a set of intermediate anchor pairs. Obviously, CAR is source-initiated routing and has to keep a complete routing path, which can not cope with the rapid topology changes of VANETs, especially in large-scale urban scenarios. Besides, the broadcasting feature of routing discovery increases redundant overheads and exacerbates network congestions.

VADD (Vehicle-Assisted Data Delivery routing) [23] is a delay sensitive routing protocol. The packet forwarding mechanism of this routing protocol varies with the position of forwarding nodes. In other words, a forwarding vehicle makes a routing decision at the intersection and forwards the packet to the road which has minimum packet delivery delay. Making use of some traffic parameters such as road length, average vehicle velocity and road traffic density, the estimation of delay through certain roads is modeled and expressed by a set of linear system equations ($n \times n$) using Gaussian elimination method, where n is the number of junctions. Once the junction is selected, a forwarding node at the road tries to find the next relay node. On straight-aways, the priority is given to a node which is closest to the next intersection. In cases where there are no direct neighbor nodes within the transmission range of the forwarding node, it carries its packet until it meet an appropriate neighbor. However, VADD has some drawbacks, one of which is its complexity growing with the intersections' number increase in the scoped area and its performance is not good in large-scale networks. In addition, when estimating local road segment delay, VADD neglects the distribution of vehicles which plays a key role in network connectivity and ignores the effects of the 1-hop delay being relevant to traffic load, channel condition, channel transmission rate and so on.

IGRP (Intersection-based Geographical Routing Protocol) [74] is a road-based QoS routing protocol. In IGRP, the routing path is composed of a succession of intersections. The selection of the road intersections is made in a way that maximizes the connectivity probability of the selected path while satisfying QoS constraints in terms of end-to-end delay, hop count, and BER (Bit Error Rate). Geographical forwarding is still used to transfer packets between any two intersections within the path, reducing the path's sensitivity to individual node movements. However, IGRP needs additional traffic statistics service to obtain the required node density and average speed information for QoS metrics estimation. In addition, IGRP is a source-driven routing protocol and the header of each data data packet attaches a complete list of intersections, which is not beneficial to cope with topology changes and routing scalability. Moreover, the mathematical estimations of delay and hop count are not accurate due to the lack of the partly connected road segments' case.

ARP-QD (Adaptive Routing Protocol based on QoS and vehicular Density) [75] is an intersection-based routing protocol to find the best path for end-to-end data delivery, which can satisfy diverse QoS requirements based on hop count, link duration and connectivity so as to cope with dynamic topology as well as intermittent connectivity, and keep the balance between stability and efficiency of the algorithm. To reduce the network overhead, an adaptive neighbor discovery algorithm is proposed to obtain neighbors' information based on local vehicular density. However, connectivity is estimated by broadcasting beacon packets which may cause channel congestion in the case of high traffic load, and this metric is an instant value and it is not accurate in dynamic scenarios. In addition, using only global distance is not enough to reflect the complete QoS of a routing path, and packets may suffer from network partitions/congestions in the upcoming road segments.

MURU (MUlti-hop Routing protocol for Urban VANETs) [11] is a completely distributed routing protocol without the need of any pre-installed infrastructure and it is able to find robust paths in urban VANETs to achieve high end-to-end packet delivery ratio with low overhead. In order to evaluate the stable level of a routing path, a new metric called EDD (Expected Disconnection Degree) is proposed, and it is defined as the probability that a path would be broken in a predefined time period. EDD is calculated according to the predicted speed and movement trajectory of each vehicle and the route with smallest EDD is chosen. In addition, in order to reduce the overhead, MURU is proposed with a backoff mechanism by utilizing the road map geometry to suppress unnecessary control messages. However, MURU is susceptible to local optimums which would significantly decrease the scalability of the routing protocol.

From the observations in QoS-based routing protocols, we can see that it is very important to solve the following problems: 1) by means of appropriately selected QoS, how to efficiently explore networks and search candidate routing paths with the limited number of overhead, and 2) how to estimate real-time road QoS in dynamic environments. These problems will be studied in this thesis.

2.4.4 ACO-based routing protocols

VANETs supply various applications for customers to satisfy with different QoS requirements, as a result, QoS routing is actually multi-objective problem. Besides, we know that vehicular routing problem (VRP) is a NP-hard (Non-deterministic Polynomial) issue [21] and it can not be solved using conventional methods. Therefore, it is essential to develop an efficient heuristic [76] algorithm which is skillful in solving NP-hard problems.

An impressive number of heuristics have been proposed for VRPs, such as SA (Simulated Annealing) [77–79], GA (Genetic Algorithm) [80, 81], TS (Tabu Search) [82, 83] and ACO (Ant Colony Optimization) [84–87]. Among these heuristic algorithms, ACO algorithm is an efficient optimization method and it has been successfully applied as a solution to some classic compounding optimization problems, e.g., traveling salesman [88], job-shop scheduling [89], telecommunication routing [90, 91], etc. Actually, The ACO algorithm is inspired by an analogy with real ant colonies foraging for food [87]. In the searching process of ants for food, they label the passed through routes by leaving an aromatic essence called pheromone. The quantity of pheromone left on a path depends on the length of the path and the quality of the food source, for example, food source which are close to the nest and have large quantities of food are explored more frequently and marked with larger amounts of pheromone, which are used to attract other ants. Overall, this process leads to an efficient procedure for procuring food by ant colonies. Based on above observation, [92] propose an ACO algorithm for solving combinatorial problems in terms of the following correspondences: 1) artificial ants searching the solution space simulate real ants exploring their environment, 2) objective function values are associated with the quality of food sources, and 3) values recorded in an adaptive memory imitate the pheromone trails.

The ACO algorithm is a probabilistic optimization method and presents a number of interesting properties. First of all, it is highly distributed and self-organized. There is no central control mechanism in the ACO algorithm, and behavior rules for optimal targets are followed by the individual ants. Secondly, it is highly robust. This is related to the property of self-organization and ACO system is composed of a number of individually unimportant agents, so that even there are some disabled agents, which have little impact on the whole performance and can not result in catastrophic failures. Thirdly, the process is adaptive. None of the ant behavior is deterministic, so some individual ants keep exploring low-QoS paths as well, and the system can adapt to changes in dynamic environments. Finally, the process is scalable. The number of ants can be adjusted based on network size, and more ants is used to cope with larger network. Besides, the interaction and cooperation among different ant colonies can also improve the scalability.

There have been some proposed ACO-based algorithms for the routing problems in VANETs and MANETs. POSANT [76] is a reactive routing protocol which combines the idea of ACO algorithm with the position information of nodes, and it has a relatively short route establishment time by using a small number of control messages. IACO (Improved Ant Colony Optimization) [87] propose an ant-weight strategy to update the increased pheromone, and makes use of the mutation operator to conduct customer exchanges in a random fashion so as to solve VRPs. The computational results of 14 benchmark problems indicates that the proposed IACO is an effective and efficient method. [93] describes an ACO-based algorithm, which is composed of three main elements: 1) Event manager, which is used to collect new orders, keeps track of the already served orders and maintain the current position of each vehicle. 2) ACO algorithm. The information collected by the event manager is used to establish a sequence of static VRP-like instances, which are solved heuristically by ACO method. 3) Pheromone conservation procedure, which is strictly connected with ACO algorithm and used to transmit information about characteristics of good solutions from a static VRP to the following one. The proposed method has been tested on a set of benchmarks defined starting from a set of widely available problems. By means of ACO-based algorithm, S. Ganguly and S. Das [94] propose novel pheromone deposition, local search and mutation strategies to solve VRPs efficiently and facilitate rapid convergence. A robust multiple ant colony system is proposed in [95] so as to solve VRP with uncertain travel costs. The multiple ant colonies work in parallel to collect various solutions indicating different levels of protection against the uncertainty, which is handled by incorporating linear formulations from the field of robust optimization into the meta-heuristic approach. [96] makes use of ACO to design a multi-objective heuristic algorithm, which is used to find routes considering the best commitment in terms of the shortest path and the lowest probability of disconnection. Simulations are implemented in three different scenarios, namely static routing, static routing with obstacles and dynamic routing. Results are very promising and they are obtained with small computational effort. ANTHOCNET [90] is a hybrid routing algorithm that combines the reactive route establishment with the proactive route maintenance process. When there is a route request, ANTHOCNET first checks the routing table of the source node to see whether there is any routing information about the destination, and if being unavailable, the source node will broadcast forward ants to establish usable routes. Route maintenance process is implemented by proactive ants during the data forwarding session. Nevertheless, each ant in ANTHOCNET stores the list of visited nodes, which can expand the ant's size especially for long routes and hence increases the overhead.

Obviously, based on the aforementioned introductions, the ACO algorithm is an efficient optimization method to solve the routing problem with multi-QoS requirements in dynamic environments. In this thesis, making use of the features and functions of ACO, we will propose a class of adaptive routing protocols to search the best QoS (namely connectivity probability, delay and packet delivery ratio) route for various applications.

2.5 Packet forwarding algorithms in VANETs

An appropriate packet forwarding algorithm plays a key role in designing available routing protocols for VANETs and some related works in this field are given in this section.

AODV [22] makes use of the routing table of each node to select next hop, but the route discovery phase of AODV introduces enormous network overhead, which may become more crucial when the wireless link is unreliable. In [97], a data packet simply choose the next hop according to its packet header in which the complete route list is stored. However, the complete node-based route make this routing protocol suffer from routing overhead and lead to scalability issues.

In order to cope with the problems of scalability and reliability, geographical forwarding is used to transfer data packets. In previous works on geographical forwarding [12, 14, 16, 98], each forwarding node picks the next hop using its list of neighbors and their geographical positions. The next hop is chosen in such a way as to maximize the forwarding progress (e.g., typically, this is the neighbor closest to the destination). This process continues until the packet reaches the destination. Obviously, to successfully choose next hops, it is vital for each node to maintain an accurate neighbor list, otherwise the best next hop could be missed or even worse, e.g., a node which is already out of the transmission range is chosen as the next hop. So as to solve this problem, Greedy+AGF (Greedy perimeter stateless routing with Advanced Greedy Forwarding) [18, 99] mechanism is proposed. In this algorithm, both the source and destination node inform each other about their velocity vectors. Besides, packet processing time and packet traveling time are added into each packet header. When forwarding data packet to the next hop, a node firstly checks whether the destination node is listed in its table of neighboring nodes and the entry is still available based on the packet traveling time and the velocity vectors of both this node and the destination node. If the destination node is in its neighbor table, but the new position prediction indicates that the destination node may be out of its communication range during data packet relaying process, then the node closest to the new position of the destination is chosen as the next hop. If the destination node is not found in the neighbor table, the forwarding node consults the packet traveling time and estimates whether it may potentially reach the position of the destination node within one hop transmission. If yes, data packet is directly forwarded to the destination node. If no answer is received (either from the destination, or the node that has the destination node in its table and is closer to the destination node than the current forwarding node), then the next closest to the destination node is chosen, and the process repeats. However, above two geographic forwarding algorithms sometimes make data packets fall into local maximums and then initiate repair strategy, which does not perform well in city scenarios because they rely on a distributed algorithm to planar the graph [16]. [15] just makes use of a restricted greedy forwarding algorithm to overcome the local maximum problem. In this algorithm, data packet should be forwarded to a node on intersections in greedy manner rather than to a node which is most far from the current forwarding node but within its communication range. In addition, some link-aware routing schemes have been recently reported [100, 101], but the link duration between vehicles in the vicinity is very short due to high mobility. Moreover, GeOpps [10] utilizes a trajectory-based geographic method to choose next hop. In this method, according to the suggested routes to their own destination, neighboring nodes firstly calculate the nearest point that they will pass through to the data packet's destination, and then they make use of a function expression (based on the information of the nearest point and digital map) to estimate the minimum time that this data packet requires to reach its destination. Finally, the neighboring node that can deliver this data packet to its destination with shortest time becomes the next hop. However, these geographic forwarding algorithms require proactive Hello message broadcast, which consumes enormous resources and occupies more bandwidth in VANET environments. So the performance of VANET routing protocols is affected, especially in peek working hours in urban scenarios.

So as to eliminate the effects of Hello message broadcast, the distributed next-hop selection algorithms are proposed in ad hoc and sensor networks [102–104] based on the receiver-based concept. In these relay selection approaches, the sender broadcasts a control packet informing its neighbors about a pending data packet transmission, and then each neighboring node utilizes certain criteria to determine if it can be selected as a next hop candidate, and if so, it calculates a waiting time, which is used to allow the better candidate to answer first. If a neighbor does not overhear a better candidate before its waiting time expires, it informs the sender that it is the best next hop. The current implementations of these approaches use only one criterion to compute the waiting time, namely the distance between potential next hops and the destination, which works well under the unit disk assumption [105] (for example, the wireless channel is ideal and the transmission range is a circle of a fixed radius). However, many studies [106, 107] have proven that real wireless radios do not follow the unit disk assumption especially in VANET scenarios where there are a lot of buildings and other obstacles to impact radio propagation. Therefore, selecting the neighbor that optimizes the forwarding progress alone does not guarantee an best selection of the next hop. In order to solve above challenges, some multiple criteria receiver-based next hop selection approaches [108, 109] have been described. However, these methods do not consider real wireless channel model, neighboring interferences and signal propagation models.

Apparently, the challenges still exist on how to efficiently select the next forwarding hop with less expenses (such as bandwidth and overhead), therefore we will propose an available packet forwarding algorithm in this thesis.

2.6 Summary

The background and related works of VANETs are introduced in this chapter. We firstly presented the characteristics and practical applications of VANETs, then the existing challenges and main problems in VANETs are stated. Besides, we introduce some typical projects implemented in USA, European Union and Japan to trace the progress of vehicular networks research. Afterwards, most relevant VANET routing protocols, which are based on topology, geographic, QoS and ACO, were given. Finally, we investigate several forwarding algorithms for 1-hop selection. Based on above discussions, there are still many challenges in the field of VANET routing, and we will focus on how to enable QoS VANET routing in the following chapters.

Chapter 3

Adaptive QoS-based Routing for VANETs using ACO (AQRV)

3.1 Introduction

VANETs are self-organized wireless networks, in which vehicles involve themselves as servers and/or clients to exchange and share information [58]. In this thesis, we mainly focus on the routing issue. Routing protocols in VANETs have been investigated widely and can be categorized into two types: topology-based routing protocols and geographic-based routing protocols.

Topology-based routing protocols (for example, TORA [64] and AODV [22]) make use of node-to-node link's information to forward the data packets from source to destination. However, these traditional routing protocols with node-centric concept cause frequent broken links, for example, as shown in Fig. 3.1, the routing path from S_1 to D_1 is established as a fixed succession of nodes $S_1 \to N_1 \to D_1$ at time $T = t$, but this route breaks at time $T = t + \Delta t$, because N_1 moves out of the communication range of S_1. As a consequence, many data packets are to be dropped and the overhead may increase significantly because of route repairs or failure notifications, which degrade the performance in terms of delay and packet delivery ratio.

Geographic-based routing protocols utilize the geographic position of neighbor nodes to decide the next hop towards the destination and do not need to maintain a whole routing table, such as GPSR [14]. Compared to topology-based routing, geographic-based routing has been proved more scalable and efficient for the highly dynamic environments [110][111]. However, many challenges in geographic routing are still required to

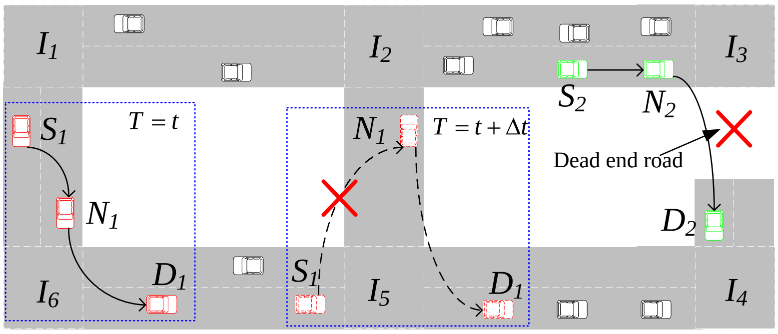

FIGURE 3.1: Illustration of routing problems in existing VANET protocols.

be addressed. GPSR [14] frequently suffers from local optimums and the recovery strategies may not work in urban scenarios due to radio obstacles. In addition, GPSR may forward data packets toward dead end road segments, which causes longer end-to-end delay for packets. For example, as shown in Fig. 3.1, because of shortest route concept, S_2 forwards data packets to N_2, which suffers from a dead end road and can not moves ahead. GSR [16] is a static intersection-based routing that makes use of city digital map to find the shortest path towards destination. Like GPSR, GSR neglects the traffic information along the route and suffers from the network routing holes problem. CAR [18] is a source-initiated routing protocol and has to keep a complete routing path towards the destination, which can not cope with the rapid topology changes of VANETs, especially in large-scale urban scenarios. Besides, the broadcasting feature of routing discovery process increases redundant overheads and exacerbates network congestions. Gytar [112] utilizes local vehicle traffic density and road distance towards the destination to dynamically relay data packets. However, the global vehicle density is not considered, which may make Gytar suffer from extreme network conditions (network partitions and network congestions) in the upcoming data forwarding processes. A-STAR [17] is also an intersection-based routing that employs city bus route to estimate road segment quality, but the busy bus routes are not necessarily equal to the routing paths with good communication characteristics. Besides, VADD [23] utilizes the historical routing information to forward data packets, but such routing information is not good and likely to be out-of-date in dynamic VANET environments.

Ant Colony Optimization (ACO) originates from the food foraging behavior of real ants [21, 76], and it is usually used to solve multi-objective problems with high computational complexity, such as the traveling salesman problem [88]. ACO can also be suitable to the VANET routing problem [71, 72, 113] because of following reasons. (1) Scalability: the ants number in ACO for network exploration is adaptive according to the network size, and the scalability is also promoted using the interactions among different ant colonies. (2) Adaptation: ants can change, die or reproduce by themselves depending on the network changes. (3) Parallelism: ants operations are inherently parallel, which can speed up the convergence process. (4) Fault Tolerance: the loss of a few nodes or links can not result in catastrophic failures, as ACO intrinsically shows an uncentralized control mechanism. Based on above arguments, ACO owns excellent adaptation, robustness and decentralized nature which satisfy with the necessary features of dynamic routing optimization problems.

According to above discussion and analysis, we propose a new routing protocol called Adaptive QoS-based Routing for VANETs using ACO (AQRV). Based on ACO concept, AQRV combines both reactive and proactive components to respectively establish and maintain best routing path. Reactive forward and backward ants are sent between source and destination to explore and set up best route consisting of a list of intersections, respectively. The key feature of the route selection is to rely on a periodically estimated road segment relaying quality which is expressed in terms of three combined QoS parameters, namely: delay, connectivity probability, and packet delivery ratio. AQRV implements a proactive route maintenance using proactive ants to update, expand and improve the routing information. In the data packets forwarding session, AQRV dynamically chooses the best next intersection for data packets, and when forwarded between two adjacent intersections, data packets make use of a simple but efficient greedy carry-and-forward mechanism [111], which can reduce the effects of individual vehicle movement on routing paths. Fig. 3.2 presents the simple concept of AQRV routing protocol. The source vehicle S firstly sends several groups of reactive forward ants to its destination D. When arriving at the intersection I_1, a reactive forward ant FA_m adds I_1's ID to its header and then chooses the next intersection I_5 or I_6 based on the global pheromone stored in I_1 with certain probability (the global pheromone reflects the route's QoS, and the higher global pheromone corresponds to the higher probability), here the global pheromone of the route from I_1 to D going through I_6 is higher than that passing through I_5 because of the congested road segment from I_1 to I_5, so FA_m prefers to selecting I_6 as the next intersection. The above process is repeated until FA_m arrives at D (shown in the green arrow line). Once reaching D, FA_m is converted into the corresponding reactive backward ant BA_m, which is sent back to S following the reverse path. When arriving at an intersection, for example I_5, BA_m updates the global pheromone of the route from I_5 to D ($I_5 \rightarrow I_4 \rightarrow D$) based on the latest estimated local QoS of road segments, and this process is iterated until reaching S (presented in the black arrow line), then a candidate routing path is established (indicated in the green bold line). Making use of global pheromone updated by previous reactive ants, some other candidate routes are set up, such as displayed in the red and blue bold lines. When all reactive backward ants reach S, the routing path owning highest global pheromone is selected as the best route (for example, shown in the red bold line). Obviously, Compared with other RREQ-RREP-based (Route REQuest-Route REPly) routing protocols,

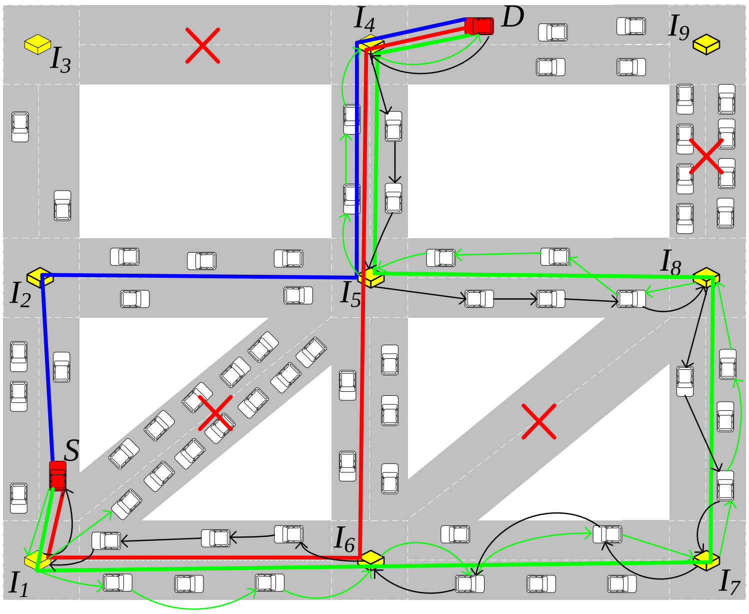

FIGURE 3.2: Simple concept of AQRV over an example.

the routing establishment process of AQRV is unicast rather broadcast, oriented rather than blind, collaborative rather than independent, and it is beneficial to decrease the network overhead and probability of choosing road semgents with bad QoS. When the best routing path is selected, we initiate data packet forward session by dynamically choosing the next intersection based on the maximum updated global pheromone, for example, while arriving at I_6, data packets may be forwarded to I_7 rather than I_5, as the global pheromone of the route from I_6 to D going through I_7 is updated by proactive ants and it is higher currently. This adaptive behavior enables to cope with the network topology changes.

The main contributions in AQRV are as follows:

1) We propose a new mechanism to estimate real-time local road segment QoS (connectivity probability, packet delivery ratio and delay), which is more accurate compared with historical or instant traffic information.

2) We make use of an opportunistic method to relay forward ants based on global QoS. Compared to the blind flooding mechanism (CAR [18] and AODV [22]), our method can accelerate the convergence of the best route and decrease network overhead. In addition, the use of the global QoS can improve route stability and avoid extreme routing conditions in the upcoming route selections.

3) ACO-based algorithm is proposed to search the best QoS route. AQRV makes different forward ants collaborate closely to search candidate available routes and update the latest

routing information, which helps adaptively choose routing paths and cope with rapid topology changes.

4) AQRV is an intersection-based routing, and it is more stable and scalable compared with node-based routing protocols.

The rest of this chapter is organized as follows. We firstly set up the system model and formulize the solved routing problems in Section 3.2. The QoS estimation for a road segment scenario is proposed in Section 3.3. In Section 3.4, we illustrate the proposed routing protocol AQRV, followed by the descriptions of simulation environments and obtained results analysis in Section 3.5. Finally, we conclude this chapter in Section 3.6.

3.2 System model and problem statement

In this chapter, we assume that each vehicle is equipped with GPS facility, digital map and navigation system, which can help vehicles find their own speed and geographical position, as well as the position of intersections. A source vehicle is supposed to obtain the geographic location of its respective destination using the location service [114], and there is a static node on each intersection to store traffic information and relay packets. In addition, our channel model is assumed as Rayleigh Fading Channel [115], which is an appropriate model for city radio environments due to the obstacles' scattering. The propagation model is selected as Shadowing Model [116], and it is employed to characterize the probabilistic multiple path fading during the radio propagation. Moreover, we assume that the urban street map is abstracted as a graph $G(I, E)$, where we represent the set of intersections I and road segments E, and for any two intersections, there is a 2-lane road segment to connect them. Obviously, we can define that a backbone route y from source S to its destination D consists of a succession of intersections $\{I_1, I_2, ..., I_{m-1}, I_m\}$, which are connected by a set of road segments $\{e_1, e_2, ..., e_{n-1}, e_n\}$, where $n = m - 1$. Note that the intersection I_1 is the first intersection connected to the source vehicle S, and the intersection I_m is the last intersection connected to the destination vehicle D.

As the target of AQRV is to establish the best route that maximizes QoS in terms of connectivity probability, packet delivery ratio and delay while satisfying the delay constraint, the best routing issue can be formulated as an optimization problem, and the objective function is given as

$$\max F(y) = \varphi_1 \cdot PC(y) + \varphi_2 \cdot PDR(y) + \varphi_3 \cdot \frac{D_{th} - D(y)}{D_{th}} \cdot \frac{1}{(1 + DV(y))} \tag{3.1}$$

where

$$\begin{cases} PC\left(y\right) = \left(\prod_{k=1}^{n} PC\left(e_k\right)\right) \cdot PC\left(e_{SI_1}\right) \cdot PC\left(e_{I_mD}\right) \\ PDR\left(y\right) = \left(\prod_{k=1}^{n} PDR\left(e_k\right)\right) \cdot PDR\left(e_{SI_1}\right) \cdot PDR\left(e_{I_mD}\right) \\ D\left(y\right) = \sum_{k=1}^{n} D\left(e_k\right) + D\left(e_{SI_1}\right) + D\left(e_{I_mD}\right) \\ DV\left(y\right) = \frac{\sum_{k=1}^{n} DV(e_k) + DV\left(e_{SI_1}\right) + DV(e_{I_mD})}{n+2} \end{cases} \tag{3.2}$$

subject to

$$D\left(y\right) \leq D_{th} \tag{3.3}$$

where $F\left(y\right)$ denotes our objective function and represents the global QoS of the route y from S to D. $PC\left(y\right)$, $PDR\left(y\right)$, $D\left(y\right)$ and $DV\left(y\right)$ stand for the connectivity probability, packet delivery ratio, delay and delay variance of the route y, respectively. $PC\left(e_k\right)$, $PDR\left(e_k\right)$, $D\left(e_k\right)$ and $DV\left(e_k\right)$ represent the same QoS metrics of a road segment e_k, respectively. D_{th} is a delay threshold and φ_1, φ_2 as well as φ_3 are weight values, and $\varphi_1 + \varphi_2 + \varphi_3 = 1$. In addition, $PC\left(e_{SI_1}\right)$, $PDR\left(e_{SI_1}\right)$, $D\left(e_{SI_1}\right)$ and $DV\left(e_{SI_1}\right)$ mean the corresponding same QoS metrics of the road segment from the source vehicle S to the first intersection I_1. While $PC\left(e_{I_mD}\right)$, $PDR\left(e_{I_mD}\right)$, $D\left(e_{I_mD}\right)$ and $DV\left(e_{I_mD}\right)$ denote the corresponding same QoS metrics of the road segment from the last intersection I_m to the destination vehicle D. During the normalization process of the three QoS parameters, in order to remove the dimensional characteristic effect of the delay and avoid the overwhelming influence of $DV\left(y\right)$, we use $\frac{D_{th}-D(y)}{D_{th}} \cdot \frac{1}{(1+DV(y))}$ to make its value less than 1.

3.3 Local QoS estimation of road segment

To resolve the routing problem formulated by the expressions 3.1, 3.2 and 3.3, the estimations of local road segment QoS are very essential and they are a key mechanism of AQRV routing protocols. As we know, local QoS of a road segment is changing with the variation of the numerous traffic parameters such as vehicle density, vehicle distribution, traffic load and so on. In this section, we propose to make use of periodic packets forwarding from two neighboring intersections to evaluate the local QoS expressed in terms of three metrics: delay, packet delivery ratio and connectivity probability. The main motivations behind choice are as follows: 1) these metrics are highly dependent on the communication parameters such as wireless channel fading, communication range, road

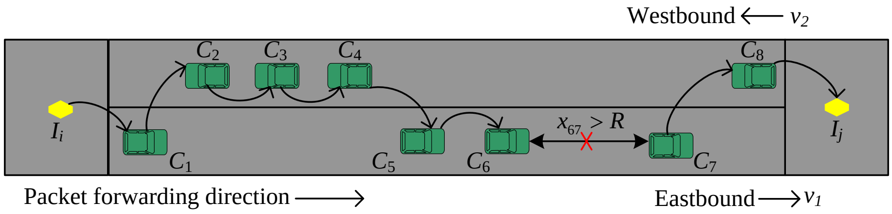

FIGURE 3.3: A 2-lane road segment scenario.

segment length, vehicle density and distribution, etc., which almost reflect the complete traffic information of a road segment, 2) these metrics may antagonise each other in different VANET scenarios. For example, ascending vehicle density is advantageous to link connectivity improvement and delay decrease, but may aggravate end-to-end packet delivery ratio due to more influences from the channel congestion. Based on above analysis, these three metrics are selected to evaluate complete and accurate local road segment QoS. A 2-lane road segment scenario is given in Fig. 3.3, where R denotes the communication range, and these two lanes go in opposite directions referred to Westbound and Eastbound. Here, we assume that each intersection I_i periodically generates packets towards its neighboring intersection I_j. By means of a simple greedy carry-and-forward mechanism, the packets are forwarded hop by hop between two intersections I_i and I_j to estimate related QoS metrics.

3.3.1 Connectivity probability

In a two-lane road segment scenario, the moving vehicles have transient contacts with the ones travelling in opposite direction. These opportunistic contacts can be used to improve connectivity. Link connectivity is maintained as long as the distance X between any two consecutive vehicles in a direction satisfies $X \leq R$ (where R denotes the communication range), or $X > R$ but the vehicles travelling in the opposing direction can bridge this gap (such as the link between C_1 and C_5 in Fig. 3.3). Note that, because of the influences of channel fading model and signal propagation model, a packet can not be always transmitted successfully even if the distance between the transmitter and the receiver is within communication range R. Obviously, the successful packet transmission is totally different from the link connectivity.

The vehicle network on a 2-lane road segment is regarded as being fully connected if there are not any broken links on a directional lane, or the broken links exist but all of them can be fixable by other vehicles moving on the opposite lane. If at least one of the broken links is not fixable, the network is regarded as being disconnected. Besides, in dynamic VANET environments, the traffic information shows stable characteristics during a short period [12], so the QoS of a road segment is able to remain a steady level within certain time period. Based on above remarks, the connectivity probability $pc\left(e_{ij}\right)$ of the road segment e_{ij} between the intersection I_i and intersection I_j is represented as

$$pc\left(e_{ij}\right) = \frac{N_c}{N_{total}} \tag{3.4}$$

where N_c denotes the number of simulation trials in which the network on road segment between I_i and I_j is fully connected, and N_{total} is the number of total simulation trials during the time interval T.

3.3.2 Delay

As an important metric of QoS, the delay can indirectly reflect current transmission channels loads, vehicles density and vehicles distribution over a road segment. Here, we let $TS(e_{ij})_n$ be the time instant of a packet n sent by the intersection I_i, and $TR(e_{ij})_n$ denotes the time instant of this packet received at the intersection I_j. The forwarding delay of this packet through the road segment e_{ij} between I_i and I_j can be simply derived as

$$d(e_{ij})_n = TR(e_{ij})_n - TS(e_{ij})_n \tag{3.5}$$

In order to alleviate the influence of instantaneous delay values, we utilize temporal discussions and the average delay in a given time interval T is expressed as

$$d\left(e_{ij}\right) = \frac{\sum\limits_{n=1}^{N_{rev}} d(e_{ij})_n}{N_{rev}} \tag{3.6}$$

where N_{rev} denotes the number of received packets during T.

In addition, the delay variance on e_{ij} over time interval T is given as

$$dv\left(e_{ij}\right) = \frac{\sum\limits_{n=1}^{N_{rev}} \left(d(e_{ij})_n - d\left(e_{ij}\right)\right)^2}{N_{rev}} \tag{3.7}$$

3.3.3 Packet delivery ratio

Packet delivery ratio reflects the efficiency and reliability of a designed routing protocol, and it is defined as the ratio of the packets successfully received by the destinations to the packets sent by the sources. According to this definition, we can express it as follows

$$pdr\left(e_{ij}\right) = \frac{N_{rev}}{N_{snd}} \tag{3.8}$$

where N_{snd} and N_{rev} denote the number of sent and received packets at the corresponding intersections during the time interval T, respectively. $N_{snd} = PR \cdot T$, where PR represents the periodic packet sending rate.

Note that the instantaneous values of QoS metrics are not accurate and can not cope with the rapid topology changes of dynamic networks, hence we capture the global characteristics of QoS metrics based on instant and historical values, and then make use of the following equations to obtain more stable simulations of a road segment's QoS.

$$\begin{cases} PC\left(e_{ij}\right) \leftarrow (1-\delta) \cdot PC\left(e_{ij}\right) + \delta \cdot pc\left(e_{ij}\right) \\ D\left(e_{ij}\right) \leftarrow (1-\delta) \cdot D\left(e_{ij}\right) + \delta \cdot d\left(e_{ij}\right) \\ DV\left(e_{ij}\right) \leftarrow (1-\delta) \cdot DV\left(e_{ij}\right) + \delta \cdot dv\left(e_{ij}\right) \\ PDR\left(e_{ij}\right) \leftarrow (1-\delta) \cdot PDR\left(e_{ij}\right) + \delta \cdot pdr\left(e_{ij}\right) \end{cases} \tag{3.9}$$

where δ is a weight value $(0 < \delta < 1)$, which regulates the effect of the new measured values. $PC\left(e_{ij}\right)$, $D\left(e_{ij}\right)$, $DV\left(e_{ij}\right)$ and $PDR\left(e_{ij}\right)$ denote the average values of connectivity probability, delay, delay variance and packet delivery ratio of the road segment e_{ij}, respectively, $pc\left(e_{ij}\right)$, $d\left(e_{ij}\right)$, $dv\left(e_{ij}\right)$ and $pdr\left(e_{ij}\right)$ mean the instant values of the corresponding QoS metrics.

It is important to emphasize that the estimation of all the above-mentioned metrics requires time synchronization between adjacent intersections. This time synchronization issue can be easily solved by using the embedded GPS facilities which can provide the same global time reference.

3.4 AQRV routing protocol description

In this section, we give a detailed description of the different components of our proposed AQRV routing protocol. AQRV aims to find the best route from the source to the destination in terms of several QoS metrics, namely connectivity probability, packet delivery ratio and delay, and these metrics are combined to periodically estimate the relaying quality of each road segment. As previously mentioned, AQRV associates both reactive and proactive components to respectively establish and maintain routes for data packets. Initially, when a routing path from the source to the destination is not available, a reactive route setup is executed by this source, and in this process, reactive forward ants are used to explore the wireless network and search candidate routing paths and reactive backward ants are in charge of establishing the best route and updating pheromone at passing through intersections. When the route establishment process is finished, the source vehicle implements data packets forwarding process, and data packets are carried out by dynamic intersection selections based on the updated global pheromone. Then, a simple greedy carry-and-forward mechanism [111] is adopted to relay packets between two adjacent intersections so as to reduce the effects of individual vehicle movement on the routing paths. Finally, the routing maintenance process is implemented by both proactive forward and backward ants, and this procedure lasts for the whole data sessions lifetime.

3.4.1 Reactive candidate routing paths exploration

Before initiating data forwarding sessions, the source vehicle S firstly sends route request packets to its two neighboring intersections to check whether there is available routing information towards the destination vehicle D. If the routing information exists at a neighboring intersection and it is not out of date, this intersection replies a positive message to S, and then S directly implements data packets forwarding. Otherwise, S starts to explore the best backbone routing path between S and D utilizing several reactive forward ants.

At the beginning of the routing exploration process, the source vehicle S randomly sends N_{fant} reactive forward ants to its neighboring intersections using greedy carry-and-forward mechanism to find candidate routing paths towards D. When arriving at the intersection I_i, the reactive forward ant k stores the identifier of I_i and a neighboring chooses the next intersection I_j using certain probability p_{ij} based on the global pheromone deposited on the intersection I_i. This probability helps in avoiding upcoming road segments with extreme traffic conditions (network partitions/network congestion), and p_{ij} is expressed as follows

$$p_{ij} = \begin{cases} \frac{[GP_{ij}]^{\beta}}{\sum\limits_{m \in Nb(i)} [GP_{im}]^{\beta}} & \text{if} j \in Nb(i) \\ 0 & \text{otherwise} \end{cases} \tag{3.10}$$

where p_{ij} denotes the probability with which the forward ant k (located at intersection I_i) chooses the next neighboring intersection I_j. $Nb\,(i)$ depicts the set of neighboring intersections of I_i. β is a weight value and $\beta > 1$. GP_{ij} is the global pheromone that reflects the global QoS of a route from the intersection I_i to D when going through intersection I_j, and it is derived as

$$GP_{ij} = \varphi_1 \cdot PC\,(y_{ij}) + \varphi_2 \cdot PDR\,(y_{ij}) + \varphi_3 \cdot \frac{D_{th} - D\,(y_{ij})}{D_{th}} \cdot \frac{1}{(1 + DV\,(y_{ij}))} \tag{3.11}$$

where $PC(y_{ij})$, $PDR(y_{ij})$, $D(y_{ij})$ and $DV(y_{ij})$ denote the connectivity probability, packet delivery ratio, delay and delay variance for the route y_{ij} from I_i to the destination vehicle D when going through I_j.

Obviously, compared with other blind flooding mechanisms, our network exploration method is beneficial to accelerate routing exploration processes and avoid low quality routing paths.

3.4.2 Reactive best routing path establishment

When a reactive forward ant arrives at D and its end-to-end delay is less than D_{th}, a corresponding reactive backward ant is generated and then returned back (using unicast transmission) to the source vehicle S following the reverse path. The reactive backward ants are aimed to collect the QoS of road segments along the routing path, and then deposit and update pheromone at each going through intersection.

Initially, when arriving at the intersection I_i (coming from the intersection I_j), the reactive backward ant collects the global QoS metrics based on the estimated routing quality of the passing through road segments from the destination D, and this process can be described as follows

$$\begin{cases} PC(y_{ij}) = \prod\limits_{k=1}^{K} PC(e_k) \cdot PC(e_{I_m D}) \\ PDR(y_{ij}) = \prod\limits_{k=1}^{K} PDR(e_k) \cdot PDR(e_{I_m D}) \\ D(y_{ij}) = \sum\limits_{k=1}^{K} D(e_k) + D(e_{I_m D}) \\ DV(y_{ij}) = \frac{\sum\limits_{k=1}^{K} DV(e_k) + D(e_{I_m D})}{K+1} \end{cases} \tag{3.12}$$

where we define the route y_{ij} is composed of a set of road segments $\{e_1, e_2, \cdots, e_{K-1}, e_K, e_{I_m D}\}$.

Then, based on the QoS metrics deduced in equation 3.12, this backward ant updates the global pheromone value GP_{ij} (equation 3.11) for the route y_{ij} follows

$$GP_{ij} \leftarrow (1-\delta) \cdot PGP_{ij} + \delta \cdot GP_{ij} \tag{3.13}$$

where δ is a weight parameter $(0 < \delta < 1)$ regulating the influence of the new measured values on the global pheromone. PGP_{ij} denotes the previously updated global pheromone of the route y_{ij} stored in the intersection I_i. Obviously, this pheromone update process can avoid the exploration stagnancy of a routing path and alleviate the effects of instant value of GP_{ij}.

The above processes are repeated until the backward ant arrives at the first intersection for the source vehicle S. When all backward ants (corresponding to all generated forwarding ants) reach S, the route owing the highest global pheromone ($\max F(y)$) is regarded as the best route.

3.4.3 Pheromone evaporation and data packet forwarding

A process of pheromone evaporation process is necessary to avoid a rapid algorithm convergence towards a suboptimal region. In other words, it is a way to escape from a local optimum. From an implementation standpoint, in each time interval, the pheromone level of all road segment links decreases following a mathematical model, which tries to imitate the evaporation mechanism of the real ants pheromone. In AQRV routing protocol, we make use of a simple formula shown in equation 3.14 to model this evaporation mechanism, which is derived as

$$GP_{ij}(t+T_{eva}) = \begin{cases} \eta \cdot GP_{ij}(t) & \text{If } GP_{ij}(t) > \tau_{min} \\ \tau_{min} & \text{Otherwise} \end{cases} \tag{3.14}$$

where η denotes the pheromone evaporation factor ($0 < \eta < 1$), T_{eva} means the evaporation time interval and τ_{min} stands for the lower threshold of the pheromone. $GP_{ij}(t+T_{eva})$ and $GP_{ij}(t)$ represent the global pheromone for the route from the intersection I_i to the destination D going through the intersection I_j at $t+T_{eva}$ and t time instants, respectively.

Once the best routing path is established, the source vehicle S initiates the data packets forwarding session. We employ a simple greedy carry-and-forward mechanism to relay data packets between two intersections. While arriving at intersection I_i, the data packets are dynamically forwarded toward the next intersection using the maximum global pheromone, which is given as $GP_{ij} = \max\limits_{m=1}^{M} \{GP_{im}\}$, where M denotes the number of I_i's neighboring intersections. The above procedures are repeated until the data packets reach the destination.

3.4.4 Proactive route maintenance

Once the best route is established, the source vehicle S starts its data packets forwarding. However, because of rapid changes of network topology, the alteration of road segment QoS and variability of traffic load on selected road segments, the performance of the established best routing path is almost likely be out of date.

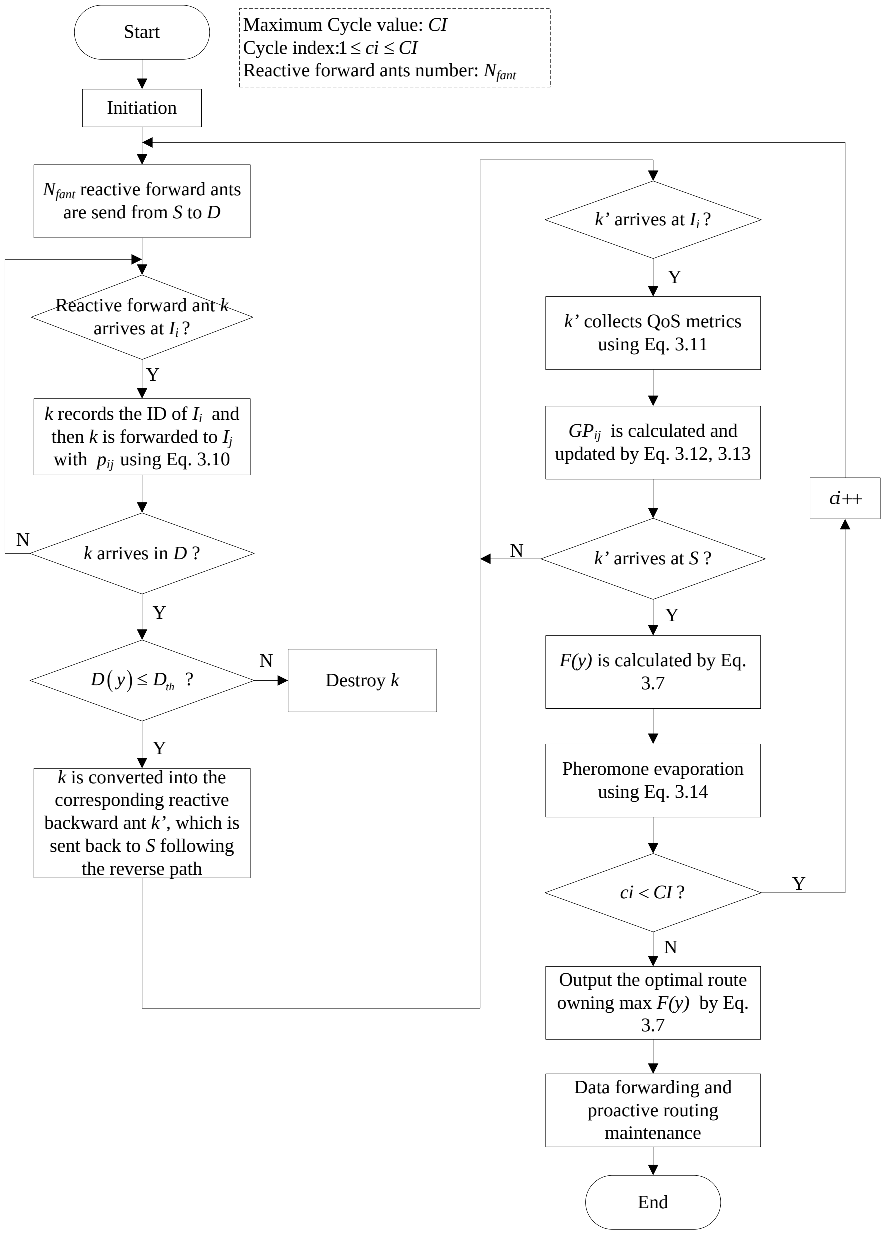

FIGURE 3.4: Flowchart of AQRV routing protocol.

In order to cope with above issue, we propose a proactive route maintenance scheme. Making use of proactive forward ants and backward ants, the source S implements the proactive route maintenance process during the whole data forwarding lifetime to adaptively update, extend and improve the real-time global pheromone. S schedules a periodic transmission of proactive forward ants to the destination D. At each intersection I_i, a proactive forward ant adds the identifier of I_i into its header and makes a new routing decision using the same probability formula given in equation 3.10. However, it is worth to notice here that a smaller value of β parameter is chosen for proactive forward ants compared to the one used for reactive forward ants in the routing setup phase. This

TABLE 3.1: Simulation setup parameters

Parameter	Value
Number of vehicles	$150 \sim 400$
Data packet sending rate DPR	$5 \sim 15$ packets/s
Periodic packet rate PR	1 packets/s
Data packet size	512 Bytes
Reactive forward ants N_{fant}	10
Reactive route exploration factor β	10
Proactive route maintenance factor β	5
Weight values of QoS metrics φ_1, φ_2 and φ_3	0.2, 0.2 and 0.6
Weight value of data process δ	0.3
Weight value of pheromone evaporation η	0.95

decision is helpful in extending the exploration range of paths towards D and uniformly spreading the traffic load over the whole network. When the proactive forward ant reaches D, a proactive backward ant is generated and it has the same behavior as the reactive backward ant for pheromone update on the reverse path. The main steps of AQRV routing protocol are given in the flowchart illustrated in Fig. 3.4.

3.5 Performance analysis and evaluation

3.5.1 Experimental environment

In this section, we investigate the performance evaluation of our routing protocol AQRV. For comparison purposes, we also implemented two classical geographical routing protocols (GSR [16] and CAR [18]) used in urban environment. GSR is a static intersection-based routing protocol and utilizes city digital map to search the shortest path towards destination, and CAR is a source-driven routing protocol and explores the minimum delay route by means of real-time routing information. In the simulation scenario, vehicles are placed in a 1500 m $\times$ 1500 m region, which consists of 15 intersections and 28 road segments. In each road segment, vehicles move with a velocity randomly selected between 15 km/h and 30 km/h. The transmission range of vehicles is set to 250 m. At the MAC layer, an IEEE 802.11p mechanism is adopted with a channel capacity of 3 Mbps. Further simulation parameters are listed in Table 3.1. In our experiments, we generated 50 data flows which send data packets at different constant bit rates. The simulation time duration is fixed to 3000 seconds and each simulated scenario is repeated 30 times with different seeds to guarantee good confidence intervals for the results.

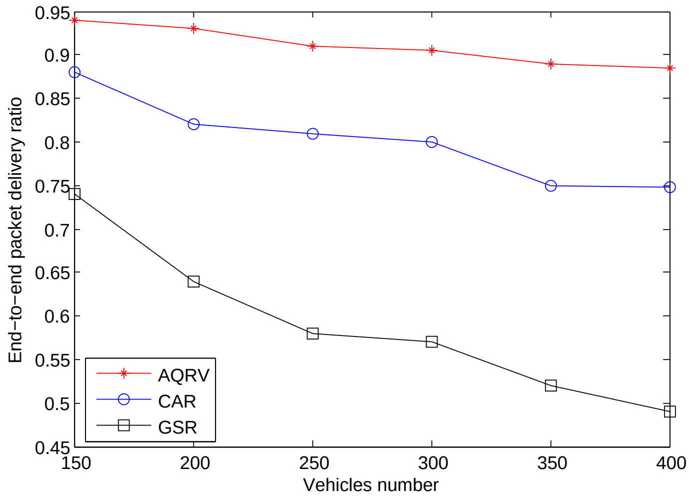

FIGURE 3.5: End-to-end packet delivery ratio (data packet sending rate $DPR = 10$ packet/s).

3.5.2 AQRV routing protocol performance evaluation

(1) End-to-end packet delivery ratio

Fig. 3.5 and Fig. 3.6 present the end-to-end packet delivery ratio as a function of the vehicles number and data packet sending rate, respectively. Fig. 3.5 shows that our routing protocol AQRV outperforms other two reference protocols with 13.78% and 56.63% growth compared with CAR and GSR, respectively. Similarly, in Fig. 3.6, the packet delivery ratio of AQRV indicates 14.07% and 35.90% increase in comparison with CAR and GSR, respectively. There are three main reasons to explain such results. Firstly, when establishing the best routing path process, AQRV protocol dynamically chooses the highest quality paths based on packet delivery ratio metric. Secondly, when forwarding data packets at each intersection, AQRV adopts an adaptive path selection so that the changes affecting the routing information collected at setup phase will be considered. Moreover, AQRV initiates the proactive routing maintenance process during data packets forwarding sessions, so that the latest routing information will be updated to cope with the topology changes and the routing path can be selected dynamically. From Fig. 3.5 and Fig. 3.6, we can also observe that the packet delivery ratio decreases with the rise of the vehicles number and data packet sending rate. The reasons are as follows: 1) when the number of vehicles grows, the network connectivity is better and more data packets are transmitted hop by hop, which implies more interference effects, and 2) higher data packet sending rate increases the traffic load, aggravates network condition and even leads to network congestions, which is not advantageous to the successful data transmission.

(2) End-to-end packet delay

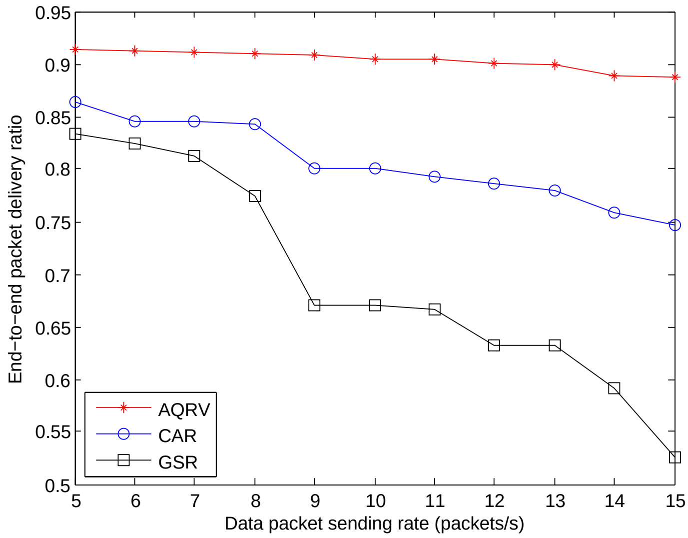

FIGURE 3.6: End-to-end packet delivery ratio (number of vehicles = 300).

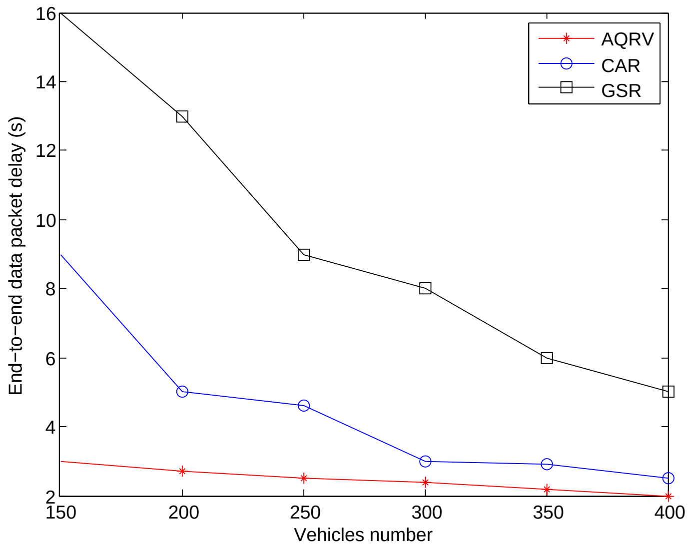

FIGURE 3.7: End-to-end packet delay ($DPR = 10$ packet/s).

Fig. 3.7 and Fig. 3.8 show the end-to-end packet delay while varying the number of vehicles and data packets sending rate, respectively. In Fig. 3.7, we see that the packet delay for all routing protocols reduces with the increase of vehicles number, as the network holes along the routing paths can be repaired with the increment of vehicles, and more and more data packets are forwarded hop by hop rather than carried by moving vehicles. Fig. 3.8 reveals that packet delay is proportional to data packet sending rate, which can increase traffic load and yield to data packets retransmissions because of network congestions. In addition, in both figures, we observe that AQRV outperforms the reference protocols, as AQRV can dynamically make routing decisions at intersections based on the latest global routing QoS, which is beneficial to coping with the rapid topology changes. In the case of GSR, data packets may be forwarded using the same path

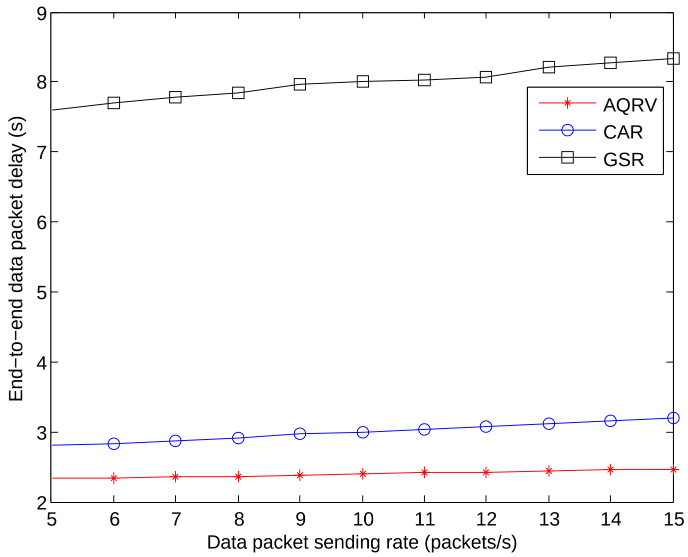

FIGURE 3.8: End-to-end packet delay (number of vehicles = 300).

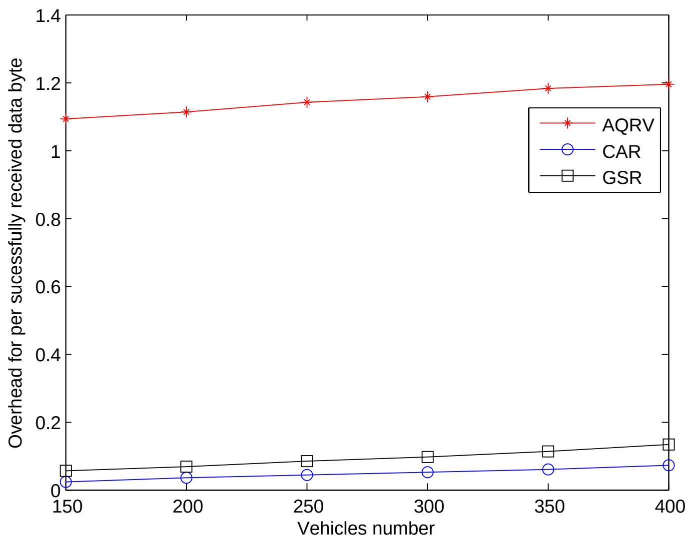

FIGURE 3.9: Overhead ($DPR = 10$ packet/s).

because of the shortest distance rule, which may make data packets forwarding suffer from intense channel congestion or routing holes. In the case of CAR routing protocol, the routing path selection depends only on the number of hops and neighboring nodes along the links, which is not enough to reflect the accurate delay. CAR is also a source routing protocol where anchor intersections are selected at route setup, and it does not provide any backup path, so in dynamic VANET environments, this routing protocol has to implement the routing recovery scheme frequently which results in longer end-to-end delay.

(3) Overhead

In these simulation experiments, we evaluate the amount of overhead generated by AQRV

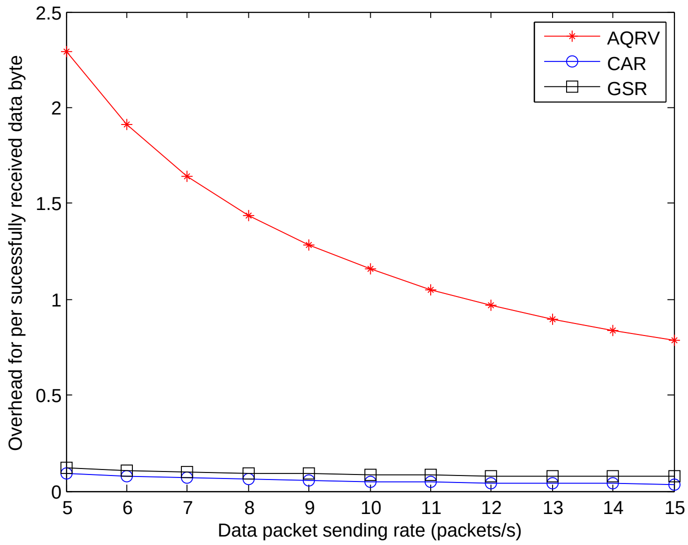

FIGURE 3.10: Overhead (number of vehicles = 300).

routing protocol and then compare it with CAR and GSR. Note that for a fair comparison, we define the overhead as the ratio between total control packets bytes and the cumulative bytes of successfully received data packets. Fig. 3.9 and Fig. 3.10 represents that the overhead of AQRV is higher than both reference routing protocols, as AQRV protocol relies on periodic packets forwarding to derive real-time QoS estimation of road segments. In addition, the proactive routing maintenance scheme of AQRV generates non negligible amount of overhead. From Fig. 3.9, we can observe that the overhead for all routing protocols has slight increase with rise of the number of vehicles which generate more Hello packets to exchange routing information among neighboring nodes. Finally, in Fig. 3.10, we observe that the overhead level of AQRV decreases as more data packets are successfully received with the increment of data packet sending rate.

3.6 Summary

In this chapter, we described a new vehicular routing protocol called AQRV. Our protocol adaptively chooses the best routing path in terms of three QoS metrics, namely connectivity probability, delay and packet delivery ratio, which are estimated by periodic packets forwarding between two neighboring intersections. AQRV makes use of reactive forward ants and backward ants to explore available routing paths and establish best route based on the updated pheromone, respectively. Routing decision for data packets is realized at each intersection to select the next intersection according to the maximum latest pheromone stored in the current intersection. Proactive route maintenance is implemented to continuously update the pheromone values by periodic proactive ants sampling. The simulation results show the preferences of our protocol, and indicate that

AQRV outperforms the reference protocols (GSR and CAR) in terms of packet delivery ratio and delay but at the cost of higher overhead. Therefore, our main objective in the following chapters is to reduce the redundant overhead of our protocol. To do so, we will propose mathematical QoS models for road segments instead of the estimations by periodic packets forwarding. In addition, we will design a new routing maintenance method to replace the proactive routing maintenance scheme adopted by AQRV.

Chapter 4

Adaptive QoS-based Routing for VANETs using ACO in 1-lane scenarios (AQRV-1)

4.1 Introduction

In this chapter, we propose an extended version of AQRV routing protocol and it is named after AQRV-1 suitable for 1-lane road segment scenarios. Though AQRV routing protocol presented in Chapter 3 offers the best dynamic QoS routing path, it still shows some drawbacks which require to be solved: 1) Real-time road segment QoS is obtained by forwarding periodic packets , which generate significant overhead participating in network congestion. 2) AQRV explores the best route between two end-to-end vehicles, but some communication pairs moving on the corresponding same or neighboring road segments (for example, two communication pairs $S \rightarrow D$ and $S_1 \rightarrow D_1$ in Fig. 4.1) may have same backbone routing path. Obviously, the derived best route between two end-to-end vehicles is less efficient than between two end-to-end intersections in terms of the routing exploration time and overhead. Enable such function would make new communication pairs directly use already explored routing paths. 3) In AQRV, the forwarding ants explore the candidate routing paths only in terms of the global pheromone, which is beneficial to the algorithm convergence and the avoidance of the extreme forwarding conditions on the upcoming road segments, but this scheme makes the forward ants be inclined to explore the established best routes. This behavior reduces the randomness of the algorithm and is not advantageous to the new routing paths exploration. 4) The routing maintenance mechanism of AQRV is a proactive process, which may create large overhead and deteriorate the traffic load especially in urban environments.

In order to address the aforementioned challenges, we propose an improved verson of AQRV routing protocol called AQRV-1 suitable for 1-lane urban environments, where the challenges of research (such as vehicles distribution, neighboring interferences and link connection, etc.) are simple and easy to cope with, and then we will further extend AQRV-1 to be available in 2-lane city scenarios in the next chapter. AQRV-1 routing protocol is to find the best route between two Terminal Intersections (TI) while meeting the same QoS objective as AQRV. To achieve the above objective, we firstly establish the system model and then local QoS models (LQM) are defined to derive these three metrics in a 1-lane road scenario. Finally, based on the concept of AQRV, we propose an ACO-based algorithm using both the local and global pheromone to solve the best routing selection problem.

Compared with AQRV, the main contributions of AQRV-1 are as follows:

(1) We propose three mathematical models to estimate real-time local road segment QoS (connectivity probability, packet delivery ratio and delay) by means of vehicle density, vehicle speed, vehicle distribution and road length, etc. Obviously, our models can easily evaluate more accurate local road segment QoS, decrease operation time, reduce energy consumption and alleviate network congestion.

(2) We present a Terminal Intersection (TI) model. AQRV-1 explores the best backbone route between two terminal intersections instead of end-to-end vehicle communication pairs to enable a group of communication pairs with the same TID (Terminal Intersection of the Destination vehicle) and QoS requirements directly implement data packets forwarding sessions by sharing the already explored paths, and such behavior helps in decreasing the routing exploration time and network overhead. In addition, TI concept is beneficial to make different communication pairs closely collaborate to update the latest routing information and cope with rapid topology changes.

(3) We make use of an opportunistic method to relay forward ants using the local and global QoS. This scheme can keep the balance between the new routing paths exploration and the current best route exploitation.

(4) A new reactive routing maintenance mechanism is proposed. This method can decrease redundant overhead and mitigate network congestion caused by the proactive routing maintenance scheme of AQRV routing protocol.

Fig. 4.1 illustrates the simple idea of AQRV-1, where the destination vehicles D, D_1 and D_2 own the same Terminal Intersection of the Destination vehicle (TID = I_4). Before sending data packets to the destination vehicle D, the source vehicle S firstly sends a RREQ message to its terminal intersection (here Terminal Intersection of the Source vehicle TIS = I_1). If TIS does not own available routing information to TID, a negative

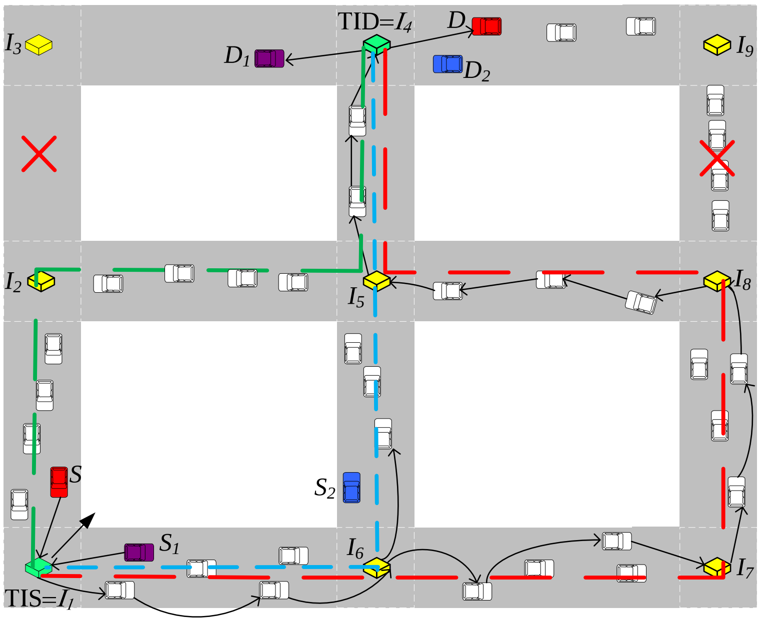

FIGURE 4.1: Backbone paths illustration in AQRV-1.

message is sent back to S and then TIS initiates the best route establishment processes (from TIS to TID). Three candidate routes ($I_1 \rightarrow I_2 \rightarrow I_5 \rightarrow I_4$, $I_1 \rightarrow I_6 \rightarrow I_5 \rightarrow I_4$ and $I_1 \rightarrow I_6 \rightarrow I_7 \rightarrow I_8 \rightarrow I_5 \rightarrow I_4$) are obtained by forward ants based on both global and local road segment pheromone. Note that the QoS routing exploring process avoids the candidate routes including road segments with extreme network situations (network partition ($I_2 \rightarrow I_3$) and/or heavy channel congestion ($I_8 \rightarrow I_9$)). After updating the global pheromone by backward ants, TIS obtains the best backbone routing path ($I_1 \rightarrow I_6 \rightarrow I_7 \rightarrow I_8 \rightarrow I_5 \rightarrow I_4$) and then sends a positive message to inform S the established best route. Finally, S initiates data packets transmission to D (shown in black arrow lines). When arriving at the intersection I_6, data packets are dynamically forwarded to the next intersection (I_7 or I_5) according to the latest global pheromone stored in the routing table of I_6 (in the example of Fig. 4.1, it is still the best next intersection of TIS towards TID). Note that, S_1 can directly forward data packets to D_1 using the explored route by S. Afterwards, the communication pair ($S_2 \rightarrow D_2$) may update the global pheromone from I_6 to TID (I_4) if the local/global QoS is changed. This behavior during the data transmission session indicates the collaboration feature of ACO and it is advantageous to the latest routing information acquisition, and makes other communication pairs ($S \rightarrow D$ and $S_1 \rightarrow D_1$) adaptively choose the best routing path for data packets forwarding.

The rest of this chapter is organized as follows. The system model and problem statement are given in Section 4.2. Then we describe the mathematical models of local QoS for 1-lane road segments in Section 4.3. AQRV-1 routing protocol is detailed in Section 4.4.

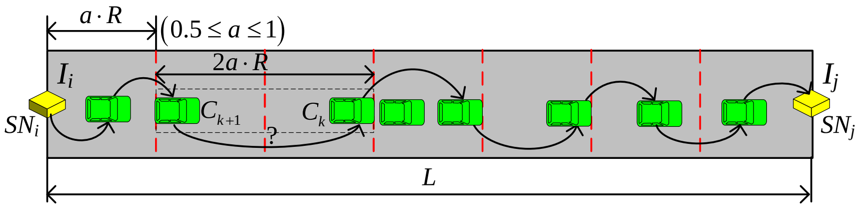

FIGURE 4.2: Vehicle distribution analysis on a 1-lane road segment.

In Section 4.5, we present the simulation environments and analyze the obtained results. Finally, Section 4.6 concludes this chapter.

4.2 System model and problem statement

In this chapter, we make some assumptions as AQRV regarding the availability of GPS facility, digital map, navigation system, location service and static nodes. We also take advantage of the Shadowing Model [116] as the propagation path loss model and assume the wireless channel as a Rayleigh Fading Channel [115]. At the MAC layer, we adopt RTS/CTS (Request To Send/Clear To Send) mechanism, and utilize simple BPSK modulation technique for physical transmission. In addition, It is known that the local QoS of road segments is a critical component of AQRV-1 routing protocol. In order to derive the mathematical models for local QoS, some suppositions are presented as follows: 1) We consider a 1-lane road segment e_{ij} connecting two intersections I_i and I_j with L in length referred to Fig. 4.2, where the vehicles on this road segment are identified as C_k ($k \geq 0$). 2) The number of vehicles on the roadway follows Poisson Distribution. This assumption has been proved valid in [117, 118] by Kolmogorov-Smirnov Test. Therefore, to simplify our 1-lane road segment scenario, we use Poisson Distribution and set the vehicle spacing density to λ. 3) The vehicle velocity is assumed constant and referred to as v, and the length of vehicles is negligible compared to the road segment length. 4) Wireless communication range is set as R. 5) A simple greedy carry-and-forward mechanism is used to relay packets within a road segment, and when packets are carried by a moving vehicle, they do not suffer from packet loss influences.

Likewise AQRV routing protocol, the urban street map is abstracted as a graph $G(I, E)$, where I and E denote the set of intersections and road segments, respectively. Therefore, a backbone route y is defined as a succession of intersections $\{I_1, I_2, ..., I_{m-1}, I_m\}$, which are connected by a set of road segments $\{e_1, e_2, ..., e_{n-1}, e_n\}$, where $n = m - 1$. As the best route established by AQRV-1 owns the same QoS as AQRV, but it is explored between two terminal intersections rather than between an end-to-end communication pair in AQRV, the objective function of AQRV-1 is given as

$$\max F(y) = \varphi_1 \cdot PC(y) + \varphi_2 \cdot PDR(y) + \varphi_3 \cdot \frac{D_{th} - D(y)}{D_{th}} \cdot \frac{1}{(1 + DV(y))} \tag{4.1}$$

where

$$\begin{cases} PC(y) = \prod\limits_{i=1}^{n} PC(e_i) \\ PDR(y) = \prod\limits_{i=1}^{n} PDR(e_i) \\ D(y) = \sum\limits_{i=1}^{n} D(e_i) \\ DV(y) = \sum\limits_{i=1}^{n} \frac{DV(e_i)}{n} \end{cases} \tag{4.2}$$

subject to

$$D(y) \leq D_{th} \tag{4.3}$$

where $F(y)$ represents the global QoS of the route from TIS to TID. $PC(y)$, $PDR(y)$, $D(y)$ and $DV(y)$ stand for the connectivity probability, packet delivery ratio, delay and delay variance of the route y, respectively. $PC(e_i)$, $PDR(e_i)$, $D(e_i)$ and $DV(e_i)$ represent the road segment e_i's connectivity probability, packet delivery ratio, delay and delay variance, respectively. D_{th} is a delay threshold. φ_1, φ_2 and φ_3 are weight values, and $\varphi_1 + \varphi_2 + \varphi_3 = 1$.

4.3 Mathematical models of local QoS for 1-lane road segment

In this section, the mathematical models for three local QoS metrics: connectivity probability, packet delivery ratio and delay are proposed for 1-lane road segment scenarios. These models play an important role in the routing selection and accurate evaluation of QoS for urban environments.

4.3.1 Connectivity probability

In the 1-lane scenario, we define that a link between two consecutive vehicles is supposed to be connected as long as this link length is within the communication range. In this section, we derive the multi-hop link connectivity probability for a given 1-lane road segment. Due to the variability of vehicles number, the vehicle distribution on a road segment is timely varying and the exact connectivity probability is far difficult to be derived. In our model, we divide the road segment into several cells to capture the connectivity characteristics. As shown in Fig. 4.2, we define the cell size as $cs = a \cdot R$, where a is a weight value $(0.5 \leq a \leq 1)$ and R denotes the communication range. In the case of the cell size $cs = 0.5R$, the maximum distance between any two vehicles in two adjacent cells equals R, which definitely guarantees the link connectivity between them. In the case of $cs = R$, the location distribution of vehicles is random and the distance between vehicles separately located in two consecutive cells may vary from 0 to $2R$, so the link (e.g. the link between two vehicles C_k and C_{k+1} as shown in Fig. 4.2) may be not connected. Obviously, the case of $cs = 0.5R$ is a sufficient but not always necessary condition for the connectivity of a link between any two vehicles which are respectively located in two adjacent cells, while $cs = R$ is a necessary but insufficient condition. According to aforementioned interpretations, we set $cs = a \cdot R$ $(0.5 < a < 1)$ to confirm the necessary and sufficient condition for the link connectivity. Let K be a random variable denoting the number of vehicles in an interval $a \cdot R$. Based on our assumptions, K follows Poisson Distribution and its Probability Mass Function (PMF) is given as

$$P\left(K = k\right) = \frac{\left(aR\lambda\right)^k}{k!} e^{-aR\lambda} \tag{4.4}$$

Obviously, in the case of $cs = a \cdot R$, the probability PC_{1-cell} that one cell contains at least one vehicle is expressed as

$$PC_{1-cell} = 1 - P\left(K = 0\right) = 1 - e^{-aR\lambda} \tag{4.5}$$

As shown in Fig. 4.2, the multi-hop link between I_i and I_j is regarded as connected as long as each link distance between any two consecutive vehicles does not exceed R. This implies that there is at least one vehicle in each cell of this road segment, so the link connectivity probability of the road segment between I_i and I_j is derived as

$$PC = \left(PC_{1-cell}\right)^N = \left(1 - e^{-aR\lambda}\right)^N \tag{4.6}$$

where $N = \left\lceil \frac{L}{a \cdot R} \right\rceil$ denotes the number of cells on the road segment between I_i and I_j. Equation (4.6) expresses the connectivity probability as a function of vehicle spacing density, communication range, cell size and road segment length.

4.3.2 Packet delivery ratio

As a key metric to measure the reliability of the multi-hop wireless network, Packet Delivery Ratio (PDR) for a given 1-lane road segment is deduced in this section. The

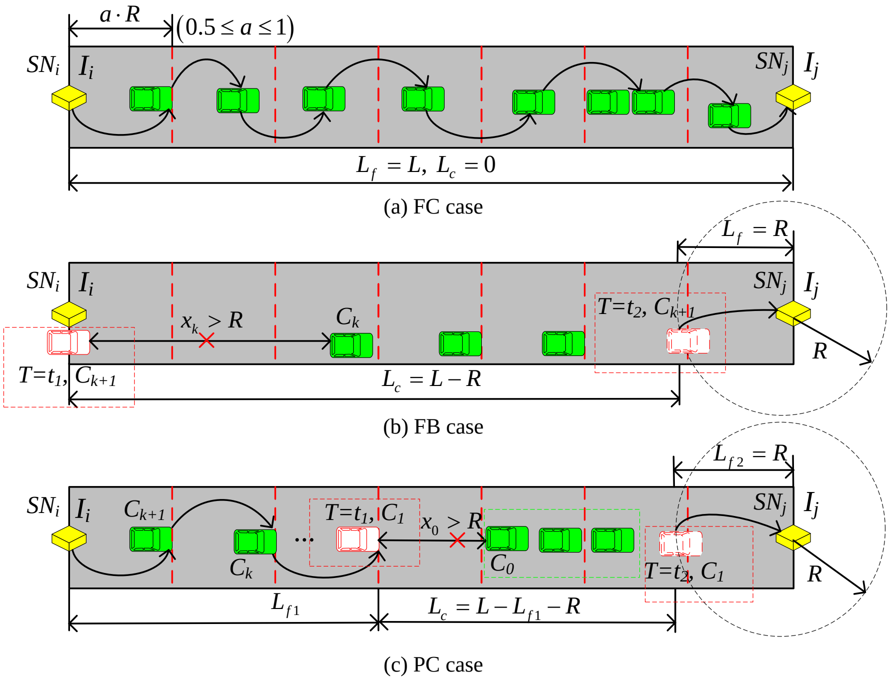

FIGURE 4.3: Three cases analysis for a road segment scenario.

statistical and real time traffic information of vehicles have demonstrated that vehicles tend to move in clusters on the road [119]. Consequently, based on the scale size of vehicles clusters, an analytical PDR model can be deduced by taking into account three different cases illustrated in Fig. 4.3: the Fully Connected road segment case (FC case, where the Communication Cluster Scale $ccs \geq L$), Fully Broken road segment case (FB case, $ccs = 0$) and Partly Connected road segment case (PC case, $0 < ccs < L$). In the FC case, links on the road segment between the intersection I_i and I_j are fully connected and packets are relayed hop by hop. Because the velocities of vehicles on a road segment are supposed to be constant and same, as long as the distance between the latest arrival vehicle C_{k+1} and the second latest arrival vehicle C_k is beyond the communication range R, this road segment scenario can be regards as the FB case and packets are carried by C_{k+1} until arriving the communication range R of the next intersection I_j. In the PC case, the links of the latest arrival vehicles are connected, but the link between the header vehicle of this connected cluster C_1 and its neighboring vehicle in front C_0 is broken, so packets are forwarded from I_i to C_1 via wireless communication, and then C_1 carries these packets until entering I_j's communication range. In addition, we define the forwarding link length L_f as the distance traveled by packets when forwarded via the wireless multi-hop links within the road segment, while the carry link length L_c is the distance crossed by packets when carried by a vehicle at speed v.

(1) 1-hop packet delivery ratio

In order to derive the multi-hop packet delivery ratio model of a road segment, we first need to model the packet delivery ratio of a single hop. In this chapter, as assuming the use of RTS/CTS mechanism in the wireless channel, the interferences introduced by hidden terminals and concurrent transmissions can be reduced. However, there are still some potential interferences from the neighboring nodes located in the segment that is outside the communication ranges of the transmitter and the receiver but inside the interference range of the receiver, as shown in Fig. 4.4. Therefore, we consider the components of the channel fading and potential interferences to deduce our PDR model.

Based on the derivations in [116], the overall Shadowing Model is given as

$$\left[\frac{P_r(x)}{P_r(x_0)}\right]_{dB} = -10\beta_1 \log\left(\frac{x}{x_0}\right) + X_{dB} \tag{4.7}$$

where $P_r(x)$ delegates the received signal power at the 1-hop distance x from the transmitter, X_{dB} is a random variable following Gaussian Distribution (GD) with zero mean and standard deviation σ_{dB} ($\sigma_{dB} = 4 \sim 12$), β_1 denotes the path loss exponent ($\beta_1 = 2.7 \sim 5$ for shadowed urban areas), and $P_r(x_0)$ is the reference value of received signal power given by

$$P_r(x_0) = \frac{P_t}{{x_0}^2} \cdot \frac{G_t G_r}{L_s} \cdot \left(\frac{\lambda_c}{4\pi}\right)^2 \tag{4.8}$$

where P_t is the transmitted signal power, G_t and G_r denote the antenna gains of the transmitter and the receiver, respectively, L_s represents the system loss and λ_c means the carrier wave length.

In addition, in terms of the coherent BPSK modulation and Rayleigh Fading channel, a link BER (Bit Error Rate) can be expressed as [115]

$$BER = \frac{1}{2}\left(1 - \sqrt{\frac{\gamma_0}{\gamma_0 + 1}}\right) \tag{4.9}$$

where γ_0 denotes the mean ratio value of the received signal to the interferences plus noise, and it is given as follows

$$\gamma_0 = 2\sigma^2 \cdot \frac{P_r(x)}{P_{therm} + \sum_{i=1}^{N_{inf}} {P^i}_{inf}} \tag{4.10}$$

where $2\sigma^2$ is the mean value of the random variable in Rayleigh Distribution, $P_{therm} = F_k \cdot CTR$ denotes the thermal noise power, F_k is a constant parameter, CTR stands for the channel transmission data rate, ${P^i}_{inf}$ is the interference from the neighbor node C_i and N_{inf} represents the number of interfering nodes.

According to our assumptions, RTS/CTS scheme is used to reduce the frame collisions introduced by the hidden terminals, so during the communication from C_{k+1} to C_k as

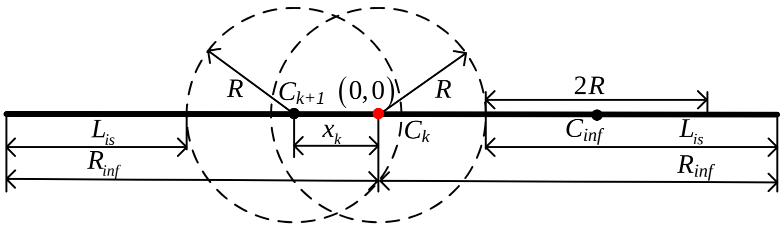

FIGURE 4.4: The analysis of potential interfering nodes. The vehicle C_{k+1} is sending packets to C_k (located in the origin of coordinates (0,0)). The distance between C_k and C_{k+1} is x_k, R_{inf} denotes the interference range, R means the communication range, L_{is} represents the length of interfering segment and C_{inf} is an interfering node located in the interfering segment.

shown in Fig. 4.4, the nodes located in their communication ranges are not allowed to transmit packets. Therefore, the potential interfering nodes must be in the segments that are outside the communication ranges of C_{k+1} and C_k but inside C_k's interference range and these consist of two parts: (R, R_{inf}) as well as $(-R_{inf}, -R - x_k)$. Within these segments, there is maximum one interfering node in a circle with a radius of R, so $\max N_{inf} = \left\lceil \frac{R_{inf}-R}{2R} \right\rceil + \left\lceil \frac{R_{inf}-R-x_k}{2R} \right\rceil$.

By substituting equation (4.10) into equation (4.9), we can derive

$$BER(x) = \frac{1}{2} - \frac{1}{2}\sqrt{\frac{2\sigma^2 P_r(x)}{2\sigma^2 P_r(x) + P_{therm} + \sum\limits_{i=1}^{N_{inf}} P_{inf}^i}} \tag{4.11}$$

So the 1-hop packet delivery ratio is given as

$$PDR_{1hop}(x) = (1 - (1 - cr)\, BER(x))^{psize} \tag{4.12}$$

where $psize$ denotes the packet size, cr means the error correction ratio and x depicts the one hop distance.

(2) Packet delivery ratio in the FC case

In this case, the links on the road segment are totally connected, and packets are forwarded from the intersection I_i to the intersection I_j hop by hop. The hop counts are closely relevant to the connectivity probability of the road segment, so we set cell size $cs = a \cdot R\,(0.5 < a < 1)$ to investigate the 1-lane road segment scenario based on the discussion in section 4.3.1. As shown in Fig. 4.3(a), the forwarding link length $L_f = L$, and the carry link length $L_c = 0$, so the hop counts between I_i and I_j in this case is expressed as

$$H_{FC} = \left\lceil \frac{L_f}{a \cdot R} \right\rceil + 1 = \left\lceil \frac{L}{a \cdot R} \right\rceil + 1 \tag{4.13}$$

where L means the road segment length, R denotes the communication range and a is the cell size parameter.

Therefore, the packet delivery ratio of the 1-lane road segment in the FC case can be given as follows

$$PDR_{FC} = PDR_{1hop}(x)^{H_{FC}} \cdot PCR_C \cdot P_{FC} = PDR_{1hop}(x)^{H_{FC}} \cdot P_{FC} \tag{4.14}$$

where PCR_C is the packet carrying ratio when packets are carried by a forwarding vehicle and $PCR_C = 1$, P_{FC} represents the probability of the FC case and $P_{FC} = PC = \left(1 - e^{-aR\lambda}\right)^N$ (deduced from equation (4.6)) and the average 1-hop distance $x = L/H_{FC}$.

(3) Packet delivery ratio in the FB case
In this case, the road segment is fully disconnected and no vehicle is available to forward packets, so packets from the intersection I_i are carried by the forwarding vehicle at speed v until this vehicle enters the communication range of the intersection I_j. Here, we define the link length between two successive vehicles C_k and C_{k+1} as x_k, as shown in Fig. 4.3(b). Since we assume that vehicle speed keeps constant on a road segment, as long as the link length between two latest arrival vehicles C_{k+1} and C_k satisfies with $x_k > R$, packets hold by C_{k+1} will be carried at vehicle speed v until arriving in the communication range of intersection I_j. Based on above considerations, $L_c = L - R$, $L_f = R$ and the packet delivery ratio in the FB case is given as

$$PDR_{FB} = PDR_{1hop}\left(R\right) \cdot PCR_C \cdot P_{FB} = PDR_{1hop}\left(R\right) \cdot P_{FB} \tag{4.15}$$

where P_{FB} means the probability of the FB case.

On the basis of the previously mentioned assumptions, the vehicles number on a road segment follows Poisson Distribution, so the distance X between any two consecutive vehicles obeys exponential distribution [117]. More precisely, the Cumulative Distribution Function (CDF) of X could be expressed as follows:

$$F\left(x\right) = P\left(X \le x\right) = 1 - e^{-\lambda x} \tag{4.16}$$

where λ denotes the vehicle spacing density of the road segment.

Consequently, the probability of the FB case is expressed as

$$P_{FB} = P\left(X > R\right) = 1 - F\left(R\right) = e^{-\lambda R} \tag{4.17}$$

Finally, by substituting equation (4.17) into equation (4.15), the packet delivery ratio in the FB case is derived as

$$PDR_{FB} = PDR_{1hop}\left(R\right) \cdot e^{-\lambda R} \tag{4.18}$$

(4) Packet delivery ratio in the PC case
In this case, the road segment is partly connected, for example, as shown in Fig. 4.3(c), the network links from the intersection I_i to the vehicle C_1 are fully connected, but the link between C_1 and C_0 is broken because of the distance between them $x_0 > R$. As a result, packets are forwarded hop by hop from I_i to C_1, and then carried by C_1 until C_1 enters the communication range of I_j. Here, the forwarding link length $L_f = L_{f1} + L_{f2}$, L_{f1} is equal to the distance between I_i and C_1, and $L_{f2} = R$.

The packet delivery ratio in the the PC case is illustrated as follows:

$$\begin{aligned} PDR_{PC} &= PDR_{1hop}(x)^{H_{PC1}} \cdot PCR_C \cdot PDR_{1hop}\left(R\right) \cdot P_{PC} \\ &= PDR_{1hop}(x)^{H_{PC1}} \cdot PDR_{1hop}\left(R\right) \cdot P_{PC} \end{aligned} \tag{4.19}$$

where $H_{PC1} = \left\lceil \frac{L_{f1}}{a \cdot R} \right\rceil$ denotes the hop counts within L_{f1}, $x = L_{f1}/H_{PC1}$ is the average 1-hop distance and P_{PC} is the PC case probability, which is derived as

$$P_{PC}{=}1 - P_{FC} - P_{FB}{=}1 - \left(1 - e^{-aR\lambda}\right)^N - e^{-\lambda R} \tag{4.20}$$

According to equation (4.19), if the forwarding links length L_{f1} is derived, the expression of packet delivery ratio in the PC case can be deduced.

We define $Cd\left(m\right)$ as a constraint condition for the connected cluster composed of m vehicles $(C_1, C_2, ..., C_{m-1}, C_m)$, and it means that the link length of any two successive vehicles in this cluster satisfies with $x_k \le R \; for \; k = 1, ..., m$, and $x_0 > R$. Obviously, we can express L_{f1} as the sum of each link length in the connected cluster, and $L_{f1}\left(m\right) = \sum\limits_{k=1}^{m} x_k$, where m denotes the number of connected links. Hence $E(L_{f1})$ is deduced in equation (4.21), where $E\left[x|x \le R\right]$ is the average link length with the constraint $x \le R$, and M is the largest integer that makes $L_{f1}\left(m\right) \le L$.

The link length X follows the exponential distribution, so the Cumulative Distribution Function (CDF) of X with constraint $X \le R$ is expressed as

$$G\left(X\right) = P\left(X \le x | X \le R\right) = \frac{P\left(X \le x, X \le R\right)}{P\left(X \le R\right)} = \begin{cases} \frac{1-e^{-\lambda \cdot x}}{1-e^{-\lambda \cdot R}}, & 0 \le x \le R \\ 0, & \text{otherwise} \end{cases} \tag{4.22}$$

$$
\begin{aligned}
&E\left(L_{f1}\right)=\sum_{m=1}^{\infty}E\left[L_{f1}\left(m\right)|Cd\left(m\right)\right]\cdot P\left[Cd\left(m\right)\right]\\
&=\sum_{m=1}^{\infty}E\left[\sum_{k=1}^{m}x_k|x_k\leq R\text{ for }i=1,...,m,\text{ and }x_0>R\right]\cdot P\left[x_k\leq R\text{ for }i=1,...,m,\text{ and }x_0>R\right]\\
&=\sum_{m=1}^{\infty}m\cdot E\left[x|x\leq R\right]\cdot P\left[x_0>R\right]\cdot P(x\leq R)^m=\sum_{m=1}^{\infty}m\cdot E\left[x|x\leq R\right]\cdot e^{-\lambda R}\cdot\left(1-e^{-\lambda R}\right)^m
\end{aligned}
$$

As the road segment is finite and its length equals L, the length of connected cluster should satisfy with $L_{f1}\left(m\right)\leq L$. Consequently, $E\left(L_{f1}\right)$ is rewritten as

$$
\begin{aligned}
&E\left(L_{f1}\right)=\left(\sum_{m=1}^{M}m\cdot E\left[x|x\leq R\right]+\sum_{m=M+1}^{\infty}L\right)\cdot e^{-\lambda R}\cdot\left(1-e^{-\lambda R}\right)^m\\
&=\left(M\cdot\left(1-e^{-\lambda R}\right)^{M+2}-(M+1)\cdot\left(1-e^{-\lambda R}\right)^{M+1}-e^{-\lambda R}+1\right)\cdot e^{\lambda R}\cdot E\left[x|x\leq R\right]\\
&+L\cdot\left(1-e^{-\lambda R}\right)^{M+1}
\end{aligned}
\tag{4.21}
$$

As a result, the expression of $E\left[x|x\leq R\right]$ can be derived as

$$
E\left(x|x\leq R\right)=\int_0^R xG'\left(X\right)dx=\int_0^R x\frac{\lambda e^{-\lambda x}}{1-e^{-\lambda R}}dx=\frac{1-\left(R\lambda+1\right)e^{-\lambda R}}{\lambda\left(1-e^{-\lambda R}\right)}
\tag{4.23}
$$

Based on equation (4.23), the largest integer M is derived as

$$
M\cdot E\left(x|x\leq R\right)\leq L\Rightarrow M=\left\lfloor\frac{L}{E\left(x|x\leq R\right)}\right\rfloor=\left\lfloor\frac{L\cdot\lambda\left(1-e^{-\lambda R}\right)}{1-\left(R\lambda+1\right)e^{-\lambda R}}\right\rfloor
\tag{4.24}
$$

By making use of equation (4.23) and (4.24), the value of $E\left(L_{f1}\right)$ in equation (4.21) can be derived.

Finally, the average packet delivery ratio between I_i and I_j is given as

$$
E\left(PDR\right)=PDR_{FC}+PDR_{FB}+PDR_{PC}
\tag{4.25}
$$

where PDR_{FC}, PDR_{FB} and PDR_{PC} are derived in equations (4.14), (4.18) and (4.19), respectively.

4.3.3 Delay

As greedy carry-and-forward algorithm is used to relay packets between two adjacent intersections, the packets delay on a road segment is closely correlated to several parameters, such as the network connectivity, 1-hop delay, hop counts and vehicle speed. In this section, we derive a delay model by considering the three cases identified in section 4.3.2: the FC case, FB case and PC case.

(1) Delay in the FC case
In this case, as shown in Fig. 4.3(a), the road segment between I_i and I_j is fully connected, and packets are forwarded hop by hop, so the delay in the FC case is simply given as

$$D_{FC} = H_{FC} \cdot t_p \cdot P_{FC} \tag{4.26}$$

where H_{FC} and P_{FC} denote the average hop counts and the probability of the FC case, respectively, and these two parameters are derived in section 4.3.2. t_p is the 1-hop delay and it consists of two parts: queue waiting time and virtual service time. From [120], we know that the calculation of t_p is closely related to several parameters, such as packet arrive rate, communication range, retransmission time, contention window size, packet size, channel transmission rate, etc.

(2) Delay in the FB case
In the FB case, since network connectivity is totally broken, packets are carried by the forwarding vehicle at speed v until this vehicle enters into the communication range of the intersection I_j (Fig. 4.3(b)). Obviously, the delay in the FB case consists of two parts including the time spent on the carry link length $L_c = L - R$ and the last vehicle 1-hop. So the delay in the FB case is expressed as

$$D_{FB} = \left(\frac{L_c}{v} + t_p\right) \cdot P_{FB} = \left(\frac{L-R}{v} + t_p\right) \cdot P_{FB} \tag{4.27}$$

where P_{FB} denotes the FB case's probability, which can be derived from equation (4.17).

(3) Delay in the PC case
In the PC case, as shown in Fig. 4.3(c), packets are relayed from I_i to C_1 via multi-hop wireless links, and then these packets are carried by C_1 until C_1 comes into I_j's communication range. The forwarding link length L_f in the PC case is composed of two parts: $L_{f2} = R$ and L_{f1} (given in equation (4.21)). Therefore, the carry link length

$L_c = L - L_{f1} - L_{f2} = L - R - L_{f1}$, and the delay in the PC case is derived as

$$\begin{aligned} D_{PC} &= \left(\frac{L_c}{v} + (H_{PC1}+1)\cdot t_p\right)\cdot P_{PC} \\ &= \left(\frac{L-R-L_{f1}}{v} + \left(\left\lceil\frac{L_{f1}}{a\cdot R}\right\rceil + 1\right)\cdot t_p\right)\cdot P_{PC} \end{aligned} \tag{4.28}$$

where P_{PC} denotes the probability of the PC case, which is derived in equation (4.20).

From the above analysis, the delay from I_i to I_j is given as

$$E(D) = D_{FC} + D_{FB} + D_{PC} \tag{4.29}$$

where D_{FC}, D_{FB} and D_{PC} are deduced from equations (4.26), (4.27) and (4.28), respectively.

Finally, the delay variance DVbetween I_i and I_j can be deduced as:

$$DV = E\left(D^2\right) - E(D)^2 = \frac{{D_{FC}}^2}{P_{FC}} + \frac{{D_{FB}}^2}{P_{FB}} + \frac{{D_{PC}}^2}{P_{PC}} - \left(D_{FC} + D_{FC} + D_{PC}\right)^2 \tag{4.30}$$

4.4 AQRV-1 routing protocol description

In this section, we detail the proposed mechanism of AQRV-1 routing protocol, which inherits from the adaptive intersection-based and ACO concept of AQRV. Likewise AQRV, the routes QoS is measured in terms of three parameters namely connectivity probability, packet delivery ratio and delay. However, unlike AQRV, which relies on periodic packets to estimate these metrics, AQRV-1 employs mathematical models presented in section 4.3. Actually, each source vehicle firstly sends a RREQ message to its TIS (deduced in section 4.4.1) for available routing information (satisfying QoS threshold and not out of date) before implementing data forwarding. If such routing information exists, a positive RREP is sent back to the source vehicle S, which can directly initiate the data packets forwarding session. Otherwise, TIS replies to S with a negative RREP, and then based on local road segment QoS and global QoS, TIS implements an best route establishment process between TIS and TID using ACO concept. AQRV-1 is mainly composed of following components: the terminal intersection selection, candidate routes derivation, best route selection and route maintenance.

4.4.1 Terminal intersection selection

In this section, we present the terminal intersections (TIS or TID) selection process for the corresponding communication pairs. A terminal intersection is determined by two factors, namely the moving direction of a communication terminal (the source vehicle or destination vehicle) and the distance to its neighboring intersections. Based on these two factors, a score is allocated to each neighboring intersection, and then the one owning the highest score is selected as the terminal intersection. The score expression is given as

$$Score\left(I_i\right) = \chi \cdot \left(1 - \frac{d\left(I_i\right)}{L}\right) + (1-\chi) \cdot Dir\left(I_i\right) \tag{4.31}$$

where L is the current road segment length, $d\left(I_i\right)$ means the distance between the communication terminal and its neighboring intersection I_i, χ denotes a weight parameter, and $Dir\left(I_i\right)$ stands for the communication terminal's moving direction value, which is given as

$$Dir\left(I_i\right) = \begin{cases} 1, \text{the terminal vehicle moves towards } I_i \\ 0, \text{otherwise} \end{cases} \tag{4.32}$$

4.4.2 Reactive candidate routing paths exploration

Once the terminal intersections for the source S and the destination D are selected respectively, S firstly sends a routing request to its TIS, and if available routing information towards TID exists at TIS and it is not out of date, TIS replies a positive message to S. Otherwise TIS sends a negative response to S and starts to search the best backbone route from TIS to TID.

To derive the candidate routes from TIS and TID, TIS launches a group of forward ants towards TID, here we set the number of forward ants to N_{fant}. When a forward ant arrives at the intersection I_i, it firstly records I_i's ID and then makes a stochastic decision to choose the next intersection based on both global and local pheromone stored locally at I_i. Compared with AQRV using only global pheromone, the network exploration mechanism of AQRV-1 is advantageous to search new candidate routing paths.

Suppose that there are K neighboring intersections of I_i, namely $I_1, I_2, ..., I_{K-1}, I_K$. The probability p_{ij} with which this forward ant selects I_j as the next intersection is given as

$$p_{ij} = \frac{{LP_{ij}}^{\alpha} \cdot {GP_{ij}}^{\beta}}{\sum_{m=1}^{K} {LP_{im}}^{\alpha} \cdot {GP_{im}}^{\beta}} \tag{4.33}$$

where α and β denote the weight values ($\alpha > 1$ and $\beta > 1$), which control the impact of local and global pheromone, respectively on the probability of the next intersection selection. LP_{ij} depicts the Local Pheromone, which reflects the local QoS of the road segment e_{ij} from I_i to I_j. GP_{ij} means the Global Pheromone, which implies the global QoS of the route y_{ij} from I_i to TID when going through I_j. The expressions of LP_{ij} and

GP_{ij} are derived as

$$\begin{aligned} LP_{ij} = F\left(e_{ij}\right) =& \varphi_1 \cdot PC\left(e_{ij}\right) + \varphi_2 \cdot PDR\left(e_{ij}\right) + \\ & \varphi_3 \cdot \frac{D_{th} - D\left(e_{ij}\right)}{D_{th}} \cdot \frac{1}{\left(1 + DV\left(e_{ij}\right)\right)} \end{aligned} \tag{4.34}$$

$$\begin{aligned} GP_{ij} = F\left(y_{ij}\right) =& \varphi_1 \cdot PC\left(y_{ij}\right) + \varphi_2 \cdot PDR\left(y_{ij}\right) + \\ & \varphi_3 \cdot \frac{D_{th} - D\left(y_{ij}\right)}{D_{th}} \cdot \frac{1}{\left(1 + DV\left(y_{ij}\right)\right)} \end{aligned} \tag{4.35}$$

where $PC\left(e_{ij}\right)$, $PDR\left(e_{ij}\right)$, $D\left(e_{ij}\right)$ and $DV\left(e_{ij}\right)$ denote the connectivity probability, packet delivery ratio, delay and delay variance of the road segment e_{ij} between I_i and I_j, respectively, and these three metrics are deduced in section 4.3. $PC\left(y_{ij}\right)$, $PDR\left(y_{ij}\right)$, $D\left(y_{ij}\right)$ and $DV\left(y_{ij}\right)$ (which are derived from equation (4.2)) represent the same QoS metrics for the route y_{ij} from I_i to TID when going through I_j. Obviously, LP_{ij} is the heuristic pheromone which can increase the algorithm's randomness, and help the forward ants get the latest local QoS information and explore new routing paths. GP_{ij} represents the global route QoS, and it makes the forward ants be inclined to select the explored best route, which is beneficial to the algorithm convergence as well as the avoidance of routing problems (routing holes and/or highly loaded links) on the upcoming road segments. Therefore, the probability p_{ij} can keep the balance between the new routing paths exploration and the prior route exploitation by adjusting α and β. In addition, it is worth noting that our stochastic forwarding method is advantageous in decreasing both the overhead and routing exploration time compared with other RREQ blind flooding mechanism.

When the forward ant arrives at TID, if the ant's delay is less than D_{th}, its explored route satisfies with the delay requirement and one candidate available route is obtained. Otherwise the explored route is ignored.

4.4.3 Reactive best routing path establishment

Backward ants are employed to implement the best route selection through the update of global pheromone. When a forward ant arrives at TID, and if its delay fulfills the delay constraint, it is transformed into a backward ant, which owns the same intersections sequence recorded by the corresponding forward ant.

The backward ant is sent back to TIS using the reverse route, and when arriving at a given I_i (moving from I_j), the backward ant firstly calculates the latest Global Pheromone GP_{ij} (by equation (4.35)) using the collected local road segment QoS (deduced in section

Algorithm 1 AQRV-1 routing algorithm concept

T_{GP}: global pheromone update time interval.
Identify TIS and TID using equation (4.31).
S sends a routing request message to TIS for the global pheromone towards TID.
if Global pheromone meeting QoS requirements exists && $CurrentTime - LastUpdateTime \leq T_{GP}$ **then**
  A positive response is sent back to S.
else
  TIS implements **Best route establishment** (refer to Algorithm 2).
end if
S initiates data packet forwarding intersection by intersection.
if TIS || TID changes **then**
  TIS implements **Best route establishment**.
end if

Algorithm 2 Best route establishment

for Each ant packet A arriving at I_i **do**
  if $A \rightarrow Type == ForwardAnt$ **then**
    Record I_i ID in A's header.
    $NextIntersection$ selection using equation (4.33).
    Send A to $NextIntersection$.
    if $NextIntersection == TID$ **then**
      if $D(y) \leq D_{th}$ **then**
        $A \rightarrow Type = BackwardAnt$.
      else
        Drop A.
      end if
    end if
  end if
  if $A \rightarrow Type == BackwardAnt$ **then**
    $UpdatePheromone$ process using equation (3.13).
    Send A to $NextIntersection$.
    if $NextIntersection == TIS$ **then**
      $UpdatePheromone$ process using equation (3.13).
      Drop A.
    end if
  end if
end for
$PheromoneEvaporation$ using equation (3.14).
Output the best route in terms of equation (4.1).
TIS sends a positive routing message to S.

4.3) along the passing through route. Then it updates the global pheromone stored at I_i based on equation 3.13 introduced in Chapter 3.

Once all backward ants arrive at TIS, we compare different $F(y)$ (equation 4.1) values of the candidate routes, and the route owning the maximum $F(y)$ is selected as the best one. Then, TIS sends a positive routing message to the source vehicle S to start data packet forwarding.

Note that the processes of pheromone evaporation and data packet forwarding are same used in AQRV routing protocol according to the descriptions given in section 3.4.3.

4.4.4 Reactive route maintenance

In AQRV routing protocol, a proactive route maintenance scheme is proposed to update latest routing information and cope with the rapid topology changes in VANET environments. However, this mechanism generates an enormous amount of overhead, which increases network congestion probability, exacerbates transmission delay and declines data packet delivery ratio.

In order to solve above challenges, a new reactive route maintenance scheme is proposed in AQRV-1. When the terminal intersection of the source or the destination vehicle changes, a new reactive routing path exploration and establishment is initiated between the current TIS and TID based on reactive forward ants and backward ants. In return, when TIS and TID keep unchanged, there is not any routing maintenance process being implemented. The detailed steps of AQRV-1 are presented in Algorithm 1 and Algorithm 2.

4.5 Performance analysis and evaluation

In this section, we firstly evaluate the accuracy of the proposed local road segment QoS models, and then analyze AQRV-1's performance compared with previously proposed AQRV routing protocol (in Chapter 3) and two reference VANET geographic routing protocols: GSR [16] and CAR [18].

4.5.1 Experimental environment

In our simulation experiments, we make use of Vehicular Ad Hoc Networks Mobility Simulator (VanetMobiSim [121]) to generate vehicles mobility. The simulation area is set to 5500 m $\times$ 5500 m consisting of 60 intersections and 98 1-lane road segments, where the vehicles move at a speed selected as 10 $\sim$ 20 m/s. The vehicle spacing density and vehicle safety time are defined as 0.01 $\sim$ 0.04 vehicles/m and 2 s, respectively. We use the Intelligent Driver Model with Intersection Management (IDM_IM) as the mobility model, and the initial positions and moving trips of vehicles are randomly selected. In addition, we take advantage of NS-2 as the network simulator and generate stochastically 350 Constant Bit Rate (CBR) sessions. In order to eliminate random seeds effects and obtain satisfactory Confidence Intervals (CI), we repeat each simulation 50 times. The remaining simulation parameters are indicated in Table 4.1.

TABLE 4.1: Simulation parameters

Parameters	Value
MAC protocol	IEEE 802.11p
CBR packet rate	5 packet/s
Communication range R	$150 \sim 350$ m
Interference range R_{inf}	$250 \sim 450$ m
Data packet size $psize$	128 and 256 Bytes
Forward Ants number N_{fant}	50
T_{GP}	10 s
Delay upper threshold T_{th}	80 s
Cell size parameter a	0.75
QoS weight parameters φ_1, φ_2 and φ_3	0.2, 0.2, 0.6
Weight value in TI selection χ	0.5
Weight parameter of local pheromone α	8
Weight parameter of global pheromone β	5

4.5.2 Validation and analysis of 1-lane local QoS models

(1) Connectivity probability of 1-lane road segment

Fig. 4.5 and Fig. 4.6 depict the impact of road segment length L, cell size cs, vehicle spacing density λ and communication range R on the road segment connectivity probability. We set $\lambda = 0.015$ vehicles/m in Fig. 4.5, which displays the upper and lower thresholds of road segment connectivity when $cs = R$ and $cs = 0.5R$, respectively. When $cs = 0.75R$, the average analytical results are in accord with the simulation results ($CI = 95\%$). In Fig. 4.6, we set $L = 1500$ m and $cs = 0.75R$, and from this figure, we can see that the average analytical results coincide with the simulation results for all R and λ. In addition, when the communication range and vehicle spacing density are increasing, the road segment network partition can be repaired, which is beneficial to the connectivity improvement. These two figures validate the accuracy of our proposed connectivity probability model.

(2) Packet delivery ratio of 1-lane road segment

In the scenario of Fig. 4.7, we set $\lambda = 0.015$ vehicles/m. This figure shows that the average error between the theoretical results and simulation results is only 4.85% when $cs = 0.75R$. In addition, when road segment length rises, the packet delivery ratio decreases due to more communication hops and hence worse the probability of loss. Moreover, the packet delivery ratio increases for smaller interference range values due to

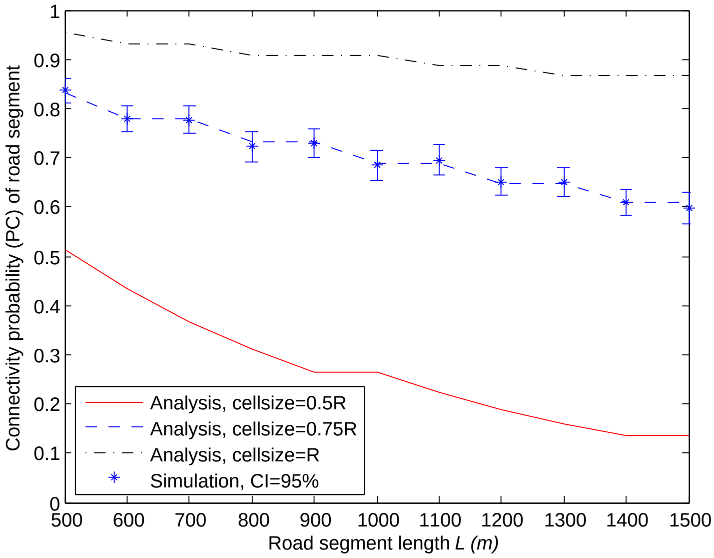

FIGURE 4.5: Road segment connectivity probability vs road segment length.

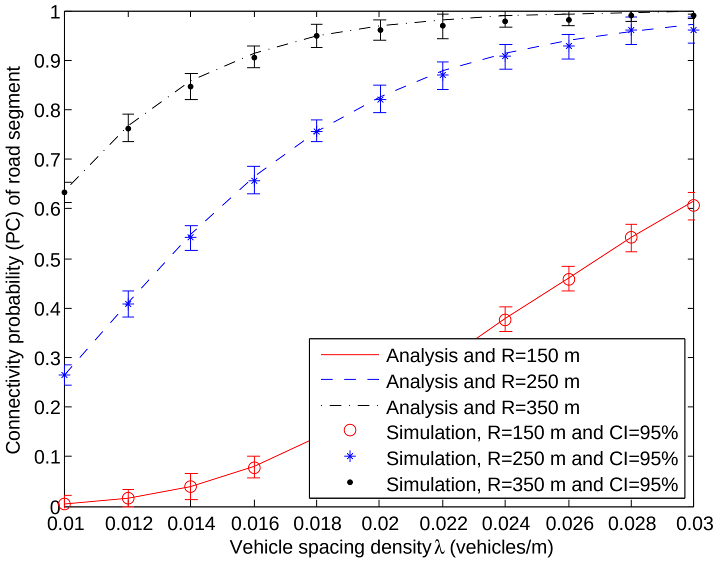

FIGURE 4.6: Road segment connectivity probability vs vehicle spacing density.

the less interference effects from the neighboring nodes. Fig. 4.8 proves the availability of the packet delivery ratio model with the varying vehicle spacing density, channel transmission data rate (CTR) and packet size. As we expected, packet delivery ratio declines with the increase of CTR, which leads to lower SINR and higher BER. Besides, packet delivery ratio deteriorates with the increase of vehicle spacing density, as higher vehicle spacing density makes more packets be forwarded using greedy rather than carry-and-forward algorithm, while greedy forwarding affords more influences from the channel fading.

(3) Delay of 1-lane road segment

Fig. 4.9 and Fig. 4.10 describe the correlation among the delay, vehicle spacing density,

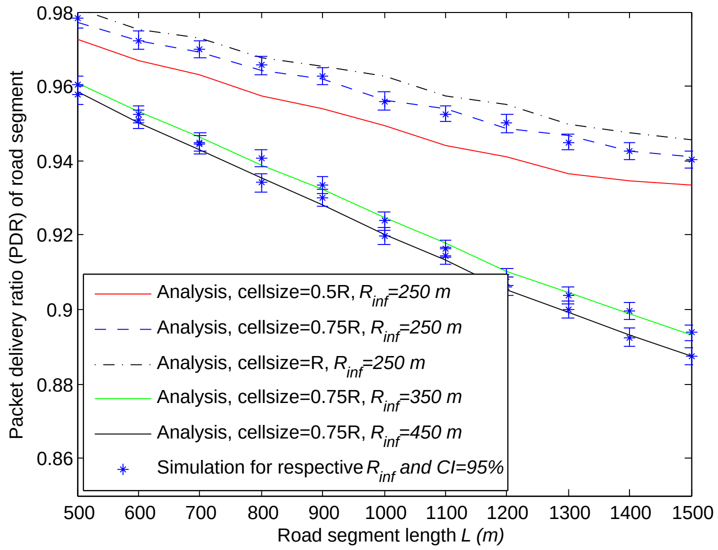

FIGURE 4.7: Road segment packet delivery ratio vs road segment length.

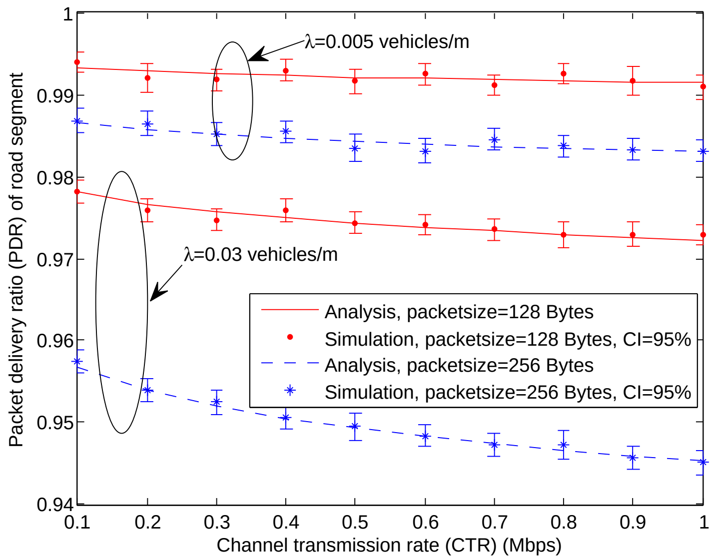

FIGURE 4.8: Road segment packet delivery ratio vs channel transmission rate.

channel transmission data rate and cell size. When $cs = 0.75R$, the analytical results and simulation results of these two figures are in good agreement, which demonstrate the accuracy of our road segment delay model. Besides, Fig. 4.9 shows that the road segment delay decreases noticeably, because network partitions can be repaired with the increase of vehicle spacing density. In Fig. 4.10, we set $\lambda = 0.03$ vehicles/m. The figure shows that road segment delay decreases when channel transmission data rate rises, the reason is that as the packets stored in the queue can be transmitted rapidly with higher channel transmission data rate, the observed delay is reduced.

According to above investigations, when $cs = 0.75R$, all average errors between analytical and simulation results are less than 5%, which proves the correctness of our proposed

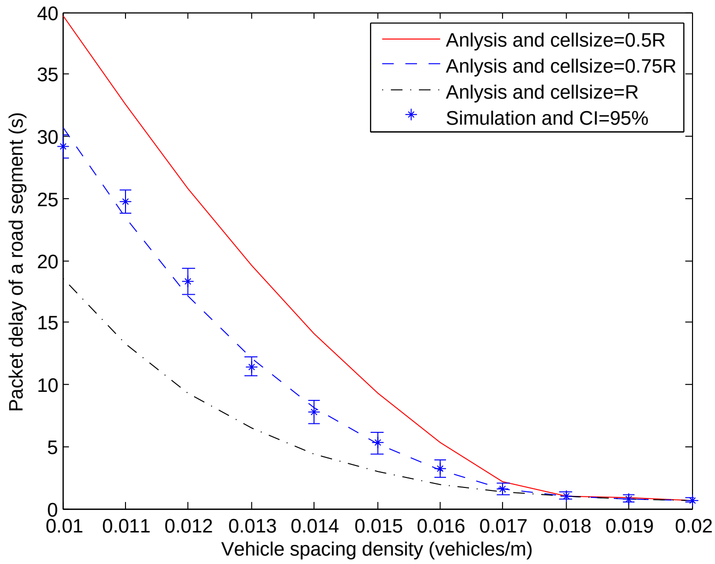

FIGURE 4.9: Road segment delay vs vehicle spacing density.

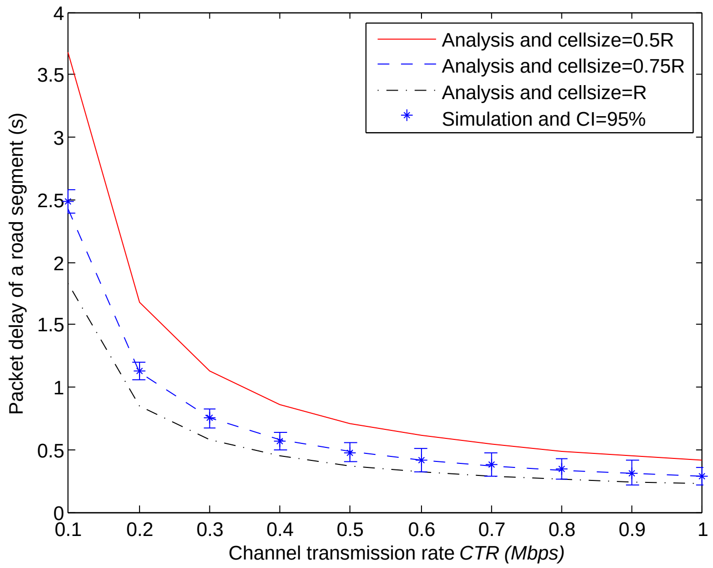

FIGURE 4.10: Road segment delay vs channel transmission rate.

analytical QoS models for the road segment. In addition, for example, when vehicle spacing density increases, connectivity probability is enhanced, delay reduces but packet delivery ratio degrades. These results justify the need for combining the three QoS metrics to meet a complete QoS routing performance.

4.5.3 AQRV-1 routing protocol performance evaluation

(1) End-to-end packet delivery ratio analysis

Fig. 4.11 displays the average packet delivery ratio for different vehicle spacing densities. We can see that all protocols show higher packet delivery ratio for lower vehicle

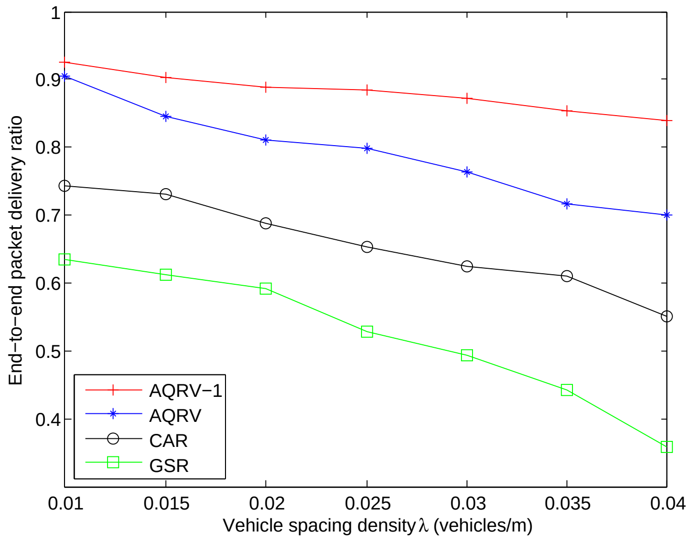

FIGURE 4.11: End-to-end packet delivery ratio for varying vehicle spacing density.

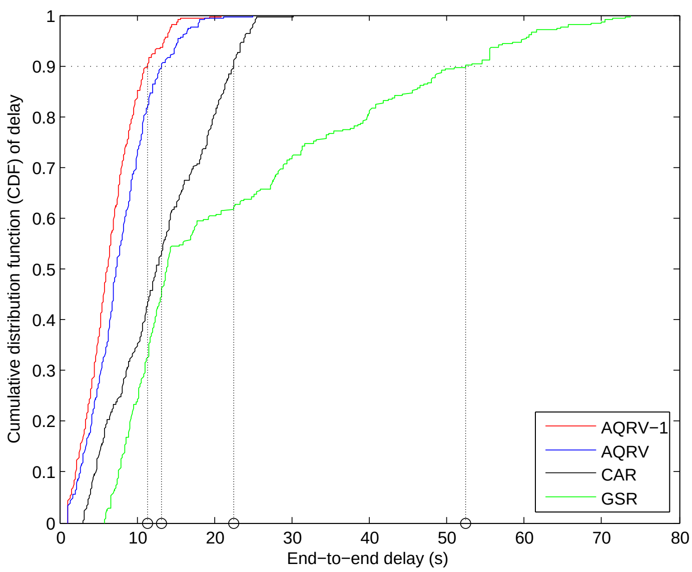

FIGURE 4.12: CDF (Cumulative Distribution Function) of end-to-end delay.

spacing density. This is because when vehicle spacing density increases, data packets prefer to be transmitted through wireless communications, which make them suffer from more interferences and channel fading effects than those carried by moving vehicles. In addition, we notice that AQRV-1 achieves the highest packet delivery ratio compared with GSR and CAR. There are two main reasons to explain such outcome. First of all, AQRV-1 dynamically selects the best routing path with highest communication QoS including packet delivery ratio. Secondly, AQRV-1 looks for available routing paths based on ACO algorithm, which makes different communication pairs cooperate with each other to update latest pheromone immediately. Obviously, it is advantageous to cope with rapid topology changes in VANET environments and thus improves packet delivery ratio. CAR does not maintain any backup routes and provides only one complete end-to-end routing path, which is far vulnerable in VANET environments and causes higher packet loss. GSR is a source driven routing protocol, and it makes routing decisions using the distance to the destination while neglecting other available routing information, so some data packets may be dropped when encountering extreme network conditions. In addition, compared with AQRV, AQRV-1 indicates higher packet delivery ratio. The main reasons are as follows: 1) the proposed local QoS models and reactive route maintenance scheme of AQRV-1 avoid redundant overhead and then alleviate network congestion and channel interference, which are beneficial to the improvement of the packet delivery ratio, and 2) when exploring candidate routes, AQRV-1 makes use of both global and local pheromone, this process helps to find the new best routes and decrease traffic load of the previous best one compared with AQRV which relies on only global pheromone.

(2) End-to-end delay analysis
Fig. 4.12 compares the Cumulative Distribution Function (CDF) of end-to-end delay for different routing protocols, here we set vehicle spacing density $\lambda = 0.015$ vehicle/m. We can notice that the delay of AQRV-1 is lower compared to the remaining protocols. Indeed, 90% delay statistics of AQRV-1 are within 11.36 s, and 90% delay records of AQRV are less than 13.11 s. While for CAR and GSR, the delay thresholds responding to 0.9 CDF value are 27.49 s and 52.37 s, respectively. The reasons of the best delay performance of AQRV-1 are as follows. In the first place, due to the ACO paradigm, AQRV-1 makes different communication pairs collaborate with each other to update available routing information, which is advantageous to cope with rapid network topology changes and adaptively chooses lower delay routes. Secondly, AQRV-1 dynamically selects next intersection using global routing information, and this behavior 1) offers the best routing decision based on latest traffic information, 2) effectively avoid network holes on the upcoming communication road segments, and 3) better reacts against high traffic load distribution compared with other source-driven routing protocols (CAR and GSR). Finally, compared with AQRV routing protocol, AQRV-1 is more efficient as it alleviates network congestion and reduces data packets retransmission times, which in return decreases the one hop delay. Fig. 4.12 also reveals that the curve of AQRV-1 offers a more rapid convergence, which implies that the delay variance of AQRV-1 is smallest. Indeed, AQRV-1 takes delay variance into account in the process of routes exploration and selection, and it also explores available routing paths using both latest local and global QoS, which is conducive to maintain the best routes, and keep low and stable packet delay. In the case of GSR, data packets are forwarded using the same path because of the shortest distance rule, and delay changes dramatically based on the varying traffic conditions along the route. CAR is a min-delay routing protocol but can not update routing information in real time, which may make upcoming data packets suffer from network partition and lead to higher delay.

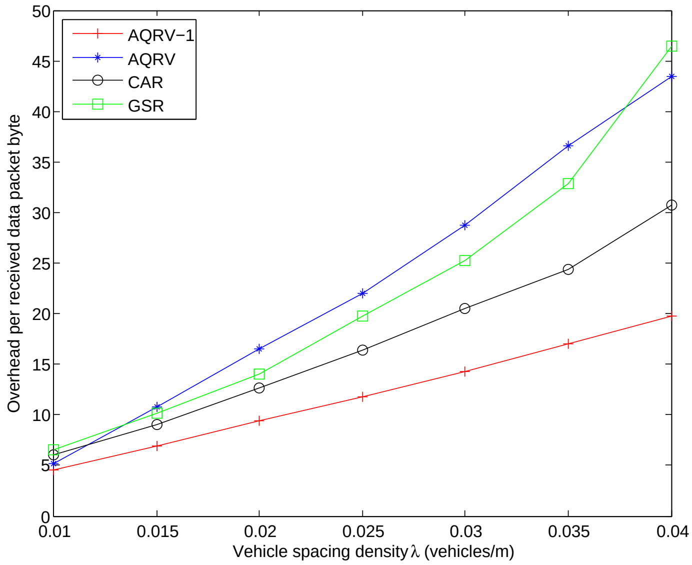

FIGURE 4.13: Overhead for per successfully received data byte.

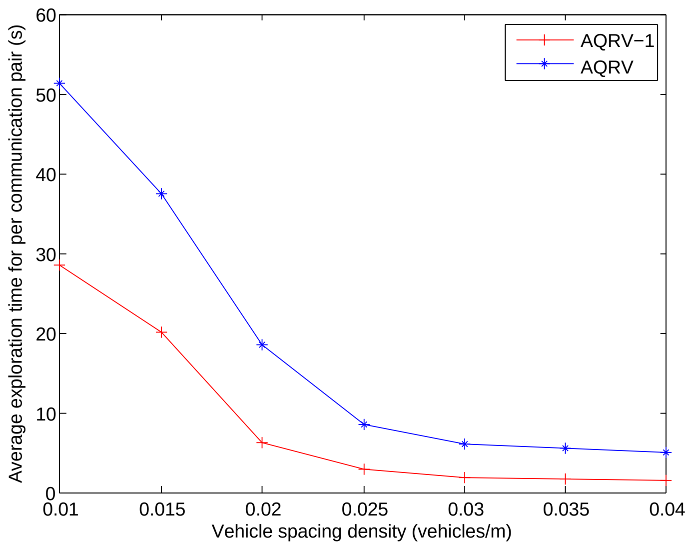

FIGURE 4.14: Average routing establishment time.

(3) Overhead analysis

Fig. 4.13 represents the generated overhead by all routing protocols as a function of vehicle spacing density. Note that for a fair comparison, we define the overhead as the ratio between the total control packet bytes and the cumulative bytes of successfully received data packets. From this figure, we find that the overhead of all routing protocols increases when vehicle spacing density goes up, since the Hello control packets occupy an important proportion of the whole overhead and their number is mainly determined by vehicle spacing density. In addition, Fig. 4.13 shows that the overhead of AQRV-1 is lowest compared with other routing protocols. The reasons are as follows: 1) AQRV-1 only explores the best route between two terminal intersections by ant unicast forwarding,

2) based on the existing best route, AQRV-1 can directly carry out data forwarding for different communication pairs with same terminal intersections and QoS requirements, 3) AQRV-1 makes use of latest routing information to dynamically choose best next intersection, which can achieve higher packet delivery ratio and thus reduce the overhead, and 4) compared with AQRV, AQRV-1 does not need to relay periodic packets between two neighboring intersections to estimate local QoS and implements a reactive rather than a proactive route maintenance process, so the amount of overhead of AQRV-1 can be decreased significantly.

(4) Route searching time analysis

Fig. 4.14 depicts the average best route's searching time for AQRV-1 and AQRV. From this figure, we can see that average searching time of best route in AQRV-1 is shorter than that in AQRV. Obviously, by using already explored best route, AQRV-1 shares the common routes and can directly implement data forwarding for different communication pairs with same terminal intersections and QoS requirements, so this scheme helps in decreasing the route searching time, while AQRV has to initiate an best route establishment process for each communication pair, which negatively impacts the network congestion and increases end-to-end delay. Besides, with the increment of vehicle spacing density, network partitions can be repaired, which is advantageous to reduce the searching time.

(5) Influence of global pheromone update interval and number of forward ants

Table 4.2 shows the normalized QoS and overhead of the selected best route, while varying the global pheromone update interval T_{GP} and forward ants number N_{fant}. Here we define the normalized QoS as $F(y)$ expressed in equation (4.1). From this table, we can observe that the normalized QoS and overhead decrease for larger T_{GP}, which implies that AQRV-1 does not need to send forward ants in time to keep up with the topology changes. Obviously, the increase of T_{GP} is advantageous to the decline of the required forward ants and overhead, but the obtained routing information may be out of date. In addition, Table 4.2 indicates that the normalized QoS is proportional to the forward ants number, because more ants can increase the routing exploration randomness and enhance AQRV-1's global exploration ability, which is beneficial to the best route search. When the forward ants number rises from 50 to 200, the QoS obtains a little improvement, but the overhead increases rapidly. Therefore, in light of these results, in order to make AQRV-1 own a good balance between the QoS and overhead, we set T_{GP} and N_{fant} for all the previous experiments to 10 s and 50, respectively.

Table 4.2: The influence of T_{GP} and N_{fant}

T_{GP}	N_{fant}	QoS	Overhead
10 s	10	0.8768	13.1241
	30	0.9001	13.9102
	50	0.9105	14.1499
	100	0.9112	15.3222
	200	0.9147	16.8726
30 s	10	0.8693	12.7760
	30	0.8916	12.9304
	50	0.9008	12.9997
	100	0.9017	13.6592
	200	0.9018	14.7214
50 s	10	0.8535	12.3167
	30	0.8629	12.4942
	50	0.8891	12.8158
	100	0.8900	13.1210
	200	0.8900	13.9870

4.6 Summary

In this chapter, we proposed an enhanced version of AQRV routing protocol called AQRV-1, for adaptively selecting the best routing path in vehicular urban environments. Firstly, we derived local QoS models in a 1-lane road segment scenario by considering three metrics, namely connectivity probability, packet delivery ratio and delay. Then, TI concept is proposed by AQRV-1 so as to explore the best route between two TIs rather than from the source to its destination in AQRV, and this behavior is beneficial to the decrease of routing delay and network overhead. Afterwards, when exploring candidate routing paths, AQRV-1 makes use of a new method which is based on both global and local pheromone instead of only global pheromone in AQRV. Moreover, a new reactive routing maintenance scheme is proposed to cope with dynamic routing changes. Finally, we validate our analytical local QoS models through extensive simulations, and demonstrate that AQRV-1 outperforms AQRV and the reference protocols. To extend this work and generalize the study, we will provide in the next chapter new mathematical QoS models suitable for 2-lane scenarios and then further improve the efficiency of our routing protocol.

Chapter 5

Adaptive QoS-based Routing for VANETs using ACO in 2-lane scenarios (AQRV-2)

5.1 Introduction

In chapter 4, we describe the routing protocol AQRV-1, which makes use of ACO-based algorithm to establish the best QoS routing path between two terminal intersections in 1-lane road environments in terms of both local and global pheromone. Nevertheless, there are yet some issues existing AQRV-1 required to be addressed.

Firstly, the proposed local road segment QoS models in AQRV-1 are available only for 1-lane road scenarios, but for 2-lane roads in urban environments, accurate mathematical QoS models are also required to estimate real-time routing performance.

Secondly, AQRV-1 is a QoS-based routing protocol but which satisfies with only the delay constraint. This may not be sufficient for various applications with different QoS limitations.

Finally, AQRV-1 routing protocol relays packets between two intersections by simple greedy carry-and-forward algorithm [122, 123], in which each node picks the next forwarding hop using its routing table holding the geographical information of its neighbors. The neighbor closest to the next intersection is chosen as the next hop, and this process continues until packets reaches the targeted destination. Therefore, to successfully choose next hops, it is very significant for each node to keep a precise neighbor list. If the lists are not accurate, the best next hop could be missed or even worse, a node which is already out of the communication range may be selected as the next hop. However, maintaining up-to-date neighboring list requires frequent Hello packet broadcasting, which results in a large amount of overhead and even aggravates the routing QoS in congested networks.

Based on above discussion and analysis, we propose an enhanced routing protocol AQRV-2. Similar to AQRV and AQRV-1, AQRV-2 depends on the ACO concept to establish the best QoS routing path in 2-lane road layout environments considering three thresholds of QoS metrics, namely connectivity probability, delay and packet delivery ratio. These three QoS parameters are estimated by our proposed mathematical models. In addition, in AQRV-2 routing protocol, we propose a new packet forwarding algorithm to select next hop using receiver-side relay election approach, in which the selection of next relaying node is not determined by the transmitter rather than by all neighboring nodes of this transmitter.

The rest of this chapter is organized as follows. The system model and problem statement are illustrated in Section 5.2. Then the mathematical models of local QoS for 2-lane road segments are proposed in Section 5.3. Afterwards, Section 5.4 illustrates the proposed receiver-side relay-based algorithm to select next forwarding hop. Section 5.5 details the simulation environments and analyzes the related results. Finally, Section 5.6 concludes the chapter.

5.2 System model and problem statement

We assume that the assumptions in this chapter are same as the descriptions in AQRV-1. As AQRV-2 aims at finding the best route that maximizes QoS evaluated in terms of connectivity probability, packet delivery ratio and delay metrics (these three metrics for 2-lane road segments are deduced in section 5.3) while satisfying the QoS constraints, a new system model is required. In our proposed system model, a 2-lane road urban street map which is represented as a graph $G(I, E)$, and for any two intersections I_i and I_j, there is only one 2-lane road segment e_k to connect them. Obviously, likewise AQRV-1, the best backbone route y between two terminal intersections can also be assumed as a succession of intersections $\{I_1, I_2, ..., I_{m-1}, I_m\}$, which are connected by a set of road segments $\{e_1, e_2, ..., e_{n-1}, e_n\}$, where $n = m - 1$. The required QoS is expressed as

$$QOS(y) = \varphi_1 \cdot PC(y) + \varphi_2 \cdot PDR(y) + \varphi_3 \cdot \frac{D_{th} - D(y)}{D_{th}} \cdot \frac{1}{(1 + DV(y))} \tag{5.1}$$

subject to

$$\begin{cases} PC\left(y\right) = \prod\limits_{i=1}^{n} PC\left(e_i\right) \geq PC_{th} \\ PDR\left(y\right) = \prod\limits_{i=1}^{n} PDR\left(e_i\right) \geq PDR_{th} \\ D\left(y\right) = \sum\limits_{i=1}^{n} D\left(e_i\right) \leq D_{th} \end{cases} \tag{5.2}$$

where $QOS\left(y\right)$ denotes the normalized QoS of a route y from the terminal intersection of source vehicle to the terminal intersection of destination vehicle. $PC\left(y\right)$, $PDR\left(y\right)$, $D\left(y\right)$ and $DV\left(y\right)$ stand for the connectivity probability, packet delivery ratio, delay and delay variance of the route y, respectively. φ_1, φ_2 and φ_3 are weight parameters ($0 < \varphi_1 < 1$, $0 < \varphi_2 < 1$, $0 < \varphi_3 < 1$ and $\varphi_1 + \varphi_2 + \varphi_3 = 1$). In addition, $PC\left(e_i\right)$, $PDR\left(e_i\right)$, $D\left(e_i\right)$ and $Dv\left(e_i\right)$ represent road segment e_i's connectivity probability, packet delivery ratio, delay and delay variance, respectively. PC_{th}, PDR_{th} and D_{th} stand for the targeted thresholds of the corresponding QoS metrics.

In order to solve the effects of multiple QoS thresholds, we propose three measured parameters baptized $F_{PC}\left(y\right)$, $F_{PDR}\left(y\right)$ and $F_{D}\left(y\right)$ for connectivity probability, packet delivery ratio and delay of the route y, respectively, to identify whether the QoS metrics of y fulfill the corresponding QoS thresholds. If so, the relevant measured parameters are set to 1, otherwise assigned to 0.

Based on above consideration, the problem in AQRV-2 that establishing the best QoS routing path as well as satisfying with multiple QoS thresholds can be formulated as a combinatorial optimization issue suitable for ACO-based algorithm and the objective function is expressed as

$$\max F\left(y\right) = \left(\varphi_1 \cdot F_{PC}\left(y\right) + \varphi_2 \cdot F_{PDR}\left(y\right) + \varphi_3 \cdot F_{D}\left(y\right)\right) \cdot QOS\left(y\right) \tag{5.3}$$

where

$$\begin{cases} F_{PC}\left(y\right) & = & \begin{cases} 1 & \text{if } PC\left(y\right) \geq PC_{th} \\ 0 & \text{otherwise} \end{cases} \\ F_{PDR}\left(y\right) & = & \begin{cases} 1 & \text{if } PDR\left(y\right) \geq PDR_{th} \\ 0 & \text{otherwise} \end{cases} \\ F_{D}\left(y\right) & = & \begin{cases} 1 & \text{if } D\left(y\right) \leq D_{th} \\ 0 & \text{otherwise} \end{cases} \end{cases} \tag{5.4}$$

Note that, AQRV-2 consists of almost the same core mechanisms as AQRV-1, namely, terminal intersections selection, candidate routes derivation, best route selection and route maintenance, so we do not present them in this chapter again. Besides, being different from the descriptions in AQRV-1, the expressions of local and global pheromone in AQRV-2 by considering multiple QoS thresholds are given as

$$LP_{ij} = F\left(e_{ij}\right) = \left(\varphi_1 \cdot F_{PC}\left(e_{ij}\right) + \varphi_2 \cdot F_{PDR}\left(e_{ij}\right) + \varphi_3 \cdot F_D\left(e_{ij}\right)\right) \cdot QOS\left(e_{ij}\right) \quad (5.5)$$

$$GP_{ij} = F\left(y_{ij}\right) = \left(\varphi_1 \cdot F_{PC}\left(y_{ij}\right) + \varphi_2 \cdot F_{PDR}\left(y_{ij}\right) + \varphi_3 \cdot F_D\left(y_{ij}\right)\right) \cdot QOS\left(y_{ij}\right) \quad (5.6)$$

where LP_{ij} depicts the Local Pheromone, which indicates the local QoS of the road segment e_{ij} between the intersection I_i and I_j. GP_{ij} denotes the Global Pheromone showing the global QoS of the route y_{ij} from the current intersection I_i to TID (Terminal Intersection of the Destination vehicle) when going through the next intersection I_j. $F_{PC}\left(e_{ij}\right)$, $F_{PDR}\left(e_{ij}\right)$ and $F_D\left(e_{ij}\right)$ are used to measure if the QoS performance of the road segment e_{ij} is compatible with the corresponding thresholds. Similarly, $F_{PC}\left(y_{ij}\right)$, $F_{PDR}\left(y_{ij}\right)$ and $F_D\left(y_{ij}\right)$ are also used to measure whether the QoS metrics of the route y_{ij} meet the corresponding QoS thresholds. $QOS\left(e_{ij}\right)$ and $QOS\left(y_{ij}\right)$ denote the normalized QoS of the road segment e_{ij} and the route y_{ij}, respectively, and these two parameters can be derived by equation (5.1).

5.3 Mathematical models of local QoS for 2-lane road segments

In this section, we derive the local QoS models for 2-lane road segments in terms of connectivity probability, delay and packet delivery ratio. In order to achieve above goals, we consider a straight 2-lane road segment e_{ij} with length L between two intersections I_i and I_j in a city scenario. The two road segment lanes go in opposite directions referred to as the Eastbound and Westbound. In addition, we set the vehicle spacing density for the Eastbound lane and Westbound lane to λ_1 and λ_2, respectively, and the vehicle velocity for these two lanes is assumed constant and correspondingly set to v_1 and v_2.

5.3.1 Connectivity probability

According to the definition of connectivity probability in Chapter 3, if there is not any broken link in a direction of a 2-lane road segment, or the broken links exist but the nodes moving on the opposite direction can repair all of them, this road segment is regarded as being connected. Obviously, the opportunistic contacts among the nodes moving on both directions is advantageous to improve connectivity probability of a road segment.

It is far difficult to derive an exact connectivity model for a 2-lane road due to the complicated vehicle mobility and its continuous nature. As for the models in AQRV-1,

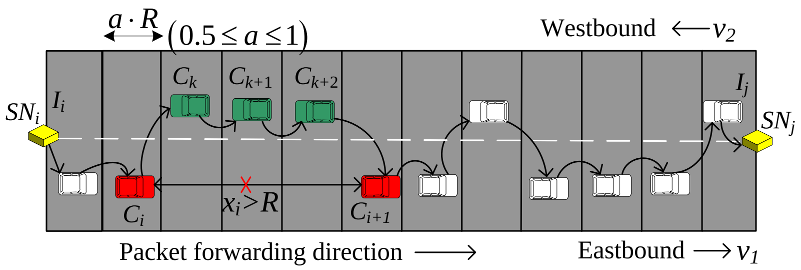

FIGURE 5.1: Vehicle distribution example on a 2-lane road segment.

in order to capture the connectivity characteristics, we divide the road segment into several cells, and two cell size threshold values referred to as $0.5R$ and R are considered, as shown in Fig. 5.1. In the case of cell size $cs = 0.5R$, the maximum vehicles distance in two adjacent cells is R, which definitely guarantees the connectivity among them. When $cs = R$, the distance of vehicles in consecutive cells may vary within the range 0 and $2R$ due to the random vehicles location distribution, so the links may be connected or not. Obviously, the case of $cs = 0.5R$ is a sufficient but not necessary condition for connectivity. Conversely, the vehicles in adjacent cells are not guaranteed to be always connected when $cs = R$, which is a necessary but insufficient condition for connectivity.

Based on above discussion, we set cell size $cs = a \cdot R$ $(0.5 < a < 1)$, and let K be a random variable denoting the number of vehicles in an interval $a \cdot R$. According to the assumption of vehicles distribution, K obviously follows Poisson Distribution and its Probability Mass Function (PMF) is given as

$$P\left(K = k\right) = \left(aR\lambda\right)^k \cdot e^{-aR\lambda} \Big/ k! \tag{5.7}$$

where λ denotes the vehicle spacing density on a road segment lane.

Since the distance between any two consecutive vehicles obeys the exponential distribution [117], the probability of a broken link between two vehicles separated by a distance X on the Eastbound lane is labeled as P_b and derived as

$$P_b = P\left(X > R\right) = e^{-\lambda_1 R} \tag{5.8}$$

where λ_1 means the vehicle spacing density on the Eastbound lane.

As shown in Fig. 5.1, two consecutive vehicles C_i and C_{i+1} on the Eastbound lane are disconnected because of the distance between them $x_i > R$. Making use of the vehicles on the Westbound lane, the broken link between C_i and C_{i+1} can be repaired as long as there is at least one vehicle in each Westbound cell within x_i. Obviously, the probability

$P_f\left(i\right)$ that a broken link between C_i and C_{i+1} can be fixable is expressed as

$$P_f\left(i\right) = \begin{cases} 1 & \text{if } x_i \leq R \\ \left(1 - P\left(K=0\right)\right)^{\left\lceil \frac{x_i}{aR} \right\rceil} & \text{if } x_i > R \end{cases} \tag{5.9}$$

where $P\left(K=0\right) = e^{-aR\lambda}$ and $\lambda = \lambda_2$, which denotes the vehicle spacing density on the Westbound lane.

Let M be a variable that denotes the number of broken links on the Eastbound lane. Obviously, road segment e_{ij} is connected if M broken links are completely fixable. The conditional connectivity probability with M broken links $P_{c|M}\left(M=m\right)$ can be written as

$$\begin{aligned} P_{c|M}\left(M=m\right) &= \prod_{i=1}^{m} P_f\left(i\right) \qquad \forall m = 1, ..., N-1 \\ &= \left(1 - e^{-aR\lambda_2}\right)^{\sum\limits_{i=1}^{m} \left\lceil \frac{x_i}{aR} \right\rceil} \\ &= \left(1 - e^{-aR\lambda_2}\right)^{\left(\frac{L}{aR} - \frac{N-1-m}{aR \cdot \lambda_1}\right)} \end{aligned} \tag{5.10}$$

where N stands for the number of vehicles and static nodes on the Eastbound lane.

When $M = m$ broken links exist among $N-1$ links on the Eastbound lane, the Probability Mass Function $P_M\left(M=m\right)$ follows a binomial distribution and is given as

$$P_M\left(M=m\right) = \begin{pmatrix} N-1 \\ m \end{pmatrix} p_b^m \left(1-p_b\right)^{N-1-m} \tag{5.11}$$

where $\forall m = 1, ..., N-1$.

Obviously, in the case of at least one broken link exists on the Eastbound lane ($m \geq 1$), the connectivity probability of the road segment is expressed as

$$P_{c1} = \sum_{m=1}^{N-1} P_{c|M}\left(M=m\right) \cdot P_M\left(M=m\right) \tag{5.12}$$

When there is no broken link on the Eastbound lane, i.e., all cells are occupied by at least one vehicle, the connectivity probability of the road segment can be given as

$$P_{c2} = \left(1 - e^{aR\lambda_1}\right)^{\left\lceil \frac{L}{aR} \right\rceil} \tag{5.13}$$

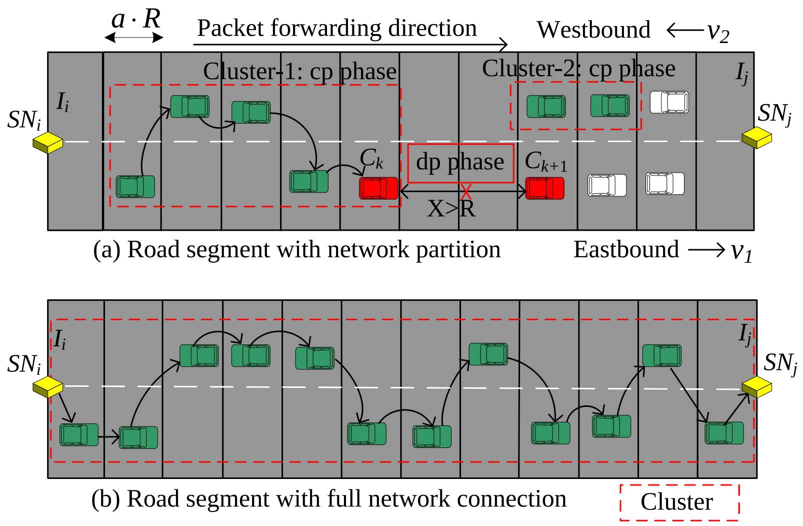

Figure 5.2: 2-lane road segment delay analysis model.

According to above analysis, the total connectivity probability of a road segment between the intersection I_i and the intersection I_j is represented as follows

$$PC = P_{c1} + P_{c2} \tag{5.14}$$

5.3.2 Delay

In this section, we derive the multi-hop transmission delay model for a given 2-lane road segment. The road traffic statistics and moving vehicles time-series snapshots have demonstrated that vehicles tend to travel in clusters on road scenarios. Obviously, a road segment may be fully connected or not in terms of the scale of the vehicles cluster. If the road segment is fully connected, data packets can be forwarded hop-by-hop, otherwise a forwarding vehicle has to carry the data packets to its neighboring vehicles. According to the discussion in section 5.3.1, we divide the road segment into several cells and set cell size $cs = a \cdot R$ to investigate the road segment delay model. Our model considers two different cases: the road segment with Network Partitions (NP) and the road segment with full Network Connections (NC), which are illustrated in Fig. 5.2.

5.3.2.1 Delay in the NP case

In this case, the road segment is partly connected, as shown in Fig. 5.2(a). An accurate delay model of a road segment is closely related to various network topologies, which are difficult to obtain due to the finite road segment length and complex vehicles movement. In order to derive an accurate road segment transmission delay model, we can expand a finite road segment into an infinite road, which can cover all kinds of network topologies, and then the road segment transmission delay D_{NP} in NP case is deduced as follows

$$D_{NP} = \frac{L}{E(\bar{v})} \tag{5.15}$$

where L denotes the road segment length and $E(\bar{v})$ is defined as the average data packets travelling speed on the road segment, and it will be estimated in equation (5.19).

With the assistance of vehicles on the Westbound lane, there are alternating periods of disconnection and connectivity on the Eastbound lane. In the disconnection phase (dp), data packets are carried by a forwarding vehicle on the Eastbound lane with the vehicle speed v_1, until next neighboring vehicle is in reach. In the connection phase (cp), data packets are propagated at wireless transmission speed v_{1hop}, which can be represented as follows

$$v_{1hop} = \frac{a \cdot R}{t_p} \tag{5.16}$$

where $a \cdot R$ means the 1-hop length and t_p indicates the 1-hop transmission delay as illustrated in Chapter 4. According to the alternating renewal process theorem [124], the respective long-run probability of data transmission time spent in *dp phase* and *cp phase* is given as

$$\begin{aligned} P_{dp} = \frac{E(T_{dp})}{E(T_{dp}) + E(T_{cp})} &= \frac{E(d_{dp})/v_1}{E(d_{dp})/v_1 + E(d_{cp})/v_{1hop}} \\ &= \frac{E(d_{dp})\, v_{1hop}}{E(d_{dp})\, v_{1hop} + E(d_{cp})\, v_1} \end{aligned} \tag{5.17}$$

$$\begin{aligned} P_{cp} = \frac{E(T_{cp})}{E(T_{dp}) + E(T_{cp})} &= \frac{E(d_{cp})/v_{1hop}}{E(d_{dp})/v_1 + E(d_{cp})/v_{1hop}} \\ &= \frac{E(d_{cp})\, v_1}{E(d_{dp})\, v_{1hop} + E(d_{cp})\, v_1} \end{aligned} \tag{5.18}$$

where $E(T_{dp})$ and $E(T_{cp})$ denote the average data transmission time spent in corresponding *dp phase* and *cp phase*. In addition, $E(d_{dp})$ and $E(d_{cp})$ stand for the distance traveled by a transmission data packet during the *dp phase* and *cp phase*, respectively. Substituting equation (5.17) and (5.18), the average data packets transmission speed $E(\bar{v})$ can be obtained as follows

$$E(\bar{v}) = v_1 \cdot P_{dp} + v_{1hop} \cdot P_{cp} = \frac{(E(d_{dp}) + E(d_{cp})) \cdot v_1 \cdot v_{1hop}}{E(d_{dp}) \cdot v_{1hop} + E(d_{cp}) \cdot v_1} \tag{5.19}$$

After substituting equation (5.16) and (5.19) into equation (5.15), road segment transmission delay can be deduced as follows

$$D_{NP} = L \cdot \frac{E\left(d_{dp}\right) \cdot aR + E\left(d_{cp}\right) \cdot v_1 \cdot t_p}{\left(E\left(d_{dp}\right) + E\left(d_{cp}\right)\right) v_1 \cdot aR} \tag{5.20}$$

Obviously, from equation (5.20), we can see that as long as $E\left(d_{dp}\right)$ and $E\left(d_{cp}\right)$ are derived, road segment transmission delay in network partition case D_{NP} can be obtained. We present in the following how these values are derived.

(1) Disconnection phase (dp)

In the *dp phase*, as shown in Fig. 5.2(a), the forwarding vehicle C_k and the next consecutive vehicle C_{k+1} on the Eastbound lane are disconnected due to their distance $x > R$, so data packets are carried by vehicle C_k until the connectivity between C_k and Cluster-2 is set up, this period is called *dp phase* of data packets transmission.

The *pattern matching* problem [124] is generally used to derive the expected number of trials until meeting consecutive successful results. From known results on pattern matching [124], the expected number of trials until k consecutive successes is given is:

$$E\left(k\right) = \frac{1 - {p_s}^k}{\left(1 - p_s\right) {p_s}^k} \tag{5.21}$$

where p_s is the probability of success for a single event. This result gives us the expected number of trials until after the pattern matching is achieved.

According to above investigation, the expected number of road cells traveled by a vehicle until meeting connected cells is analogous to the pattern matching problem described in equation (5.21). Therefore, as shown in Fig. 5.2(a), the number of road cells traversed by the vehicle C_k until it encounters connected Cluster-2 (consisting of n consecutive connected cells) along the Westbound lane is expressed as follows

$$E\left(n\right) = \left(\frac{1 - {p_a}^n}{\left(1 - p_a\right) {p_a}^n} - n\right) \cdot \frac{v_1}{v_1 + v_2} \tag{5.22}$$

where p_a denotes the probability of success that a cell of the Westbound lane is connected with its neighboring cells and this event is achieved by laying at least one vehicle in one cell, so $p_a = 1 - e^{-\lambda_2 aR}$. In addition, n connected cells along the Westbound road are used to bridge the gap between C_k and C_{k+1}, thus we can set n to $\lceil \frac{x}{aR} \rceil$.

Note that the factor $\frac{v_1}{v_1+v_2}$ is introduced in equation (5.22), because the vehicle C_k and Cluster-2 move in the opposite direction with v_1 and v_2, respectively, and the number of cells required for C_k is consequently reduced. In addition, equation (5.21) gives us the cells until after the pattern is seen, while what we expect is the number of cells traversed until before the pattern is seen. Hence, we subtract n to find the distance until connectivity.

We know that the link between C_k and C_{k+1} is broken if at least one cell on the Westbound lane is vacant along the gap x ($x > R$). The disconnection probability between C_k and C_{k+1} with distance X is given as follows

$$P\left(\bar{\mathrm{C}}|X=x\right)=\begin{cases}0 & \text{if } x\leq R\\ 1-{p_a}^{\lceil x/aR\rceil} & \text{if } x>R\end{cases}\tag{5.23}$$

Due to the Probability Density Function (PDF) of the vehicles on the Eastbound lane $f_X\left(x\right)=\lambda_1 e^{-\lambda_1 x}$, the disconnection probability is expressed as

$$P\left(\bar{C}\right)=\int_0^{\infty}P\left(\bar{\mathrm{C}}|X=x\right)\cdot f_X\left(x\right)dx=e^{-\lambda_1 R}-\frac{\lambda_1 aRe^{-\lambda_1 R}{p_a}^{1/a}}{\lambda_1 aR-\ln\left(p_a\right)}\tag{5.24}$$

Based on above analysis, the average distance of data transmission in *dp phase* is given as

$$\begin{aligned}E\left(d_{dp}\right)&=\int_0^{\infty}E\left(n\right)\cdot aR\cdot f_X\left(x|\bar{C}\right)dx\\&=\int_0^{\infty}E\left(n\right)\cdot aR\cdot\frac{f_X\left(x\right)P\left(\bar{C}|X=x\right)}{P\left(\bar{C}\right)}dx\end{aligned}\tag{5.25}$$

By substituting equation (5.22) and (5.23) into equation (5.25), we can deduce the final expression of the carrying distance in *dp phase* $E\left(d_{dp}\right)$, which is given as

$$\begin{aligned}E\left(d_{dp}\right)=&\frac{aR}{P\left(\overline{C}\right)}\cdot\frac{v_1}{v_1+v_2}\cdot\frac{\lambda_1}{1-P_a}\cdot\left(\frac{e^{-\lambda_1 R}{P_a}^{-1/a}}{\lambda_1+\frac{\ln(P_a)}{aR}}+\frac{e^{-\lambda_1 R}{P_a}^{1/a}}{\lambda_1-\frac{\ln(P_a)}{aR}}-\frac{2e^{-\lambda_1 R}}{\lambda_1}\right)\\&-\frac{\lambda_1}{P\left(\overline{C}\right)}\cdot\frac{v_1}{v_1+v_2}\cdot\left(\frac{\left(1+\lambda_1 R\right)e^{-\lambda_1 R}}{{\lambda_1}^2}-\frac{\left(\lambda_1 R-\frac{\ln(P_a)}{a}+1\right)e^{-\lambda_1 R}{P_a}^{1/a}}{\left(\lambda_1-\frac{\ln(P_a)}{aR}\right)^2}\right)\end{aligned}\tag{5.26}$$

(2) Connection phase (*cp*)

In *cp phase*, vehicles are connected with each other and data packets are transmitted at the speed v_{1hop}. The transmission distance in *cp phase* is composed of two parts. In the first part, consecutive Eastbound nodes are connected if the distance between them is not more than R, or even if the distance is greater than R, each Westbound cell within the gap is occupied by at least one vehicle, for example, Cluster-1 shown in Fig. 5.2(a). In the second part, if the gap in *dp phase* is repaired by the vehicles on the Westbound lane, the distance of gap x is also traversed by data packets at speed v_{1hop}. For instance, as represented in Fig. 5.2(a), with the movement of Cluster-1 and Cluster-2, the two vacant cells between C_k and C_{k+1} will be occupied by the vehicles in Cluster-2, and data packets can then be forwarded hop by hop when going through these two cells.

In the case of the first part, the expected transmission distance between two consecutive vehicles on the Eastbound lane is given as

$$\begin{aligned} E\left(X|C\right) &= \int_0^\infty x f_X\left(x\right) \frac{P\left(C|X=x\right)}{P\left(C\right)} dx \\ &= \int_0^\infty x f_X\left(x\right) \frac{1-P\left(\overline{C}|X=x\right)}{1-P\left(\overline{C}\right)} dx \end{aligned} \tag{5.27}$$

By substituting equation (5.23) and (5.24) into equation (5.27), $E\left(X|C\right)$ is represented as

$$\begin{aligned} E\left(X|C\right) =& \frac{\lambda_1 aR - \ln\left(p_a\right)}{\left(1-e^{-\lambda_1 R}\right)\cdot\left(\lambda_1 aR - \ln\left(p_a\right)\right) + \lambda_1 aRe^{-\lambda_1 R}{p_a}^{1/a}} \\ &\cdot \left(\frac{1-e^{-\lambda_1 R}\left(1+\lambda_1 R\right)}{\lambda_1} + \frac{\lambda_1 e^{-\lambda_1 R}{P_a}^{1/a}\left(1+\lambda_1 R - \frac{1}{a}\ln\left(P_a\right)\right)}{\left(\lambda_1 - \frac{\ln(P_a)}{aR}\right)^2} \right) \end{aligned} \tag{5.28}$$

If y consecutive links on the Eastbound lane are connected, the transmission distance covered is $y \cdot E\left(X|C\right)$. So the expected distance covered in the first part during *cp phase* $E\left(d_{cp-part1}\right)$ is shown as follows

$$\begin{aligned} E\left(d_{cp-part1}\right) &= \sum_{y=1}^{\infty} y \cdot E\left(X|C\right) P(C)^y \left(1-P\left(C\right)\right) \\ &= E\left(X|C\right)\frac{P\left(C\right)}{1-P\left(C\right)} = E\left(X|C\right)\frac{1-P\left(\overline{C}\right)}{P\left(\overline{C}\right)} \end{aligned} \tag{5.29}$$

In the case of the second part, the average transmission distance equals the gap length between C_k and C_{k+1} on the link disconnection condition. Based on the above analysis, the transmission distance is deduced as follows

$$\begin{aligned} E\left(d_{cp-part2}\right) &= E\left(X|\overline{C}\right) \\ &= \int_0^\infty x f_X\left(x\right) \frac{P\left(\overline{C}|X=x\right)}{P\left(\overline{C}\right)} dx \\ &= \frac{1}{P\left(\overline{C}\right)} \left(\frac{e^{-\lambda_1 R}\left(1+\lambda_1 R\right)}{\lambda_1} - \frac{\lambda_1 e^{-\lambda_1 R}{P_a}^{1/a}\left(1+\lambda_1 R - \frac{1}{a}\ln\left(P_a\right)\right)}{\left(\lambda_1 - \frac{\ln(P_a)}{aR}\right)^2} \right) \end{aligned} \tag{5.30}$$

In terms of the above deduction, the average distance of data transmission in *cp phase* is given as

$$\begin{aligned} E\left(d_{cp}\right) &= E\left(d_{cp-part1}\right) + E\left(d_{cp-part2}\right) \\ &= \frac{\lambda_1 a R - \ln\left(p_a\right)}{e^{-\lambda_1 R} \cdot \left(\lambda_1 a R - \ln\left(p_a\right)\right) - \lambda_1 a R e^{-\lambda_1 R} {p_a}^{1/a}} \cdot \frac{1}{\lambda_1} \end{aligned} \tag{5.31}$$

Finally, based on equation (5.26) and (5.31), road segment delay in NP case D_{NP} can be deduced by equation (5.20).

5.3.2.2 Delay in the NC case

In this case, the links of the road segment are totally connected, and the packets can be forwarded from current intersection I_i to next intersection I_j using hop by hop. As shown in Fig. 5.2(b), the cluster length $L_{cl} \geq L$. Consequently, the transmission delay between I_i and I_j in this case can be expressed as follows

$$D_{NC} = H_{NC} \cdot t_p \tag{5.32}$$

where $H_{NC} = \left\lceil \frac{L}{a \cdot R} \right\rceil + 1$ denotes the hop counts between I_i and I_j, and t_p means the 1-hop transmission delay.

From the analysis of NP case and NC case, the average transmission delay of a 2-lane road segment between two intersections I_i and I_j is given as

$$D = D_{NP} \cdot (1 - PC) + D_{NC} \cdot PC \tag{5.33}$$

where PC stands for the road segment connectivity probability (deduced in equation (5.14)).

In addition, the transmission delay variance between two intersections I_i and I_j is expressed as

$$DV = {D_{NC}}^2 \cdot PC + {D_{NP}}^2 \cdot (1 - PC) - D^2 \tag{5.34}$$

5.3.3 Packet delivery ratio

In AQRV-2 routing protocol, we make use of a new packet forwarding algorithm, which is mentioned in section 5.4, and this algorithm is based on distance-greedy carry-and-forward mechanism. When links among nodes on a road segment are connected, packets are forwarded using hop-by-hop wireless communication, whereas when suffering from broken links, packets are carried by the current forwarding node with its moving speed. Based on above consideration, we can derive the mathematical model of packet delivery ratio by considering two cases same as delay deduction, namely the case of road segment with Network Partitions (NP) and the case of road segment with full Network Connections (NC), which are illustrated in Fig. 5.2.

5.3.3.1 Packet delivery ratio in the NP case

As shown in Fig. 5.2(a), the NP case is composed of two phases including the disconnection phase (*dp phase*) and connection phase (*cp phase*), and the corresponding ratio of the packet forwarding length in the *dp phase* and the *cp phase* is given as

$$r_{dp} = \frac{E\left(d_{dp}\right)}{E\left(d_{cp}\right) + E\left(d_{dp}\right)} \tag{5.35}$$

$$r_{cp} = \frac{E\left(d_{cp}\right)}{E\left(d_{cp}\right) + E\left(d_{dp}\right)} \tag{5.36}$$

where $E\left(d_{dp}\right)$ and $E\left(d_{cp}\right)$ denote the average distance traveled by forwarded packets (over all cycles of a road segment with infinite length), in the *dp phase* and *cp phase*, respectively, and they are given in equation (5.26) and equation (5.31).

In the *dp phase*, packets are carried by the current moving node and packet delivery ratio is stable, so the value of packet delivery ratio in this phase PDR_{dp} is expressed as

$$PDR_{dp} = 1 \tag{5.37}$$

In the *cp phase*, packets are forwarded hop-by-hop with the effects of the propagation and channel fading, etc. As a result, the packet delivery ratio in this phase is derived as

$$PDR_{cp} = PDR_{1hop}\left(x\right)^{H_{cp}} \tag{5.38}$$

where $PDR_{1hop}\left(x\right)$ denotes the 1-hop packet delivery ratio and it is deduced in equation (4.12) in Chapter 4, $x = \frac{L \cdot r_{cp}}{H_{cp}}$ is the average 1-hop distance and H_{cp} means the hop count which is presented as

$$H_{cp} = \left\lceil \frac{L \cdot r_{cp}}{a \cdot R} \right\rceil = \left\lceil \frac{L \cdot E\left(d_{cp}\right)}{a \cdot R \cdot \left(E\left(d_{cp}\right) + E\left(d_{dp}\right)\right)} \right\rceil \tag{5.39}$$

where L means the length of road segment, R is the communication range and a denotes the cell size parameter.

Based on above analysis, the packet delivery ratio in NP case is given as

$$PDR_{NP} = PDR_{cp} \cdot PDR_{dp} = \left(PDR_{1hop}\left(x\right)\right)^{\left\lceil \frac{L \cdot E\left(d_{cp}\right)}{a \cdot R \cdot \left(E\left(d_{cp}\right) + E\left(d_{dp}\right)\right)} \right\rceil} \tag{5.40}$$

5.3.3.2 Packet delivery ratio in the NC case

In this case, as shown in Fig. 5.2(b), the road segment between I_i and I_j is fully connected, and packets are totally forwarded hop by hop, so the hop count between I_i and I_j is expressed as

$$H_{NC} = \left\lceil \frac{L}{a \cdot R} \right\rceil + 1 \tag{5.41}$$

Obviously, the packet delivery ratio of the 2-lane road segment in the NC case can be given as follows

$$PDR_{NC} = PDR_{1hop}(x)^{H_{NC}} = PDR_{1hop}(x)^{\left\lceil \frac{L}{a \cdot R} \right\rceil + 1} \tag{5.42}$$

where the average 1-hop distance $x = L/H_{NC}$.

Based on the derivations of both NC case and NP case, the average packet delivery ratio in a 2-lane road segment scenario is deduced as

$$PDR = PDR_{NP} \cdot (1 - PC) + PDR_{NC} \cdot PC \tag{5.43}$$

where PC stands for the road segment connectivity probability (deduced in equation (5.14)).

5.4 Packet forwarding algorithm

Many existing geographic forwarding schemes make the selection of the next forwarding hop at transmitter-side usually by means of maximizing the forwarding progress distance. In order to successfully select next forwarding hop, maintaining up-to-date routing lists in these methods are necessary and such behaviors are achieved by frequent Hello packets broadcast, which results in redundant overhead, especially in resource constrained VANET scenarios with heavy traffic load. So as to solve the above challenges, the receiver-side relay election approaches [102, 108, 109] are proposed, in which the current forwarding vehicle broadcasts a RTS message attached data packet transmission information to its neighboring vehicles. Once receiving this RTS message, each neighboring vehicle determines whether it should choose itself as the next forwarding hop by calculating waiting time in terms of several criteria. The waiting time is used to allow better next forwarding hop candidate to reply a CTS message earlier. Here some receiver-side based algorithms for next hop selection are introduced as follows. The method in [103] uses one criterion to compute the waiting time, namely the distance between potential next forwarding hop candidates and destination, but it does not consider the link quality. As a result, data drop ratio and delay increase due to the link failure. Besides, some approaches [108, 109] are proposed in terms of multiple metrics, such as forwarding progress distance, received power and best transmission range. However, they do not take into account the impacts from the interference of neighboring vehicles and wireless channel.

Inspired by the concept of receiver-side relay election approaches, we propose an improved packet forwarding algorithm accounting for forwarding progress distance and BER (derived in equation (4.11)), which is relevant to the signal propagation model, wireless channel model, neighboring interference and modulation schemes, etc. Note that, we neglect the collisions of RTS and CTS due to their short length and instantaneous transmission delay.

5.4.1 Next hop selection process

In AQRV-2 routing protocol, we make use of RTS/CTS exchange scheme to determine the next hop based on the receiver-side concept rather than the sender self-selection.

Firstly, a transmitter C_s broadcasts a RTS frame to the neighbors located in its communication area. Here RTS frames are modified to carry the geographical position of the transmitter C_s and the target next intersection I_j, both of which are used in the next hop selection. In addition, being different from the original RTS/CTS scheme statement that only the intended receiver processes and answers the RTS frame, a flag is inserted to the RTS frame in our algorithm to inform all receiving nodes to process and possibly answer this RTS frame.

Then, when receiving this modified RTS frame, each next hop candidate C_k calculates a waiting time making use of a mapping function which is derived in equation (5.45) in Section 5.4.2. The candidate node C_k broadcasts a CTS frame after this waiting time. Obviously, the waiting time is an indicator of how good a next hop candidate is: the shorter the waiting time, the better the next hop candidate is. The first CTS from one of the candidate nodes indicates that the best next hop node is determined and other candidate nodes need to give the contest up and cancel the waiting time.

Algorithm 3 Self-selection of next hop at candidate node C_k.

Notation:
I_j: target next intersection.
C_s: transmitter node C_s.
C_k: next hop candidate C_k.
C_m: next hop candidate C_m.
t_k: waiting time of C_k.
ID_s, ID_m and ID_k: corresponding ID of C_s, C_m and C_k.
X_j, X_s: corresponding coordinate position on X axis of I_j, C_s.
Y_j, Y_s: corresponding coordinate position on Y axis of I_j, C_s.
****
if receiving $RTS\,(X_s, Y_s, X_j, Y_j, flag)$ from C_s **then**
    Calculate t_k using equation (5.45).
    Set the timer to t_k.
    if $t < t_k$ **then**
        if receiving $CTS\,(ID_s, ID_m)$ from C_m **then**
            stop the timer.
        else
            Continue to overhear CTS frame.
        end if
    else
        Broadcast $CTS\,(ID_s, ID_k)$.
    end if
end if
if receiving a data packet from C_s **then**
    Send back an ACK to C_s.
end if

Finally, once receiving a CTS frame from the best next hop node, the transmitter C_s just forwards the data packet to this node, which then acknowledges this data packet. Note that, if the transmitter receives another correct CTS frame afterwards for the same data packet (for example, the earlier CTS frame broadcast was not heard by some next hop candidates in the communication zone), it simply discards the CTS to avoid any packet duplication. In case of no CTS frame received by the transmitter, it means that the local optimum is met by this transmitter, which will carry the data packets until it finds other appropriate relaying nodes. The detailed processes are presented in Algorithm 3.

5.4.2 Waiting time calculation

The waiting time of each next hop candidate is a key factor to determine the best next hop. An effective waiting time should fulfill three objectives: 1) the waiting time of the best next hop node should be the shortest such that this node can reply CTS earliest, 2) the waiting time difference between the best next hop node and the second best next hop node is large enough, which is beneficial to avoid potential CTS frame collisions,

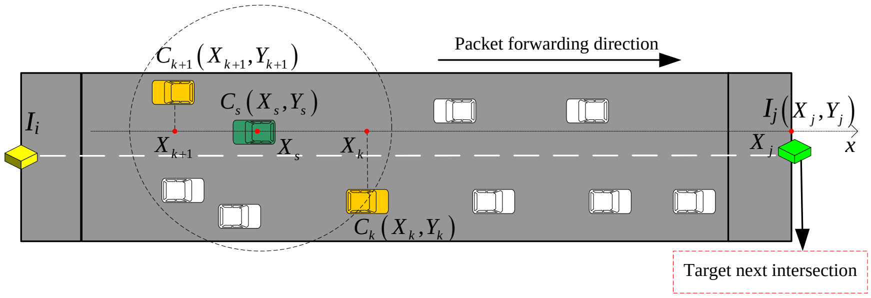

FIGURE 5.3: Forwarding progress distance on a 2-lane road segment.

and 3) the waiting time is as short as possible to avoid unnecessary packet transmission delay. To achieve these goals, we just choose the forwarding progress distance and BER as evaluating parameters for waiting time calculation.

Compared with the communication range of each node, the width of a 2-lane road segment can be neglected, so the forwarding progress distance of the next hop candidate C_k from the transmitter node C_s can be simply expressed as

$$d_{sk} = d_{sj} - d_{kj} = |X_j - X_s| - |X_j - X_k| \tag{5.44}$$

where d_{sj} and d_{kj} denote the distance from C_s to I_j and from C_k to I_j, respectively. X_s, X_k and X_j mean the corresponding coordinate position of C_s, C_k and I_j on the x axis. As shown in Fig. 5.3, we can see that $d_{sk} > 0 > d_{s(k+1)}$.

Based on above analysis, a mapping function, of which the values are restricted in selected $[0, T_{max}]$ interval, is proposed to derive the waiting time. The expression of this mapping function is given as

$$t_k = \begin{cases} \left({T_{\max}}^{\sigma_1} - {T_{\max}}^{\sigma_1} \cdot \left(\frac{d_{sk}}{R}\right)^{\sigma_2} (1 - 2 \cdot BER\,(d_{sk}))^{\sigma_3} \right)^{{\sigma_1}^{-1}} & \text{if } d_{sk} > 0 \\ +\infty & \text{if } d_{sk} \leq 0 \end{cases} \tag{5.45}$$

where t_k denotes the waiting time of C_k, R means the communication range, $BER\,(d_{sk})$ stands for the BER of packet from C_s to C_k. In addition, σ_1, σ_2 and σ_3 are weight parameters to control the nature of relative priority of potential relay nodes, regulate the influences of forwarding progress distance and BER, respectively.

Fig. 5.4 and Fig. 5.5 show the waiting time with different σ_1 values and forwarding progress distances. By means of analyzing the different curves of both the figures, we confirm that lower values of σ_1 lead to shorter waiting time, which is beneficial to decrease the forwarding delay, but far smaller σ_1 makes the curves of waiting time be more smooth in the certain range of forwarding progress distance, and these results reveal that the differences of waiting time are smaller and easily induce CTS collisions. Apparently,

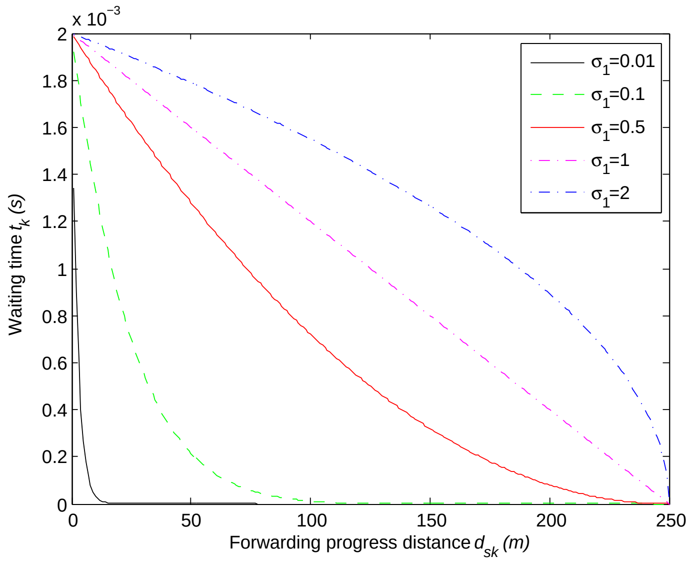

FIGURE 5.4: Waiting time calculated using only forwarding progress distance.

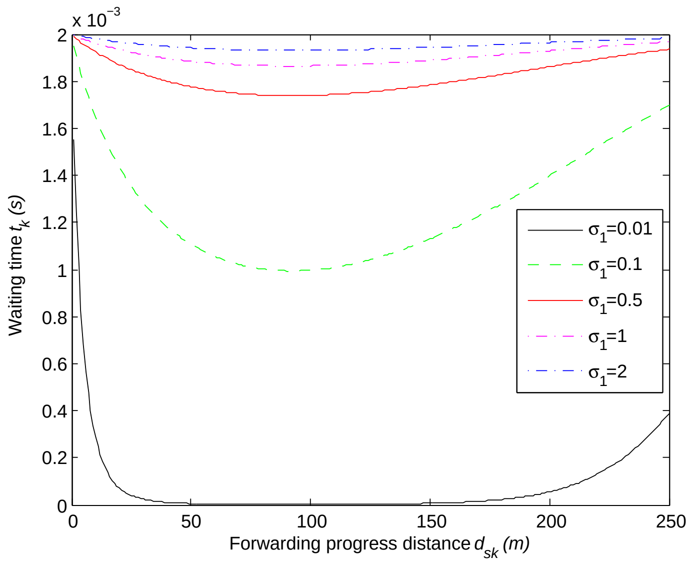

FIGURE 5.5: Waiting time calculated using forwarding progress distance and BER.

a desirable value of σ_1 is very important, here we set $\sigma_1 = 0.1$. In addition, Fig. 5.4 presents that the approach based on only forwarding progress distance favors the node farthest from the transmitter as the next hop, which may lead to packet loss. While from Fig. 5.5, we can see that our proposed method prefers to choose the node around the range $80 \sim 120$ m as the next hop, and this selection can keep a balance between the forwarding progress distance and packet loss ratio.

Fig. 5.6 shows an example that illustrates our proposed data forwarding algorithm. When the transmitter node C_s wants to send a data packet to the next intersection I_j, it first broadcasts a RTS frame to its neighbors specifying its own location and I_j's location. As shown in Fig. 5.6(a), once next hop candidates C_k, C_{k+1}, C_{k+2}, C_{k+3} and C_{k+4} receive

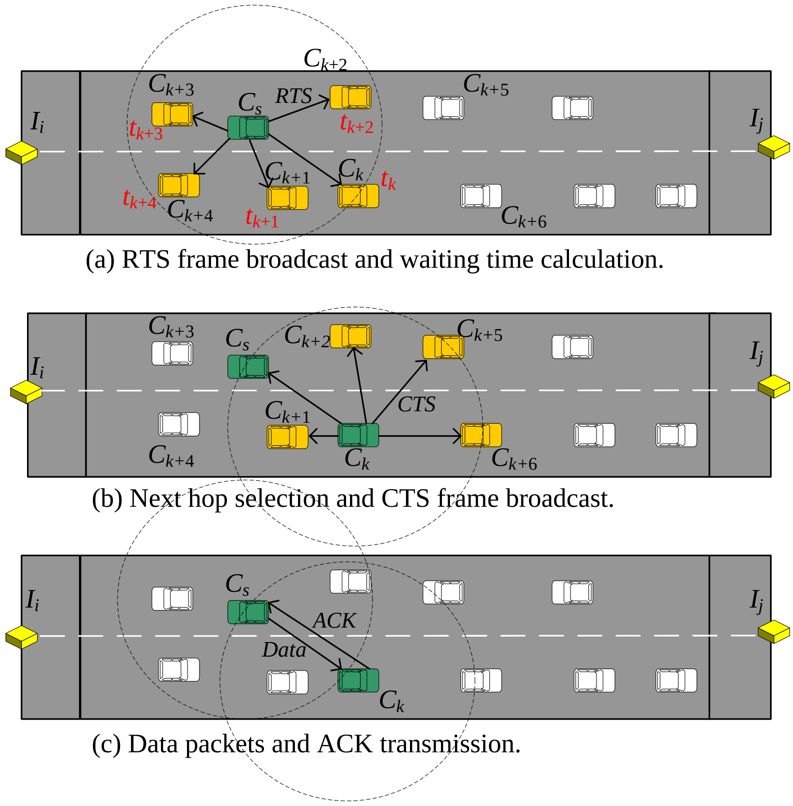

(a) RTS frame broadcast and waiting time calculation.

(b) Next hop selection and CTS frame broadcast.

(c) Data packets and ACK transmission.

FIGURE 5.6: Next hop self-selection example.

this RTS, they calculate their corresponding waiting time and set their timer to prepare to reply a CTS frame to C_s. If C_k owns the shortest waiting time, it will reply C_s a CTS earliest (Fig. 5.6(b)). When C_{k+1} and C_{k+2} hear this CTS frame, they stop their timers and give up the opportunity of next hop selection. Besides, the C_k's neighboring nodes, consisting of C_{k+1}, C_{k+2}, C_{k+5} and C_{k+6}, are not allowed to send any packets to C_k until C_k completes data transmission from C_s due to the effects of the CTS frame broadcast. While receiving CTS from C_k, C_s sends its data packet to C_k, which will reply with an ACK frame if it successfully receives this data packet (indicated in Fig. 5.6(c)). This example shows how this forwarding method can effectively choose the next hop without Hello messages which in return decreases the overhead.

5.5 Performance analysis and evaluation

In this section, the proposed local 2-lane road segment QoS models are firstly validated, and then we evaluate the performance of AQRV-2 routing protocol in comparison with previously proposed AQRV-1, CAR [18] (minimum delay intersection-based routing protocol) and GSR [16] (static shortest distance intersection-based routing protocol.)

Table 5.1: Simulation parameters.

Parameters	value
Urban area scenario size	6000 m × 6000 m
Vehicle mobility model	IDM_IM
Vehicle speed v_1 and v_2	10 ∼ 30 m/s
Vehicle spacing density λ_1 and λ_2	0.01 ∼ 0.03 vehicles/m
Number of CBR flows	300
CBR data packet rate	1 ∼ 5 packet/s
QoS metrics thresholds PC_{th}, PDR_{th} and D_{th}	0.5, 0.7 and 70 ∼ 130 s
Waiting time weight parameter σ_1, σ_2 and σ_3	0.1, 1, 200

5.5.1 Experimental environment

The simulation scenario we consider is a 6000 m × 6000 m area, which consists of 60 intersections and 103 2-lane road segments.

In our vehicle mobility model, we set vehicles safety time and recalculating movement step time as 2 s and 0.5 s, respectively, and the initial position and trip of moving vehicles are selected randomly. In addition, we utilize the IEEE 802.11p at the MAC layer, set the maximum channel transmission rate to 3 Mbps and make the communication range R varies between 200 m ∼ 350 m. Finally, we randomly initiate 300 constant bit rate (CBR) sessions and set the data packet size to 512 Bytes. In our experiments, the simulation time duration is fixed to 6000 seconds and each simulation scenario is repeated 30 times with different seeds to guarantee good confidence intervals for the results. The main simulation parameters are listed in Table 5.1, other remaining parameters about AQRV-2 are same as the ones used in AQRV-1 which are given in Table 4.1.

5.5.2 Validation and analysis of 2-lane local QoS models

(1) Connectivity probability of 2-lane road segment
Fig. 5.7 depicts the road segment connectivity probability for different communication ranges and cell sizes. As we expected, this figure shows the corresponding upper and lower thresholds of the road segment connectivity when cell size cs equals R and $0.5R$, respectively. When $cs = 0.7R$, the theoretical results are in accordance with the simulation results (95% confidence interval (CI), and average difference is 4.38%). Moreover, when increasing the communication range R, the connectivity is improved due to the repairs of the road segment network partitions. Fig. 5.8 presents the road segment connectivity probability with varying vehicle spacing densities for the Eastbound and Westbound lanes. From this figure, we can see that connectivity probability is proportional to the vehicle spacing density, as more vehicles can overcome network holes and repair broken links.

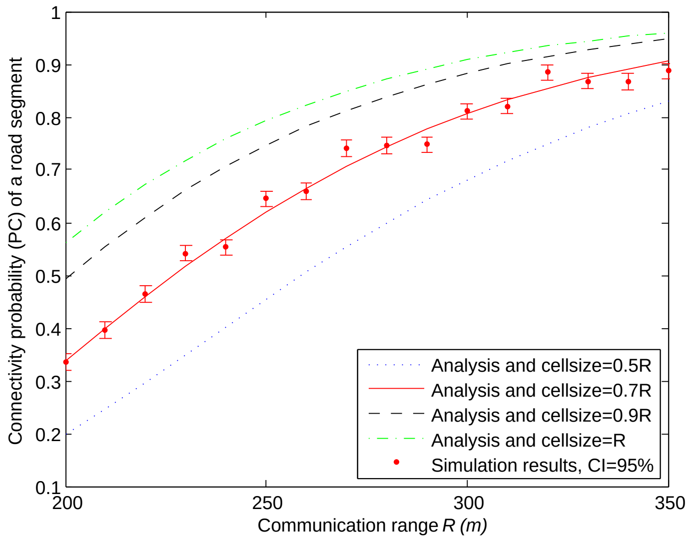

FIGURE 5.7: Road segment connectivity probability. Here road segment length $L =$ 1500 m, vehicle spacing density λ_1= 0.01 vehicles/m and λ_2= 0.005 vehicles/m.

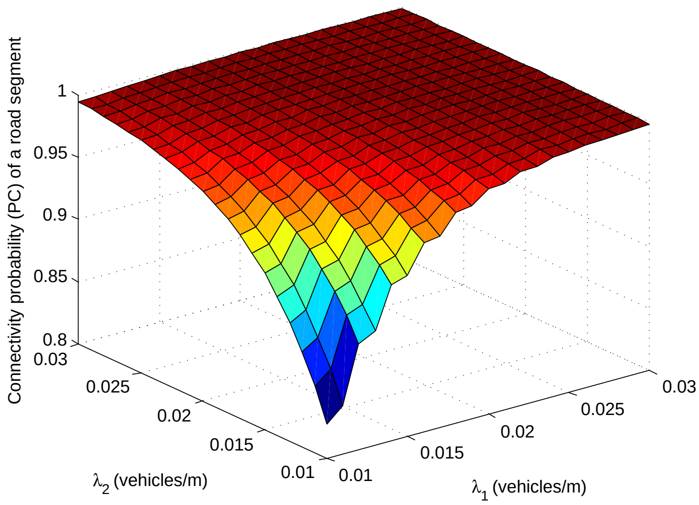

FIGURE 5.8: Road segment connectivity probability. Here communication range $R =$ 250 m,
cell size parameter a=0.7 and $L = 1500$ m.

(2) Delay of 2-lane road segment

Fig. 5.9 describes the correlations among the road segment transmission delay, communication range and cell size. When $cs = 0.7R$, the analytical and simulation results are in good agreement, and show a small difference of 3.02% in average. In addition, we observe that when the communication range increases, the road segment transmission delay significantly decreases, as the road segment connectivity is enhanced and the data packets can be transmitted mainly using wireless communications. Fig. 5.10 shows the road segment transmission delay as a function of the vehicle speed and road segment length. In this figure, the differences between analytical results and simulation results are only 2.96% and 3.17% for the curves with $L = 1000$ m and $L = 1500$ m, respectively.

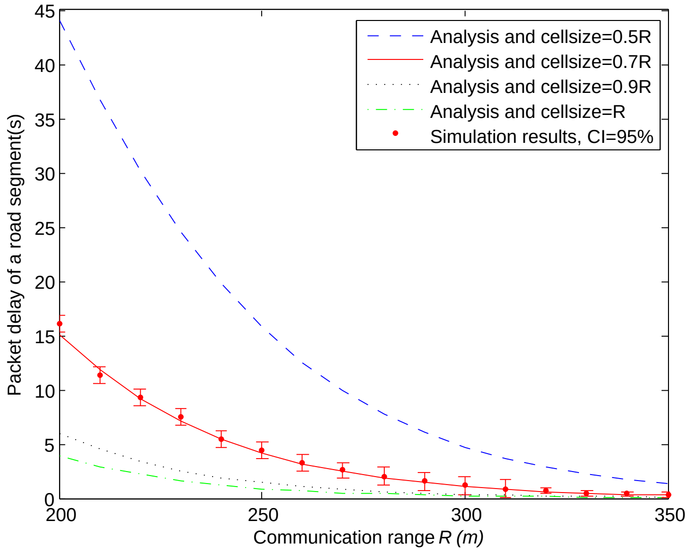

FIGURE 5.9: Road segment delay. Here $L = 1500$ m, $\lambda_1 = 0.01$ vehicles/m and $\lambda_2 = 0.005$ vehicles/m.

Besides, since we utilize greedy carry-and-forward to transmit data packets, when suffering from network partitions, data packets are carried by forwarding vehicles, and as the transmission delay mainly depends on the vehicle speed in this case, the transmission delay on the road segment decreases with the vehicle speed augmentation. In Fig. 5.11, the transmission delay on a road segment is given as a function of the vehicle spacing density and communication range. We observe that the gap between the theoretical and the simulation results are only about 3.78% and 2.70% for the curves with $R = 200$ m and $R = 250$ m, respectively. In addition, the transmission delay is inversely proportional to the vehicle spacing density, because the wireless network partitions are repaired and more packets can be forwarded through wireless communications. Moreover, higher communication range is advantageous to the improvement of network connectivity, which in return decreases the packet delay.

(3) Packet delivery ratio of 2-lane road segment

From Fig. 5.12, we see that the average error between the theoretical results and simulation results is only 3.91% when $cs = 0.7R$. In addition, when road segment length rises, the packet delivery ratio decreases due to more communication hops. Fig. 5.13 proves the availability of the packet delivery ratio model with the varying interference range and channel transmission data rate (CTR). As we expected, packet delivery ratio declines with the increase of CTR, which leads to lower SINR and higher BER. Besides, packet delivery ratio is more important for smaller interference range values, which can alleviate the interfering effects from the neighboring nodes.

According to the above investigations, when $cs = 0.7R$, the difference between theoretical results and average simulation results is within $\pm 5\%$, which proves the correctness of our

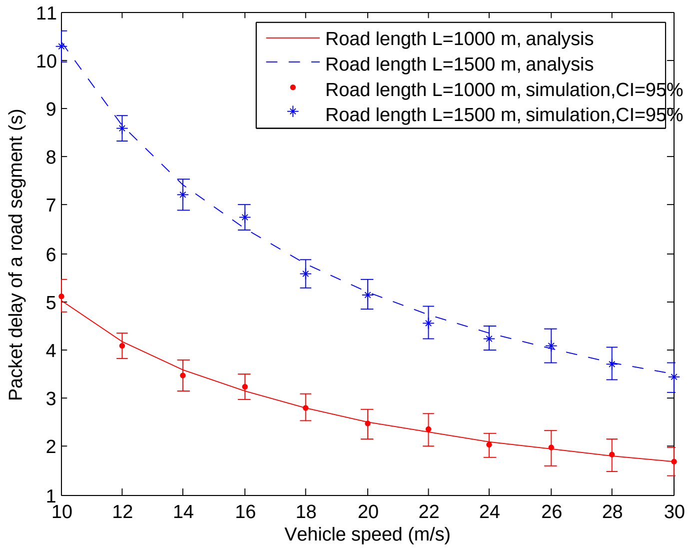

FIGURE 5.10: Road segment delay. Here $R = 250$ m, $\lambda_1 = 0.01$ vehicles/m, $\lambda_2 = 0.005$ vehicles/m and a=0.7.

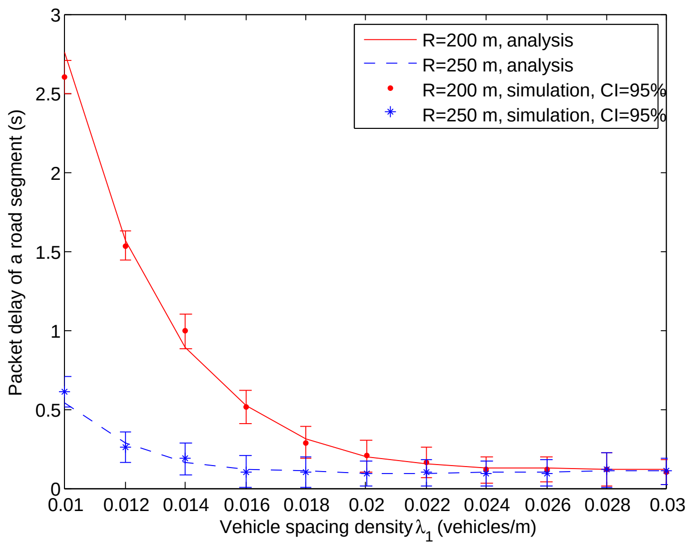

FIGURE 5.11: Road segment delay. Here $L = 1500$ m, $\lambda_2 = 0.01$ vehicles/m and a=0.7.

proposed analytical models for the QoS metrics of a 2-lane road segment.

5.5.3 AQRV-2 routing protocol performance evaluation

(1) End-to-end packet delivery ratio analysis

From Fig. 5.14, we can see that AQRV-2 achieves the highest packet delivery ratio compared with GSR and CAR. There are two main reasons to explain this outcome. Firstly, AQRV-2 dynamically chooses the best routing path with the highest communication QoS including packet delivery ratio, which makes the selected path be with appropriate

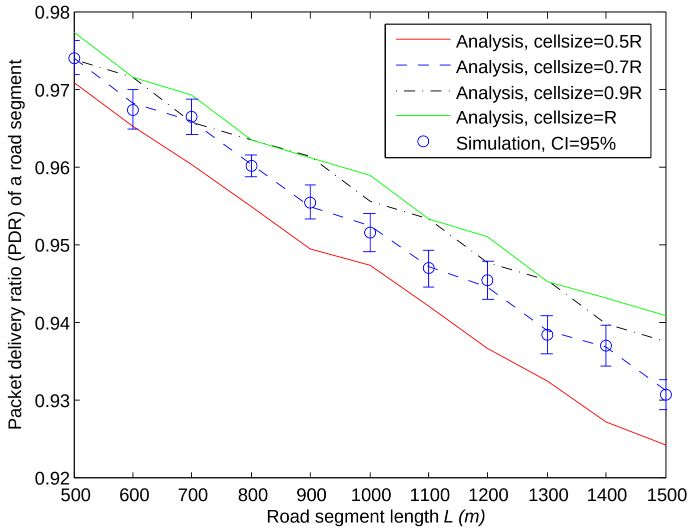

FIGURE 5.12: Road segment packet delivery ratio. Here vehicle spacing density $\lambda_1 = \lambda_2 = 0.01$ vehicles/m and interference range $R_{inf} = R = 250$ m.

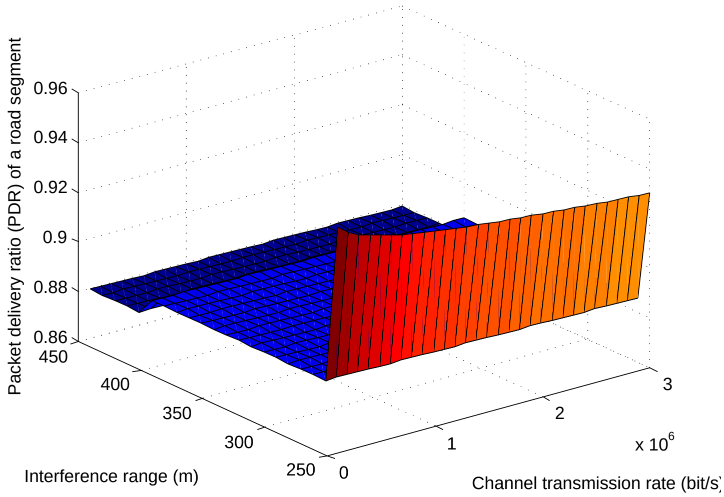

FIGURE 5.13: Road segment packet delivery ratio. Here $R = 250$ m, a=0.7, $L = 1500$ m, and $\lambda_1 = \lambda_2 = 0.02$ vehicles/m.

vehicle density and avoids congested road segments. Secondly, AQRV-2 searches available routing paths utilizing ACO algorithm, which offers a dynamic routing adaption as different communication pairs cooperate with each other to update latest pheromone immediately and cope with rapid topology changes. However, CAR provides only one complete end-to-end routing path, which is not adapted to the dynamic VANET environments and hence results in higher packet loss. GSR only considers the distance to the destination but neglects other available routing information, so some data packets may be dropped when suffering from congestions. This figure also indicates that all protocols experience higher packet delivery ratio with lower vehicle spacing density. The reason is as follows: when vehicle spacing density rises, network connectivity is better and data

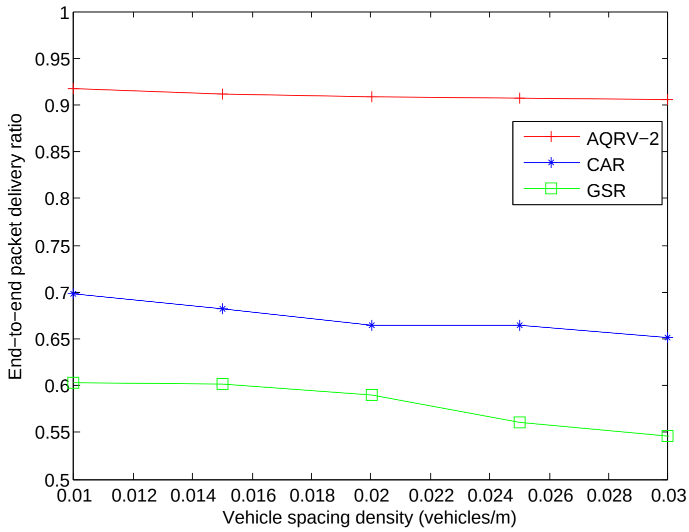

FIGURE 5.14: End-to-end packet delivery ratio.

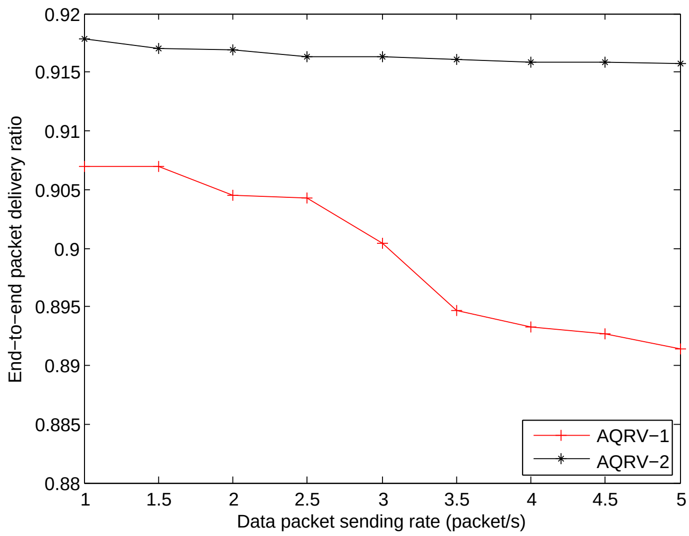

FIGURE 5.15: End-to-end packet delivery ratio.

packets are almost transmitted through wireless links, so compared with the vehicles carrying situations, these data packets may suffer from more channel fading effects, which lead to worse packet delivery ratio.

Fig. 5.15 presents the end-to-end packet delivery ratio as a function of packet sending rate. This figure shows that the packet delivery ratio of AQRV-2 is better than that of AQRV-1. The reasons are as follows. 1) In AQRV-2 routing protocol, we propose a new data forwarding scheme, which makes use of RTC/CTS scheme to choose next forwarding hop. This mechanism efficiently decreases the overhead and significantly alleviates the influences of heavy traffic load. 2) We define a threshold of packet delivery ratio in the objective function of AQRV-2, so the routes with lower packet delivery ratio are ignored.

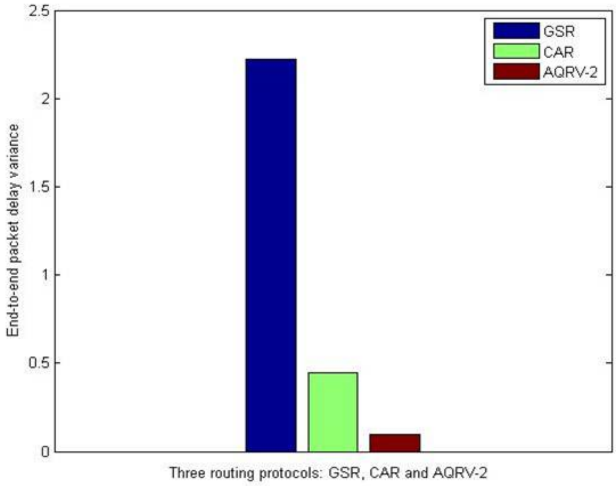

FIGURE 5.16: End-to-end delay variance.

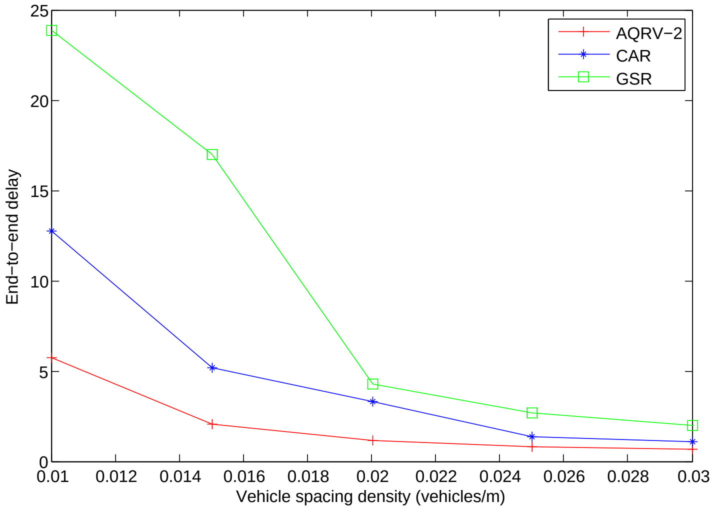

FIGURE 5.17: End-to-end delay.

(2) End-to-end delay analysis

Fig. 5.16 shows the transmission delay variance of three routing protocols, namely GSR, CAR and AQRV-2. It clearly represents that the delay variance in AQRV-2 is smaller than the corresponding one for GSR and CAR, so the routing paths selected by AQRV-2 are more stable. This is because: Firstly, AQRV-2 takes transmission delay variance into account in the processes of available routes exploration and selection. Secondly, the best route of AQRV-2 is confirmed on the basis of both local and global communication quality, which is conductive to maintain stable routes and alleviate data packets suffering from bad traffic conditions, such as routing holes or heavy congestions.

Fig. 5.17 depicts the end-to-end average transmission delay as a function of vehicle density. This figure shows that AQRV-2 provides the lowest transmission delay compared with both reference routing protocols. By using ACO algorithm, AQRV-2 enables the collaboration between different communication pairs to update latest global pheromone, which is profitable to adjust to rapid network topology changes and reduce the transmission delay. In the case of GSR, data packets are forwarded using the same path because of the shortest-distance path rule, which makes the routing protocol unable to adapt to rapid topology changes. CAR is a min-delay routing protocol but can not update routing information in time, so upcoming data packets may suffer from network partitions which result in higher transmission delays. Besides, as expected, the transmission delay of all routing protocols is inversely proportional to the vehicle spacing density. The delay increases substantially in sparse network situations due to the repairs of network holes.

In order to deepen the investigation of the end-to-end delay components, we present them in Fig. 5.18 for AQRV-2 routing protocol for different vehicle spacing density scenarios. The packet delay in AQRV-2 consists of four parts: the delay of route establishment given by ants for per data packet, the carrying delay when a packet is carried by moving vehicles, the retransmission delay and the delay without retransmission. From this figure, we can see that the ratio of the carrying delay reduces with the increase of vehicle spacing density, while the wireless communication delay ratio (including the retransmission delay and the delay without retransmission) is proportional to the vehicle spacing density. The reason is that higher vehicle spacing density is beneficial to the network partition repairs, which make more data packets be transmitted hop by hop rather than carried by moving vehicles. In addition, the retransmission delay proportion rises with the increase of vehicle spacing density, because higher vehicle spacing density implies that there may be more severe neighboring vehicles' interference, which exacerbates successful packets transmission and causes more retransmission attempts. Finally, we note that the proportion of the route establishment delay for per data packet is almost stable with various vehicle spacing densities and shows a small value compared to other delay components.

(3) Overhead analysis

Fig. 5.19 represents the network overhead for different of vehicle spacing densities. As stated in previous chapters, we define the overhead as the ratio between the total control packets bytes and the cumulative bytes of successfully received data packets. Compared with other routing protocols, AQRV-2 shows the lowest overhead. Based on the latest global pheromone, AQRV-2 protocol dynamically chooses best route to forward data packets, which can achieve better packet delivery ratio and thus reduce the overhead. Besides, AQRV-2 makes use of terminal intersection concept to reduce redundant route explorations, which in return reduce the overhead. Moreover, compared with other geographic-based routing protocols, Hello packets are not required to exchange geographical information to select next hop in the proposed data forwarding algorithm of AQRV-2. Obviously, this scheme can dramatically decrease the overhead. Fig. 5.19 also indicates

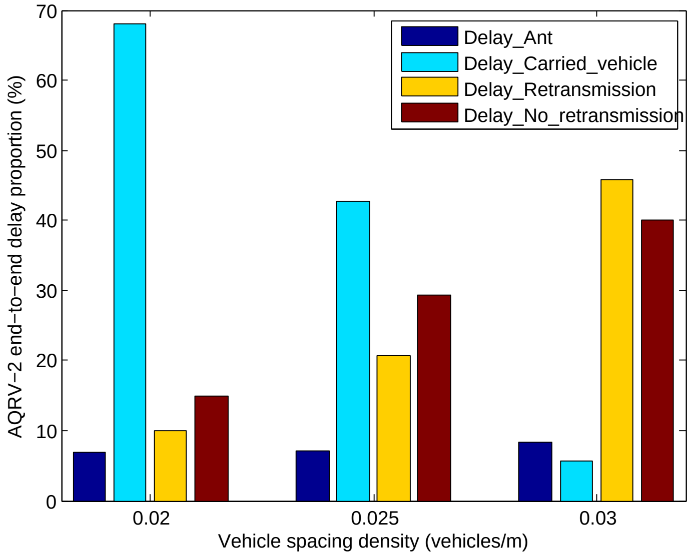

FIGURE 5.18: End-to-end delay components of AQRV-2.

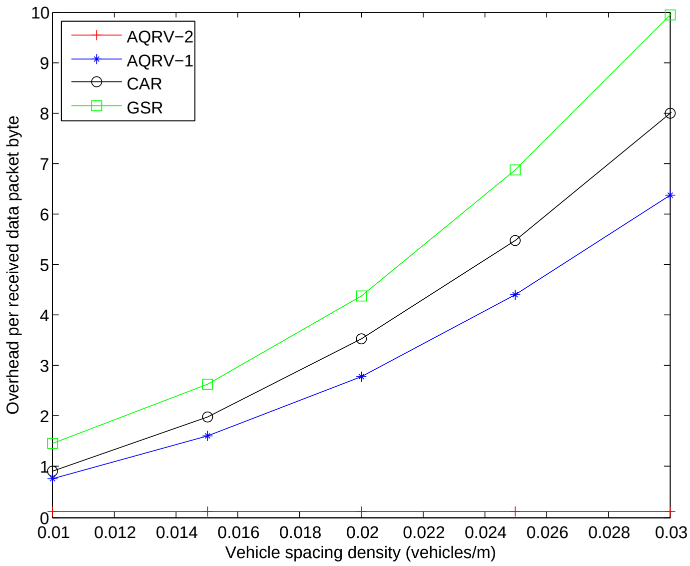

FIGURE 5.19: Overhead vs vehicle spacing density.

that the overhead for all protocols increases for higher vehicle densities, because Hello control packets occupy an important proportion of the whole generated overhead, and their number is mainly determined by vehicle spacing density.

(4) Analyzing the impact of forward ants number on AQRV-2

In this simulation experiment, we set the vehicle spacing density as 0.01 vehicles/m. Here we make use of three QoS parameters: connectivity probability, delay and packet delivery ratio (the three of them are used by ants to search the best route) to evaluate the normalized QoS. From Table 5.2, we can see that the QoS is proportional to the forward ants number, because generating more ants can enhance AQRV-2's global exploration ability and find more candidate routing paths, which is advantageous to the best route

TABLE 5.2: The influences of forward ants number.

N_{fant}	QoS	Route establishment time	Overhead
10	0.7035	0.1676 s	0.0341
20	0.8213	0.2865 s	0.0612
50	0.8805	0.3521 s	0.1704
100	0.8897	0.4890 s	0.3607
200	0.8898	1.1688 s	0.6914

confirmation. However, since the rise of forward ants improves the randomness of routing exploration, the best route's convergence rate is slower and the route establishment time for per communication pair increases. In addition, when the number of forward ants rises from 50 to 200, the QoS gains a little improvement, but the overhead and the route establishment time deteriorate rapidly. Obviously, the number of forward ants plays an important role in the performance of AQRV-2, and in our previous experiments, we set the forward ants number to 50, which makes AQRV-2 achieve a good balance between the QoS, route establishment time and overhead.

(5) Analyzing the impact of delay threshold D_{th} on AQRV-2
Fig. 5.20 and 5.21 show the effects of delay threshold on the end-to-end delay and packet delivery ratio respectively, of a selected backbone route of AQRV-2 routing protocol. The increase of the delay threshold will allow packets to be carried by more and more forwarding vehicles and the selected route might more likely be with low vehicle density, which makes packet delivery require higher delay, as shown in Fig. 5.20. On the other hand, the selected route with sparse vehicles can decrease the contention in the network and alleviate neighbors' interference, which is beneficial to improve packet delivery ratio shown in Fig. 5.21.

5.6 Summary

In this chapter, an enhanced version of AQRV-1 routing protocol naming after AQRV-2 is proposed, and it is suitable for the city environment with 2-lane roads layout and satisfies with multiple QoS requirements. In order to cope with the mentioned challenges, we firstly design a new system model to meet the demands of multiple QoS metrics and QoS thresholds in terms of connectivity probability, delay and packet delivery ratio. Then, by means of vehicles mobility characteristics, vehicles spacing density and so on, we propose mathematical models to estimate local QoS for 2-lane road segments, which are more realistic than 1-lane road segments in urban scenarios investigated in AQRV-1. In addition, an improved packet forwarding algorithm is proposed to relay packets between two neighboring intersections. The simulation results validate the accuracy

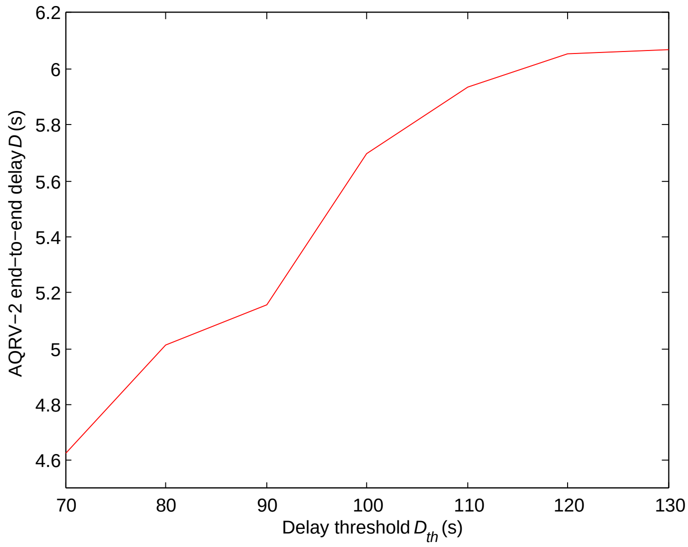

FIGURE 5.20: AQRV-2 end-to-end delay.

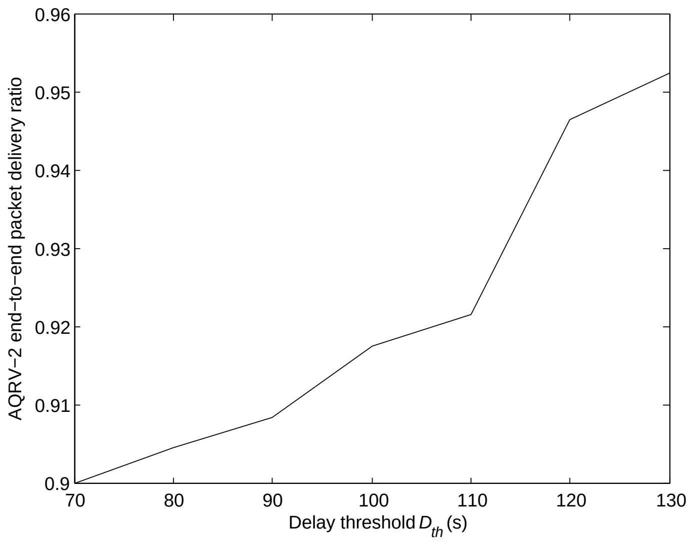

FIGURE 5.21: AQRV-2 end-to-end packet delivery ratio.

of our deduced local 2-lane road segment models for connectivity probability, packet delivery ratio and delay, and indicate that the communication performances of AQRV-2 outperform AQRV-1, GSR and CAR routing protocols. Afterwards, we present the advantages of proposed packet forwarding algorithm which is beneficial to the decrease of overhead and alleviation of network congestion, and investigate the impact of related parameters (such as QoS thresholds and forward ants number) on AQRV-2 .

Chapter 6

Conclusion and Future works

6.1 Conclusion

Many challenges characterize the VANET routing research field, such as scalability, redundant overhead, inadaptation to rapid topology changes, high exploration delay and so on. In this thesis, for the purpose of solving mentioned issues, we propose adaptive routing protocols in urban scenarios to establish the best route owning the best QoS in terms of connectivity probability, delay and packet delivery ratio. In these routing protocols, we regard the routing issues as combinatorial nonlinear optimization problems, and then propose the ACO-based algorithms to resolve them.

First of all, we propose an intersection-based routing protocol called AQRV and it makes use of reactive and proactive components to establish and maintain best QoS routing path from source to destination, respectively. Thanks to the features of ACO, AQRV can make different forward ants collaborate closely to search candidate available routes and update the latest routing information. Besides, compared to the blind flooding mechanisms (such as RREQ-RREP scheme), we implement an opportunistic method to relay forward ants based on global QoS, expressed in terms of real time connectivity probability, delay and packet delivery ratio, which are estimated by periodic packets forwarding between two neighboring intersections. This method can accelerate the convergence of the best route, decrease network overhead, improve the stability of routing path and avoid extreme routing conditions in the upcoming route selections. In data packets forwarding session, AQRV dynamically chooses the best next intersection for the data packets forwarding destination using best global pheromone available at the current intersection, and when relayed between two adjacent intersections, data packets are forwarded by a simple greedy carry-and-forward mechanism to alleviate the effects of the movements of individual nodes. The simulation results reveal that AQRV shows better routing performance in terms of packet delivery ratio and delay but generates higher overhead compared with reference routing protocols (GSR and CAR).

In order to further improve the efficiency of AQRV and decrease the amount of overhead, we proposed an enhanced routing protocol called AQRV-1 for 1-lane road layout urban scenarios. Compared with AQRV, the main contributions of AQRV-1 are as follows. Firstly, by taking advantage of traffic information in urban environments (such as vehicle density, road segment length, vehicle distribution, vehicle speed and traffic load, etc.), we propose three corresponding mathematical models for 1-lane road segment to estimate its real-time local QoS (namely connectivity probability, packet delivery ratio and delay), which can easily evaluate more accurate local road segment QoS, decrease operation time, reduce energy consumption and alleviate network congestion compared with the periodic packets forwarding scheme in AQRV. Secondly, based on the proposed TI model, AQRV-1 explores the best backbone route between two terminal intersections instead of end-to-end vehicle communication pairs, so this method can make a group of communication pairs with the same TID directly implement data packets forwarding sessions by sharing the explored paths to decrease routing exploration time and network overhead. Moreover, instead of only global pheromone in AQRV, AQRV-1 makes use of reactive forward ants to explore candidate routes based on both local and global pheromone, which helps to keep the balance between the new routing paths exploration and the best route exploitation. Finally, we proposed a new routing maintenance mechanism to contribute in network's overhead reduction. The simulation results validate our analytical local QoS models and demonstrate that AQRV-1 outperforms the reference protocols (AQRV, GSR and CAR). However, AQRV-1 is a QoS-based routing protocol with only delay constraint, which is not enough for various applications with different QoS requirements. In addition, data packets are forwarded between two intersections using the simple greedy carry-and-forward algorithm, which requires frequent Hello broadcasting to update latest geographical information among neighboring nodes, the routing QoS may be even aggravated in heavy traffic load networks because of channel congestions. Moreover, the mathematical QoS models in AQRV-1 are suitable for 1-lane road segments, and we want to design the analyzing QoS models for 2-lane road segments, which are more realistic in urban environments.

Based on above discussion and analysis of AQRV-1, we propose an improved routing protocol AQRV-2, which establishes the best QoS routing path in 2-lane road layout environments. First of all, we design a new system model considering three thresholds of QoS metrics, namely connectivity probability, delay and packet delivery ratio, to meet the requirements of various applications. In addition, making use of the basic concept of receiver-side relay election, we propose a new packet forwarding algorithm, which makes neighboring nodes select the best next hop by themselves based on waiting time. Compared with previous method used in AQRV-1, this scheme avoids Hello packets broadcasting by each node for geographic information exchange and is beneficial to significantly decrease overhead in congested networks. Furthermore, we propose three mathematical QoS models expressing the same QoS metrics: connectivity probability, packet delivery ratio and delay for 2-lane road layout scenarios. The simulation results prove that our deduced local 2-lane road segment models are valid. Besides, we analyze the communication performance of AQRV-2 by considering the impacts of various design parameters such as forward ants number and delay thresholds. The results confirm the efficiency of AQRV-2 compared to other reference protocols (AQRV-1, GSR and CAR).

6.2 Future works and perspective

There are still many challenges to cope with in VANET field, which expand several new research directions to extend some proposals or consider further complementary developments. Based on profound investigations and considerations, the possible directions are as follows.

(1) Propose available evaluation methods to analyze the effects of weight parameters in our routing protocols, such as α and β regulating the local and global pheromone, and φ_1, φ_2 and φ_3 adjusting corresponding connectivity probability, packet delivery ratio and delay.

(2) Investigate other optimization methods and compare their performance as regards to ACO algorithm, and then draw up the conclusions related to the efficiency and availability of our routing protocols.

(3) Because of the key roles of vehicle movement in VANET research field and the complexities of city scenarios characteristics, it is very challenging to design an accurate mobility model of vehicles to reflect and induce fully realistic urban environments. Therefore, it would be interesting to design some advanced mobility models and apply such models in the core of the routing functions.

(4) Security. Since VANETs information transmission is distributed in an open access environment and it is very easy to suffer from various attacks, for example, some hackers attempt to modify the forwarding public information so as to result in serious accidents and make the traffic be in chaos. It would be interesting to investigate how to integrate such security function into the design mechanisms of the routing protocol for VANETs.

(5) Big data technologies. The applications of VANETs in urban scenarios are usually in need of real-time mobility support, location awareness and efficient geo-distributed

RSU. It is very meaningful to apply the big data technologies to VANETs, and then one can gain useful insight from a huge amount of operational data to improve traffic management processes such as planning, engineering and operations.

Appendix A

A list of publications

A.1 International conference papers

[1] G. Li and L. Boukhatem. An Intersection-based Delay Sensitive Routing for VANETs Using ACO Algorithm. In *Proc. IEEE International Conference on Computer Communications and Networks (ICCCN'14)*, pages 1-8, Shanghai, China, Aug. 2014.

[2] G. Li and L. Boukhatem. Adaptive Vehicular Routing Protocol based on Ant Colony Optimization. In *Proc. ACM International Workshop on Vehicular Inter-Networking, Systems, and Applications (VANET'13)*, pages 95-98, Taipei, Taiwan, May 2013.

[3] G. Li and L. Boukhatem. A Delay-Sensitive Vehicular Routing Protocol Using Ant Colony Optimization. In *Proc. IEEE Mediterranean Ad Hoc Networking Workshop (MED-HOC-NET'13)*, pages 49-54, Ajaccio, Corsica, France, Jun. 2013.

A.2 Published journal papers

[1] G. Li, L. Boukhatem, and S. Martin. An Intersection-based QoS Routing in Vehicular Ad Hoc Networks. *ACM Mobile Networks & Applications (ACM MONET)*, 20(2):268-284, Feb. 2015.

A.3 Unpublished journal papers

[1] G. Li, L. Boukhatem. An Adaptive QoS-based Routing for VANETs using ACO Algorithm. *IEEE Transactions on Intelligent Transportation Systems (IEEE T-ITS)* (under review).

[2] G. Li, L. Boukhatem. Multiple QoS Vehicular Routing in Urban Scenarios combining ACO and Fuzzy-based Algorithms. *IEEE Transactions on Vehicular Technology (IEEE TVT)* (under review).

Bibliography

[1] V. Tiwari, K. Vyas, and N. Goyal. Gain enhancement of a cpw - fed horse shoe shaped slot antenna with defected ground structures for wimax/wlan applications. In *Proc. IEEE Recent Advances and Innovations in Engineering (ICRAIE'14)*, pages 1–5, Jaipur, India, May 2014.

[2] F. Aurzada, M. Levesque, M. Maier, and M. Reisslein. Fiwi access networks based on next-generation pon and gigabit-class wlan technologies: a capacity and delay analysis. *ACM Transactions on Networking*, 22(4):1176–1189, Aug. 2014.

[3] J. Yoon, H. Zhang, S. Banerjee, and S. Rangarajan. Video multicast with joint resource allocation and adaptive modulation and coding in 4g networks. *ACM Transactions on Networking*, 22(5):1531–1544, Oct. 2014.

[4] A. Ghazal, C. Wang, B. Ai, D. Yuan, and H. Haas. A nonstationary wideband mimo channel model for high-mobility intelligent transportation systems. *IEEE Transactions on Intelligent Transportation Systems*, 16(2):885–897, Apr. 2015.

[5] R. Jalali, K. El-khatib, and C. McGregor. Smart city architecture for community level services through the internet of things. In *Proc. IEEE Intelligence in Next Generation Networks (ICIN'15)*, pages 108–113, Paris, France, Feb. 2015.

[6] N Kumar, N Chilamkurti, and Joel J Rodrigues. Learning automata-based opportunistic data aggregation and forwarding scheme for alert generation in vehicular ad hoc networks. *IEEE Computer Communications*, 39(7):22–32, Feb. 2014.

[7] M. Conti and S. Giordano. Mobile ad hoc networking: milestones, challenges, and new research directions. *IEEE Communications Magazine*, 52(1):85–96, Jan. 2014.

[8] J. Liu, H. Nishiyama, N. Kato, J. Ma, and X. Jiang. Throughput-delay tradeoff in mobile ad hoc networks with correlated mobility. In *Proc. IEEE International Conference on Computer Communications (INFOCOM'14)*, pages 2768–2776, Toronto, Canada, Apr. 2014.

[9] S. Sultan, M. Doori, A. Bayatti, and H. Zedan. A comprehensive survey on vehicular ad hoc network. *Journal of Network and Computer Applications*, 37(1): 380–392, Jan. 2014.

[10] I. Leontiadis and C. Mascolo. Geopps: geographical opportunistic routing for vehicular networks. In *Proc. IEEE World of Wireless, Mobile and Multimedia Networks (WOWMOM'07)*, pages 1–6, Espoo, Finland, Jun. 2007.

[11] Z. Mo, H. Zhao, K. Makki, and N. Pissinou. Muru: a multi-hop routing protocol for urban vehicular ad hoc networks. In *Proc. IEEE International Conference on Mobile and Ubiquitous Systems: Networking & Services (MOBIQ'06)*, pages 1–8, California, USA, Jul. 2006.

[12] D. Yong, W. Chen, and X. Li. A static-node assisted adaptive routing protocol in vehicular networks. In *Proc. ACM International Workshop on Vehicular Ad Hoc Networks (VANET'07)*, pages 59–68, Montreal, Canada, Sep. 2007.

[13] M. Altayeb and I. Mahgoub. A survey of vehicular ad hoc networks routing protocols. *International Journal of Innovation and Applied Studies*, 3(3):829–846, Jul. 2013.

[14] B. Karp and H. Kung. Gpsr: greedy perimeter stateless routing for wireless networks. In *Proc. ACM International Conference on Mobile Computing and Networking (MOBICOM'00)*, pages 243–254, New York, USA, Aug. 2000.

[15] C. Lochert, M. Mauve, H. Fusler, and H. Hartenstein. Geographic routing in city scenarios. *ACM SIGMOBILE Mobile Computing and Communications Review*, 9 (1):69–72, Jan. 2005.

[16] C. Lochert, H. Hartenstein, D. Hermann, and M. Mauve. A routing strategy for vehicular ad hoc networks in city environments. In *Proc. IEEE Intelligent Vehicles Symposium Proceedings (IVS'03)*, pages 156–161, Columbus, USA, Jun. 2003.

[17] B. Seet, G. Liu, B. Lee, C. Foh, and K. Wong. A-star: a mobile ad hoc routing strategy for metropolis vehicular communications. In *Proc. IEEE Networking Conference (NETWORKING'04)*, pages 989–999, Athens, Greece, May 2004.

[18] V. Naumov and T. Gross. Connectivity-aware routing (car) in vehicular ad hoc networks. In *Proc. IEEE International Conference on Computer Communications (INFOCOM'07)*, pages 1919–1927, Anchorage, USA, May 2007.

[19] Q. Yang, A. Lim, S. Li, J. Fang, and P. Agrawal. Acar: adaptive connectivity aware routing protocol for vehicular ad hoc networks. In *Proc. IEEE International*

Conference on Computer Communications and Networks (ICCCN'08), pages 1–6, St. Thomas, USA, Aug. 2008.

[20] C. Ma and N. Liu. Traffic-aware data delivery scheme for urban vehicular sensor networks. *International Journal of Distributed Sensor Networks*, 9(4):1–12, Aug. 2013.

[21] S. Wankhade and M. Ali. Ant based techniques for qos routing in mobile ad hoc network: an overview. *International Journal of Advanced Networking and Applications*, 3(3):1094–1097, Jun. 2011.

[22] C. Perkins and E. Royer. Ad-hoc on-demand distance vector routing. In *Proc. IEEE Workshop on Mobile Computing Systems and Applications (WMCSA'99)*, pages 90–100, Los Angeles, USA, Feb. 1999.

[23] J. Zhao and G. Cao. Vadd: vehicle-assisted data delivery in vehicular ad hoc networks. *IEEE Transactions on Vehicular Technology*, 57(3):1910–1922, May 2008.

[24] H. Alshaer and E. Horlait. An optimized adaptive broadcast scheme for inter-vehicle communication. In *Proc. IEEE Vehicular Technology Conference (VTC'05)*, pages 2840–2844, Stockholm, Sweden, May 2005.

[25] R. Mangharam, R. Rajkumar, M. Hamilton, P. Mudalige, and B. Fan. Bounded-latency alerts in vehicular networks. In *Proc. IEEE Mobile Networking for Vehicular Environments (MOVE'05)*, pages 55–60, Anchorage, USA, May 2007.

[26] J. Lee, C. Wang, and M. Chuang. Fast and reliable emergency message dissemination mechanism in vehicular ad hoc networks. In *Proc. IEEE Wireless Communications and Networking Conference (WCNC'10)*, pages 1–6, Cancun, Mexico, Apr. 2010.

[27] Y. Zhuang, J. Pan, Y Luo, and L. Cai. Time and location critical emergency message dissemination for vehicular ad-hoc networks. *IEEE Journal on Selected Areas in Communications*, 29(1):187–196, Jan. 2011.

[28] D. Ni, S. Andrews J. Li, and H. Wang. Preliminary estimate of highway capacity benefit attainable with intelligent drive technologies. In *Proc. IEEE Conference on Intelligent Transportation Systems (ITSC'10)*, pages 819–824, Madeira Island, Portugal, Sep. 2010.

[29] Y. Liu and U. Ozguner. Effect of inter-vehicle communication on rear-end collision avoidance. In *Proc. IEEE Intelligent Vehicles Symposium (IVS'03)*, pages 168–173, Columbus, USA, Jun. 2003.

[30] R. Tatchikou, S. Biswas, and F. Dion. Cooperative vehicle collision avoidance using inter-vehicle packet forwarding. In *Proc. IEEE Global Telecommunications Conference (GLOBECOM'05)*, pages 2762–2766, Saint Louis MO, USA, Dec. 2005.

[31] P. Seiler, A. Pant, and K. Hedrick. Disturbance propagation in vehicle strings. *IEEE Transactions on Automatic Control*, 49(10):1835–1842, Oct. 2004.

[32] L. Li and F. Wang. Cooperative driving at blind crossings using inter-vehicle communication. *IEEE Transactions on Vehicular Technology*, 55(6):1712–1724, Nov. 2006.

[33] T. Delot, N. Cenerario, S. Ilarri, and S. Lecomte. A cooperative reservation protocol for parking spaces in vehicular ad hoc networks. In *Proc. ACM International Conference on Mobile Technology, Application & Systems (MOBILITY'09)*, pages 1–8, Nice, France, Sep. 2009.

[34] S. Lee, G. Pan, J. Park, M. Gerla, and S. Lu. Secure incentives for commercial dissemination in vehicular networks. In *Proc. ACM International Symposium on Mobile ad hoc Networking and Computing (MOBIHOC'07)*, pages 150–159, Quebec, Canada, Sep. 2007.

[35] T. Kitani, T. Shinkawa, N. Shibata, K. Yasumoto, M. Ito, and T. Higashino. Efficient vanet-based traffic information sharing using buses on regular routes. In *Proc. IEEE Vehicular Technology Conference (VTC'08)*, pages 3031–3036, Singapore, May 2008.

[36] L. Wischhof, A. Ebner, and H. Rohling. Information dissemination in self-organizing inter-vehicle networks. *IEEE Transactions on Intelligent Transportation Systems*, 6(1):90–101, Mar. 2005.

[37] Apple carplay, Mar. 2015. URL http://www.techradar.com/news/car-tech/apple-carplay-everything-you-need-to-know-about-ios-in-the-car-1230381.

[38] H. Hartenstein and K. Laberteaux. A tutorial survey on vehicular ad hoc networks. *IEEE Communications Magazine*, 46(6):164–171, Jun. 2008.

[39] P. Fazio, F. Rango, C. Sottile, and C. Calafate. A new channel assignment scheme for interference-aware routing in vehicular networks. In *Proc. IEEE Vehicular Technology Conference (VTC'11)*, pages 1–5, Yokohama, Japan, May 2011.

[40] W. Viriyasitavat, F. Bai, and O. Tonguz. Dynamics of network connectivity in urban vehicular networks. *IEEE Journal on Selected Areas in Communications*, 29 (3):515–533, Mar. 2011.

[41] J. Blum, A. Eskandarian, and L. Hoffman. Challenges of intervehicle ad hoc networks. *IEEE Transactions on Intelligent Transportation Systems*, 5(4):347–351, Dec. 2004.

[42] M. Artimy, W. Robertson, and J. Phillips. Connectivity in inter-vehicle ad hoc networks. In *Proc. IEEE Canadian Conference on Electrical and Computer Engineering (CCECE'11)*, pages 293–298, Saskatchewan, Canada, May 2004.

[43] Vehicle safety communications project: final report. Technical Report DOT HS 810 591, Apr. 2006.

[44] Vehicle safety communications – applications (vsc-a) project: final report. Technical Report DOT HS 811 073, Jan. 2009.

[45] Vehicle infrastructure integration proof of concept executive summary – vehicle: final report. Technical Report FHWA-JPO-09-003, May 2009.

[46] High-occupancy vehicle (hov) system analysis tools – statewide hov facility performance analysis. Technical Report CA13-1665, May 2013.

[47] Cooperative perception and communication in vehicular technologies (coopercom), Sep. 2014. URL http://www.agence-nationale-recherche.fr/?Project=ANR-10-INTB-0304.

[48] Cooperative vehicles and infrastructure systems (cvis), May 2010. URL http://www.cvisproject.org.

[49] Privacy enabled capability in co-operative systems and safety applications (preciosa), Mar. 2010. URL http://www.2020-horizon.com/PRECIOSA-Privacy-enabled-capability-in-co-operative-systems-and-safety\-applications(PRECIOSA)-s1224.html.

[50] E-safety vehicle intrusion protected applications (evita), Jul. 2012. URL http://www.2020-horizon.com/EVITA-E-safety-vehicle-intrusion-protected\-applications(EVITA)-s1011.html.

[51] Secure vehicular communication (sevecom), Sep. 2010. URL http://www.sevecom.org.

[52] Network on wheels (now), May 2008. URL http://www.network-on-wheels.de/about.html.

[53] The advanced safety vehicle programme, Sep. 2007. URL http://www.researchgate.net/publication/2340778_The_Advanced_Safety_Vehicle_Programme/links/0f316a093829de2215f2dc18.pdf.

[54] Y. Furukawa. Driver behavior and active safety (overview). *R&D Review Toyota CRDL*, 39(2):1–8, Apr. 2004.

[55] S. Oyama. Its radiocommunications in japan. In *Proc. IEEE International Symposium on Wireless Vehicular Communications (WIVEC'07)*, pages 1–6, Tokyo, Japan, May. 2012.

[56] H. Matsumoto, H. Sonoda, M. Yoshioka, and T. Tanino. Study of how to protect etc system security. In *Proc. IEEE World Congress on Intelligent Transportation Systems (WCITS'08)*, pages 1–5, New York, USA, Nov. 2008.

[57] A. Fujimoto, K. Sakai, M. Ogawa, S. Hamada, S. Handa, M. Matsumoto, and K. Takahashi. Toward realisation of smartway in japan. In *Proc. IEEE World Congress on Intelligent Transportation Systems (WCITS'08)*, pages 6–15, New York, USA, Nov. 2008.

[58] B. Paul, M. Ibrahim, and M. Bikas. Vanet routing protocols: Pros and cons. *International Journal of Computer Applications*, 20(3):28–34, Apr. 2011.

[59] S. Zeadally, R. Hunt, Y. Chen, A. Irwin, and A. Hassan. Vehicular ad hoc networks (vanets): status, results, and challenges. *Telecommunication Systems*, 50(4):217–241, Aug. 2012.

[60] M. Marina and S. Das. On-demand multipath distance vector routing in ad hoc networks. In *Proc. IEEE International Conference on Network Protocols (ICNP'01)*, pages 14–23, California, USA, Nov. 2001.

[61] Y. Chen, Z. Xiang, W. Jian, and W. Jiang. A cross-layer aomdv routing protocol for v2v communication in urban vanet. In *Proc. IEEE International Conference on Mobile Ad-hoc and Sensor Networks (MSN'09)*, pages 353–359, Fujian, China, Dec. 2009.

[62] B. Jarupan and E. Ekici. A survey of cross-layer design for vanets. *Ad Hoc Networks*, 9(5):966–983, Jul. 2011.

[63] Z. Haas and M. Pearlman. The performance of query control schemes for the zone routing protocol. *ACM Transactions on Networking*, 9(4):427–438, Aug. 2001.

[64] V. Park and M. Corson. A highly adaptive distributed routing algorithm for mobile wireless networks. In *Proc. IEEE International Conference on Computer Communications (INFOCOM'97)*, pages 1405–1413, Kobe, Japan, Apr. 1997.

[65] M. Altayeb and I. Mahgoub. A survey of vehicular ad hoc networks routing protocols. *International Journal of Innovation and Applied Studies*, 3(3):829–846, Jul. 2013.

[66] K. Lee, J. Harri, U. Lee, and M. Gerla. Enhanced perimeter routing for geographic forwarding protocols in urban vehicular scenarios. In *Proc. IEEE Globecom Workshops (GLOBECOMW'07)*, page 26–30, Washington DC, USA, Nov. 2007.

[67] K. Lee, M. Le, J. Harri, and M. Gerla. Louvre: Landmark overlays for urban vehicular routing environments. In *Proc. IEEE Vehicular Technology Conference (VTC'08)*, page 1–5, Calgary, Canada, Sep. 2008.

[68] J. Nzouonta, N. Rajgure, G. Wang, and C. Borcea. Vanet routing on city roads using real-time vehicular traffic information. *IEEE Transactions on Vehicular Technology*, 58(7):3609–3626, Sep. 2009.

[69] G. Yan, D. Rawat, and B. Bista. Provisioning vehicular ad hoc networks with quality of service. *International Journal of Space-Based and Situated Computing*, 2(2):104–111, Mar. 2012.

[70] S. Bitam and A. Mellouk. Qos swarm bee routing protocol for vehicular ad hoc networks. In *Proc. IEEE International Conference on Communications (ICC'11)*, pages 1–5, kyoto, Japan, Jun. 2011.

[71] G. Li and L. Boukhatem. An intersection-based delay sensitive routing for vanets using aco algorithm. In *Proc. IEEE International Conference on Computer Communications and Networks (ICCCN'14)*, pages 750–757, Shanghai, China, Aug. 2014.

[72] G. Li and L. Boukhatem. Adaptive vehicular routing protocol based on ant colony optimization. In *Proc. IEEE International Workshop on Vehicular Ad Hoc Networks (VANET'13)*, pages 95–98, Taipei, China, May 2013.

[73] Y. Hsieh and K. Wang. A road-based qos-aware multipath routing for urban vehicular ad hoc networks. In *Proc. IEEE Global Communications Conference (GLOBECOM'12)*, pages 189–194, California, USA, Dec. 2012.

[74] H. Saleet, R. Langar, K. Naik, R. Boutaba, A. Nayak, and N. Goel. Intersection-based geographical routing protocol for vanets: A proposal and analysis. *IEEE Transactions on Vehicular Technology*, 60(9):4560–4574, Nov. 2011.

[75] Y. Sun, S. Luo, Q. Dai, and Y. Ji. An adaptive routing protocol based on qos and vehicular density in urban vanets. *International Journal of Distributed Sensor Networks*, 1(1):1–14, Mar. 2015.

[76] S. Kamali and J. Opatrny. A position based ant colony routing algorithm for mobile ad-hoc networks. *Journal of Networks*, 3(4):459–462, Apr. 2008.

[77] W. Chiang and R. Russell. Simulated annealing metaheuristics for the vehicle routing problem with time windows. *Annals of Operations Research*, 63(1):3–27, Feb. 1996.

[78] R. Moghaddam, N. Safaei, and Y. Gholipour. A hybrid simulated annealing for capacitated vehicle routing problems with the independent route length. *Applied Mathematics and Computation*, 176(2):445–454, May 2006.

[79] C. Koulamas, S. Antony, and R. Jaen. A survey of simulated annealing applications to operations research problems. *Omega*, 22(1):41–56, Jan. 1994.

[80] M. Osmana, M. Sinnab, and A. Mousab. An effective genetic algorithm approach to multi-objective routing problems (morps). *Applied Mathematics and Computation*, 163(2):769–781, Apr. 2005.

[81] B. Baker and M. Ayechew. A genetic algorithm for the vehicle routing problem. *Computers & Operations Research*, 30(5):787–800, Apr. 2003.

[82] J. Brandão and A. Mercerb. A tabu search algorithm for the multi-trip vehicle routing and scheduling problem. *European Journal of Operational Research*, 1(1): 180–191, Jul. 1997.

[83] M. Gendreau, G. Laporte, C. Musaraganyi, and E. Taillard. A tabu search heuristic for the heterogeneous fleet vehicle routing problem. *Computers & Operations Research*, 26(12):1153–1173, Oct. 1999.

[84] M. Reimann, K. Doerner, and R. Hart. D-ants: savings based ants divide and conquer the vehicle routing problem. *Computers & Operations Research*, 31(4): 563–591, Apr. 2004.

[85] K. Doerner, R. Hart, G. Kiechle, M. Lucka, and M. Reimann. Parallel ant systems for the capacitated vehicle routing problem. *Evolutionary Computation in Combinatorial Optimization*, 30(4):72–83, Apr. 2004.

[86] S. Mazzeo and I. Loiseau. An ant colony algorithm for the capacitated vehicle routing. *Electronic Notes in Discrete Mathematics*, 18(1):181–186, Dec. 2004.

[87] Y. Bin, Z. Yang, and B. Yao. An improved ant colony optimization for vehicle routing problem. *European Journal of Operational Research*, 196(1):171–176, Jul. 2009.

[88] L. Gambardella and M. Dorigo. Ant colony system: a cooperative learning approach to the traveling salesman problem. *IEEE Transactions on Evolutionary Computation*, 1(1):53–66, Apr. 1997.

[89] A. Colorni, M. Dorigo, V. Maniezzo, and M. Trubian. Ant system for job-shop scheduling. *Jorbel–Belgian Journal of Operations Research Statistics and Computer Science*, 34(1):39–53, Feb. 1994.

[90] G. Caro, F. Ducatelle, and L. Gambardella. Anthocnet: an adaptive nature-inspired algorithm for routing in mobile ad hoc networks. *European Transactions on Telecommunications*, 16(5):443–455, Sep. 2005.

[91] G. Caro and M. Dorigo. Ant colonies for adaptive routing in packet-switched communications networks. In *Proc. ACM International Conference on Parallel Problem Solving from Nature (PPSN'98)*, pages 673–682, Amsterdam, Netherlands, Sep. 1998.

[92] A. Colorni, M. Dorigo, and V. Maniezzo. Distributed optimization by ant colonies. In *Proc. IEEE European Conference On Artificial Life (ECAL'91)*, pages 134–142, Pairs, France, Sep. 1991.

[93] R. Montemanni, L. Gambardella, A. Rizzoli, and A. Donati. A new algorithm for a dynamic vehicle routing problem based on ant colony system. *IEEE Transactions on Evolutionary Computation*, 3(7):1–22, Apr. 2003.

[94] S. Ganguly and S. Das. A novel ant colony optimization algorithm for the vehicle routing problem. *Swarm, Evolutionary, and Memetic Computing*, 82(97):401–412, Dec. 2013.

[95] N. Toklu, R. Montemanni, and L. Gambardella. A robust multiple ant colony system for the capacitated vehicle routing problem. In *Proc. IEEE International Conference on Systems, Man, and Cybernetics (SMC'13)*, pages 1871–1876, Manchester, UK, Oct. 2013.

[96] R. Silva, H. Lopes, and W. Godoy. A heuristic algorithm based on ant colony optimization for multi-objective routing in vehicle ad hoc networks. In *Proc. IEEE International Conference on Computational Intelligence and 11th Brazilian Congress on Computational Intelligence (BRICS-CCI-CBIC'13)*, pages 435–440, Ipojuca, Brazil, Sep. 2013.

[97] C. Perkins and P. Bhagwat. Highly dynamic destination-sequenced distance-vector routing (dsdv) for mobile computers. In *Proc. IEEE Conference on Communications Architectures, Protocols and Applications (SIGCOMM'94)*, pages 234–244, New York, USA, Oct. 1994.

[98] J. Luo, X. Gu, T. Zhao, and W. Yan. A mobile infrastructure based vanet routing protocol in the urban environment. In *Proc. IEEE International Conference*

on Communications and Mobile Computing (CMC'10), pages 432–437, Shenzhen, China, Apr. 2010.

[99] V. Naumov, R. Baumann, and T. Gross. An evaluation of inter-vehicle ad hoc networks based on realistic vehicular traces. In *Proc. ACM International Symposium on Mobile Ad hoc Networking and Computing (MOBIHOC'06)*, page 108–119, Florence, Italy, May 2006.

[100] M. Souryal and N. Moayeri. Channel-adaptive relaying in mobile ad hoc networks with fading. In *Proc. IEEE Communications Society Conference on Sensor and Ad Hoc Communications and Networks (SECON'05)*, pages 142–152, California, USA, Sep. 2005.

[101] S. Lee, B. Bhattacharjee, and S. Banerjee. Efficient geographic routing in multihop wireless networks. In *Proc. ACM International Symposium on Mobile Ad hoc Networking and Computing (MOBIHOC'05)*, pages 230–241, New York, USA, May 2005.

[102] F. Holger, J. Widmer, K. Michael, M. Martin, and H. Hannes. Contention-based forwarding for mobile ad hoc networks. *Ad hoc Networks*, 1(4):351–369, Nov. 2003.

[103] K. Egoh and S. De. Priority-based receiver-side relay election in wireless ad hoc sensor networks. In *Proc. ACM International Conference on Wireless Communications and Mobile Computing (IWCMC'06)*, page 1177–1182, Vancouver, Canada, Jun. 2006.

[104] M. Chawla, N. Goel, K. Kalaichelvan, A. Nayak, and I. Stojmenovic. Beaconless position based routing with guaranteed delivery for wireless ad-hoc and sensor networks. *Ad-Hoc Networking*, 32(6):847–855, Nov. 2006.

[105] M. Huson and A. Sen. Broadcast scheduling algorithms for radio networks. In *Proc. IEEE Military Communications Conference (MILCOM'95)*, page 647–651, California, USA, Nov. 1995.

[106] G. Zhou, T. He, S. Krishnamurthy, and J. Stankovic. Impact of radio irregularity on wireless sensor networks. In *Proc. IEEE International Conference on Mobile Systems, Applications, and Services (MOBISYS'04)*, page 125–138, Boston, USA, Jun. 2004.

[107] J. Zhao and R. Govindan. Understanding packet delivery performance in dense wireless sensor networks. In *Proc. IEEE International Conference on Embedded Networked Sensor Systems (SENSYS'03)*, page 1–13, Los Angeles, USA, Nov. 2003.

[108] J. Nzouonta, N. Rajgure, G. Wang, and C. Borcea. Vanet routing on city roads using real-time vehicular traffic information. *IEEE Transaction Vehicular Technology*, 58(7):3609–3626, Feb. 2009.

[109] K. Egoh and S. De. A multi-criteria receiver-side relay election approach in wireless ad hoc networks. In *Proc. IEEE Military Communications Conference (MILCOM'06)*, pages 1–7, Washington DC, USA, Oct. 2006.

[110] S. Wang, C. Lin, Y. Hwang, K. Tao, and C. L. Chou. A practical routing protocol for vehicle-formed mobile ad hoc networks on the roads. In *Proc. IEEE Intelligent Transportation Systems Proceedings (ITSC'05)*, pages 161–166, Vienna, Austria, Sep. 2005.

[111] R. Santos, A. Edwards, R. Edwards, and N. Seed. Performance evaluation of routing protocols in vehicular ad-hoc networks. *International Journal of Ad Hoc and Ubiquitous Computing*, 1(2):80–91, Nov. 2005.

[112] M. Jerbi, T. Rasheed, and Y. Doudane. Towards efficient geographic routing in urban vehicular networks. *IEEE Transactions on Vehicular Technology*, 58(9): 5048–5058, Nov. 2009.

[113] J. Bell and P. McMullen. Ant colony optimization techniques for the vehicle routing problem. *Advanced Engineering Informatics*, 18(1):41–48, Jul. 2004.

[114] G. Karagiannis, O. Altintas, E. Ekici, G. Heijenk, B. Jarupan, K. Lin, and T. Weil. Vehicular networking: A survey and tutorial on requirements, architectures, challenges, standards and solutions. *IEEE Communications Surveys & Tutorials*, 13 (4):584–616, Jul. 2011.

[115] S. Haykin and M. Moher. *Modern Wireless Communications*. Prentice Hall, Massachusetts, USA, 2004.

[116] T. Rappaport. *Wireless Communications: Principles and Practice*. Prentic Hall PTR, California, USA, 1996.

[117] P. Athanasios and P. Unnikrishna. *Probability, random variables and stochastic processes*. McGraw-Hill, New York, USA, 2002.

[118] N. Wisitpongphan, B. Fan, P. Mudalige, and O. Tonguz. On the routing problem in disconnected vehicular ad-hoc networks. In *Proc. IEEE International Conference on Computer Communications (INFOCOM'07)*, pages 2291–2295, Alaska, USA, May 2007.

[119] A. Agarwal, D. Starobinski, and T. Little. Phase transition of message propagation speed in delay-tolerant vehicular networks. *IEEE Transactions on Intelligent Transportation Systems*, 13(1):249–263, Mar. 2012.

[120] R. Oliveira, L. Bernardo, and P. Pinto. Modelling delay on ieee 802.11 mac protocol for unicast and broadcast nonsaturated traffic. In *Proc. IEEE Wireless Communications and Networking Conference (WCNC'07)*, pages 463–467, Hongkong, China, Mar. 2007.

[121] J. Harri, F. Filali, C. Bonnet, and M. Fiore. Vanetmobisim: generating realistic mobility patterns for vanets. In *Proc. IEEE International Workshop on Vehicular Ad Hoc Networks (VANET'06)*, pages 96–97, Los Angeles, USA, Sep. 2006.

[122] F. Kuhn, R. Wattenhofer, Y. Zhang, and A. Zollinger. Geometric ad-hoc routing of theory and practice. In *Proc. IEEE Annual Symposium on Principles of Distributed Computing (PODC'03)*, pages 63–72, Boston, USA, Jul. 2003.

[123] P. Bose, P. Morin, I. Stojmenovic, and J. Urrutia. Routing with guaranteed delivery in ad hoc wireless networks. *ACM Wireless Networks*, 7(6):609–616, Nov. 2001.

[124] M. Sheldon. *Introduction to Probability Models.* Academic Press, Los Angeles, USA, 2004.